Powder binder interactions in 3D inkjet printing

by

RHYS M. LEWIS

Diploma work No. 124/2014

at Department of Materials and Manufacturing Technology

CHALMERS UNIVERSITY OF TECHNOLOGY

Gothenburg, Sweden

Diploma work in the Master programme Materials Engineering

Performed at: Digital Metal, Molndal / Chalmers University of Technology

Supervisor(s): Bo Goran Andersson

Company Name: Digital Metal

Address: Argongatan 30,Molndal 431 53,Sweden

Examiner: Dr. Sven Bengtsson

Department of Materials and Manufacturing Technology

Chalmers University of Technology, SE - 412 96, Gothenburg

Powder Binder Interactions in 3D inkjet printing

RHYS M. LEWIS

Powder binder interactions in 3D inkjet printing

RHYS M. LEWIS

Department of Materials and Manufacturing Technology

Chalmers University of Technology

SUMMARY

Three dimensional printing is an additive manufacturing technique that is the next step in the development of additive manufacturing technology. It is a tool less process which can be used to fabricate parts having complex geometries in a single step process with minimal material wastage. It involves the deposition of metal powder in successive layers followed by the selective local deposition of ink which functions as a binder using a print head. On completion of the printing process the part is cured, cleaned of loose powder and placed in an oven for debinding followed by sintering in a sintering furnace. The parts so produced may then be processed as desired by techniques such as polishing to achieve the desired surface finish.

In order to maintain high quality product each processing stage needs to be evaluated as a source of error. One of the most important variables in this process is the interaction between the metal powder and the ink during printing. The speed of printing as well as the accuracy, surface finish and yield of the print are dependent on the quality of the powder ink interactions.

The focus of this thesis is the study of powder ink interactions by studying the characteristics of both the powder and the ink and consequently improving the quality of their interactions. This involves testing both existing metal powder ink combinations and new combinations through controlled tailoring of their properties. The powders assessed include different batches of 316L powders. The combinations are assessed based on the goals of ease of processing, handling, sintering and product quality. The variables modified include particle size distribution of the powder, powder bed temperature, ink viscosity, surface tension and powder bed packing. The differences between the powder ink interactions in the case of both virgin and recycled powder are also assessed to establish better process control and improve quality.

TABLE OF CONTENTS

TABLE OF FIGURES

1. INTRODUCTION

1.1 BACKGROUND

During 3D printing of products made of 316L powder it was observed that the printing performance of the powder supplied from the same supplier varied from batch to batch. The quality of the printed parts produced by the same ink was also found to differ for different batches of powder printed with the same ink. These differences in behaviour pose significant challenges to standardization and maintenance of product quality. Based on real life shop floor experience of the operator working with different batches of powder the powder found to function best in the machine was identified. A number of different powder blends were prepared from different batches of powders including powder obtained from crushed green parts. This crushed powder is quite crucial to reduce material wastage as currently these parts are discarded thus reducing process efficiency. The effect of additional variables such as temperature on the printing process is quite important as the machine runs at an elevated temperature of 80^0C and the powders are stored in a heating cabinet maintained at 60^0C to minimize the deleterious effects of moisture on the powders. A special heated plate apparatus is fabricated to that end during the investigation of powder wettability however this could not be done during the investigation of powder rheology due to possibility of permanent damage to the equipment. In addition a green printed part was examined using optical microscopy to understand the spreading of the printed ink on the surface of the powder particles. The effect of differing quantities of ink and binder content in the ink was also studied to examine possibilities of ink modification to produce products with a higher green strength. This is important as stronger green parts facilitate easier handling and process automation.

1.2 OBJECTIVES

The objectives of this master thesis are as follows:

- Comparison of the powder rheology of eight different powders for the selection of one that is found to function best in the machine based on shop floor experience
- Investigation of the differences in wetting characteristics of two different batches of 316L powders sourced from the same producer using the same production process
- Examination of process variables such as temperature on the printing process
- Investigation of the change in green strength of parts resulting from ink modification

1.3 LITERATURE SURVEY

Additive manufacturing is a term that has garnered increasing attention from the mainstream media and is a field of growing interest to people all over the world. Often hailed as a transformative technology by scientists and policy makers it is seen as the solution to the problems of deindustrialization in the developed world. Though initially used to develop prototypes its usage has expanded over the last couple of years to applications far beyond prototyping. Over the past decade the usage of this technology to manufacture parts for direct use has grown and now accounts for 28 % of additive manufacturing product and service revenues [1]. Additive manufacturing is itself a technique of manufacturing three dimension parts by depositing materials in layers as opposed to conventional subtractive manufacturing processes which involve primarily material removal. The main advantages of additive manufacturing over other conventional manufacturing processes are:

- Production of intricate parts with no special tooling or modifications thus resulting in parts with better functionality as opposed to conventional manufacturing machine shop processes where design complexity requires complex and additional tool paths increasing costs.
- Near net shape production thus minimizing the amount of processing required as compared to traditional subtractive manufacturing processes.

- Manufacture of even a small number of parts at a reasonable cost as it does not require the traditional tool fabrication and setup time and allows the manufacture of complex shapes in one single piece thus reducing need for assembly and simplifying logistics.

The various additive manufacturing processes can be classified based on the form of the material used as follows.
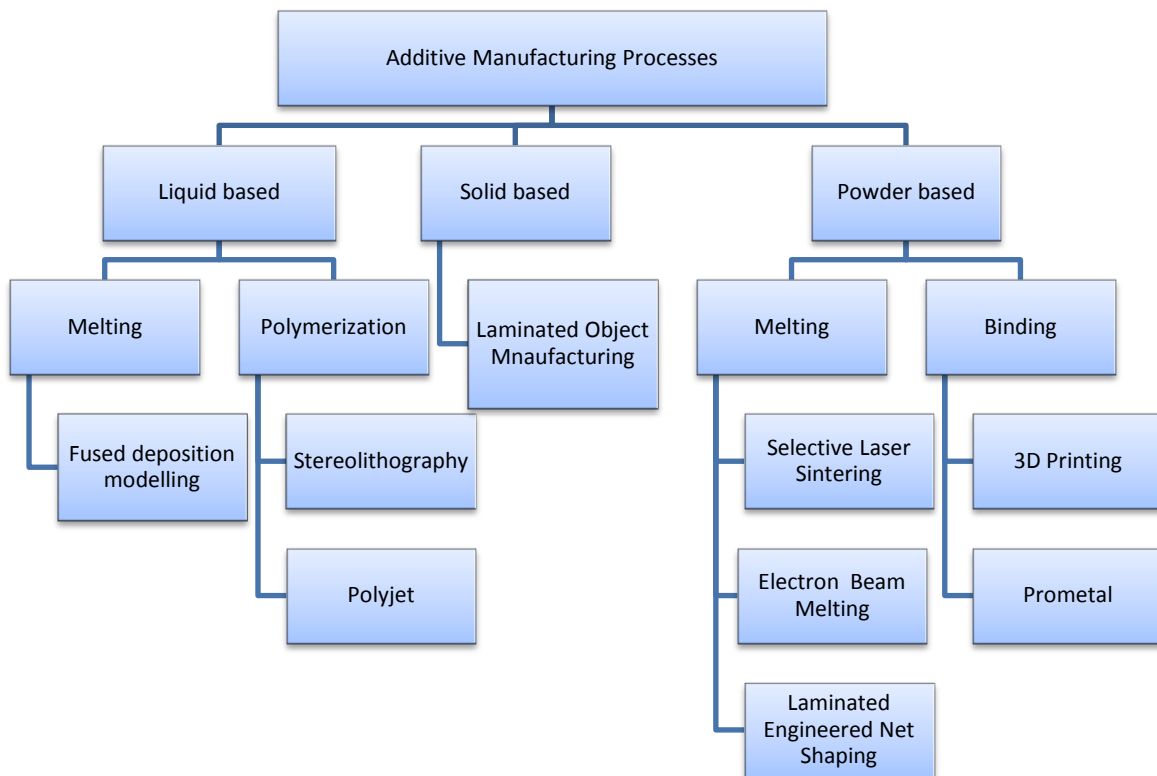
Figure 1: Classification of additive manufacturing processes [2]

The focus of this work is three dimensional inkjet printing a technique of fabricating three dimensional parts from powder and ink as a binder which is based on the same principle as an inkjet printer.

The basic process structure and description is given below in the Figure.2 :

| Object design | Slicing | Recoating | Physical object |

Figure 2: 3D printing process layout [3]

- The three dimensional CAD file created based on requirements of the engineering team or by scanning an existing product using Magnetic Resonance Imaging (MRI), Computer Tomography (CT) or Reverse Engineering (RE) is prepared [4].
- The CAD file is then converted into an STL (Stereolithography) file using software which transforms the data into triangles whose number can be changed as per the requirements of accuracy and convenience
- The STL file so obtained is sliced into two dimensional layers to be printed after positioning the objects in the printing box to minimize printing time. Additional supports may be added using the software to support delicate overhangs, avoid sagging during sintering, etc.
- The file is then used by the machine to print the part using the powdered materials and ink supplied through an inkjet. The ink functions as a binder and binds the powder particles in the pattern required to form primitives which combine to form a single layer. The blade deposits a layer of powder after printing each layer.

Some of the primary advantages and limitations are given in Figure 3 below

Advantages

Cost of 3D printing mahcines is significantly lower than other additive manufacturing machines esp laser based ones

Simpler to assemble from more commonly available parts as compared to laser based techniques

Easier and cheaper to scale up capacity by adding more print heads

Applicable to many materials [5]

Limitations

Many materials still cannot be printed

Limited accuracy for large parts compared to SLS [5]

Ink formulation

Droplet shape and splashing [5]

 Nozzle clogging

Figure 3 : Advantages and limitations of 3D printing

1.3.1 INK FORMULATION

Since 3D printing involves printing of ink ejected through a print head onto the powder bed a significant amount of effort has been dedicated to the development of suitable inks. Since the technology used in 3D printing borrows significantly from inkjet printing on a paper, an examination of the literature relating to the formulation and modification of ink and inkjet is relevant.

The main requirements for the proper functioning of the printing system are [6]

- Ability to maintain fluidity in the cartridge to avoid clogging up the capillary channels and nozzles
- Quick drying once printed
- Good printing resolution

The above conflicting requirements are managed through use of humectants, solvents and good equipment design [6].It is necessary to look at the composition of the ink given in the Figure 4 in detail to look at possible areas for modification.
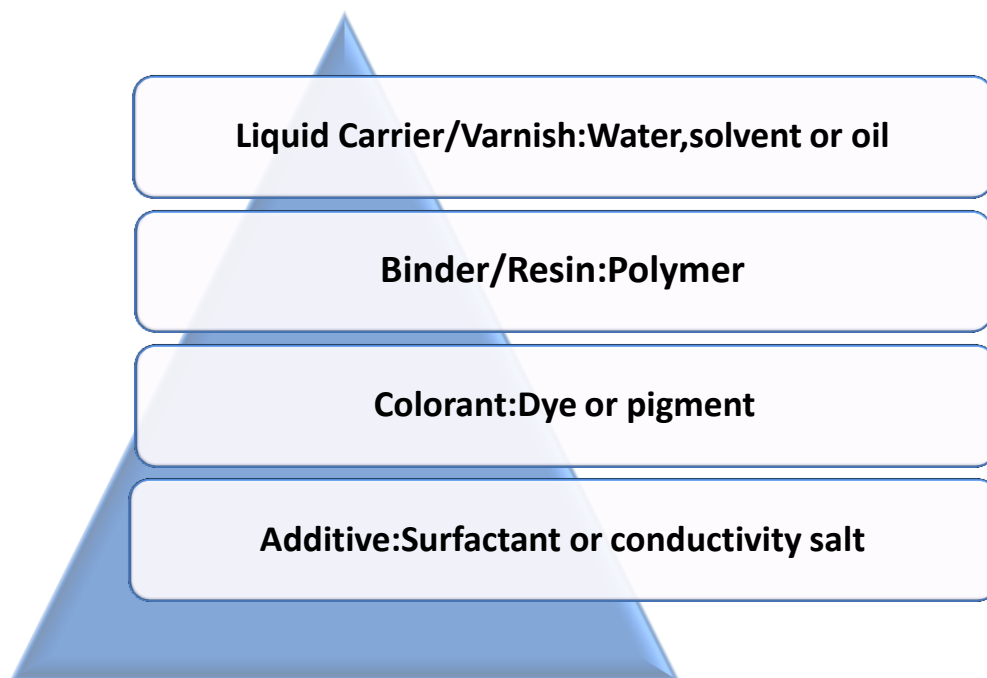
Figure 4 : Key ingredients in inkjet ink

Important factors affecting the performance of inks in 3D printing are the surface tension, viscosity, molecular weight, conductivity, material compatibility and safety [7]. Of these the most critical factors in the proper penetration of the ink and its wettability are the viscosity and surface tension. To ensure problem free ejection of ink from the nozzle the maximum permitted viscosity for the inks is about 20 mPas [8].The viscosity affects droplet formation and droplet velocity [9]. A general rule for this is that the maximum particle size in the ink should be 100 times smaller than the nozzle diameter to avoid clogging [10]. Modifying viscosity is tricky because it is affected by many different factors such as pH, solid loading, polymer loading and polymer length. The viscosity can be lowered by decreasing particle loading [11], adding a dispersant and increasing particle size although this may clog the nozzles [12][13][14][15]. The surface tension is also usually limited. It has a large influence of the wetting characteristics of the ink on the powder bed and can be changed through the addition of a fluid with different surface tension. Another important factor to be considered is the binder residue due to thermal decomposition of the binder during the thermal de-binding stage carried out on the recycled powder at 200^{0}C and its possible effects on wettability. This is examined with the help of an SEM to detect

organic residue from the ink i.e. mainly carbon. Polyvinylpyrrolidone (PVP) is often used as a binder in inks [16] and is also the primary binder material studied here. The effect on increasing the PVP content on green strength can also be evaluated. Increasing green strength could facilitate easier handling, cleaning and possible process automation.

1.3.2 INKJET PRINTING

In inkjet printing tiny droplets of ink are propelled onto paper form the basis of 3D printing of metal parts. The print head, ink and substrate are the three related factors in an inkjet printing system that affect the quality of printed parts. As commercially available inkjet print heads are used in Digital Metals 3D printing system the focus will remain on the ink and substrate. During the early days of inkjet technology only low viscosity inks were used at ambient temperatures. Today developments in inkjet technology allowing use of higher pressures allow use of inks with higher viscosity [17]. Selective printing of the ink onto the powder bed allows low cost and high precision parts conveniently. The two main technologies employed in inkjet printers today are

- Continuous jet: It was first developed by IBM in the 1970's. Pressurized ink is forced through a nozzle to form a continuous jet of ink which is broken up an external vibration produced by a piezo crystal to form a stream of droplets which acquire an electrical charge during passage through a charge electrode and deflector plates which deflect them and subsequently guide them to the substrate while the unused ink is collected by suction and for reuse [18].

- Drop-on-demand: First developed by Siemens in the PT-80 serial character printer this technology ensures ink droplet ejection only when needed. Ink flows to a chamber which has a nozzle and a piezoelectric crystal which is excited during printing creating a pressure wave. This pressure wave creates an ink droplet that is ejected through the nozzle resulting in better consistency and control and avoids the deflection and recirculation of recovered ink seen in continuous jet printing systems [18].Today most printers utilize this technology. Thermal print heads are also used here.

On ejection of the droplet from the print head it moves toward and impacts the powder bed. The droplet is drawn into the powder bed by capillary action. The successive droplets added merge with the previous droplets in the powder bed. This may cause some splashing. The fluid quickly sinks into the bed and the time for penetration can be monitored.

1.3.3 POWDER RHEOLOGY

The properties of stainless steel powders are affected to a large degree by the nature of the process used to manufacture them. The specific process chosen has a large impact on a number of factors such as the composition, particle size, particle size distribution and particle shape. The properties of the powder vary depending on the production route. The main techniques of powder production by atomization are show in Figure 5 below:
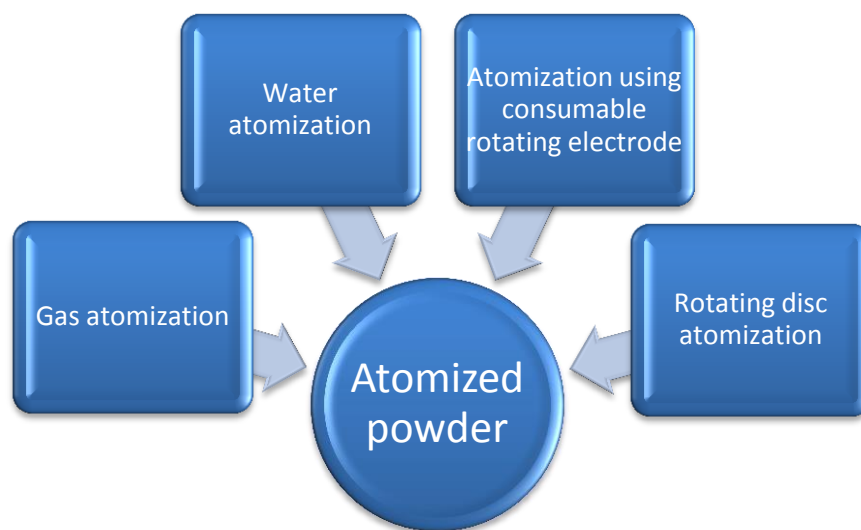
Figure 5: Techniques of powder atomization

Of the above methods the two main methods used for 3D printing are gas atomization and atomization using a consumable rotating electrode [19].The powder used in these experiments as ins commonly used   was 316L gas atomized powder. Gas atomization produces powder particles with reproducible particle size distribution, perfectly spherical shape which imparts the powders with excellent fluidity resulting in excellent packing density. Molten metal is prepared in an inert atmosphere or vacuum to prevent oxidation. In this process a molten metal stream is disrupted by a jet of air, nitrogen, argon or helium at a

high velocity. The gas is chosen based on the metal, surface texture and the rate of atomization. The size of the powder particles can be controlled by carefully controlling the ratio of gas-to-metal [20].The tanks used are usually quite tall to allow sufficient time for solidification of the metal as it falls to the bottom of the tank. By maintaining control over the momentum of the disrupting gas jet the production rate of the metal powder can be carefully controlled. Any oxidation of the powders produced by this process is minimal with oxide thicknesses of just a few atomic layers. To ensure good powder flow in a 3D printing machine a detailed investigation and control of powder rheology is crucial. A powder with a good rheological profile minimizes manufacturing problems and enhances product quality. Traditional characterization techniques such as angle of repose, flow through an orifice and Carr's index have limited industrial relevance due to poor reproducibility of test conditions. While the effect of factors such as particle shape, size distribution, texture and surface energy are relatively easily quantified ,in industry a number of additional factors such as air flow and moisture due to the environment also have a significant effect on powder behaviour [21]. The flow of the powder is dependent not only on the powder characteristics but also on the handling, storage and processing equipment. To characterize flowability of different powders the density, cohesiveness and wall friction need to be measured [22].If any problems are uncovered by testing suitable remedial action such as process, powder or environment modification may be undertaken. Thus proper characterization of powder rheology can prevent processing problems and thus save valuable time and money for an additive manufacturer.

1.3.4 WETTABILITY

Wettability of a solid is mainly studied through the determination of the surface energies of the solid and liquid to be discussed. This is assessed through measurement of the contact angle between the powder bed and the ink as shown in Figure 6 applying the Young's equation of force balance at the three phase interface using a goniometer. At the triple point the following three interfacial forces are balanced

- Interfacial force between the drop and the ambient vapour(γ_{LV})
- Interfacial force between the drop and the powder bed(γ_{SL})

- Interfacial force between the powder bed and the ambient vapour (γ_{SV}) [23]

$$cos\theta = \frac{(\gamma_{sv} - \gamma_{sl})}{\gamma_{LV}} \qquad (1)$$

$\Theta < 90^0 C$

Tangent

Ink
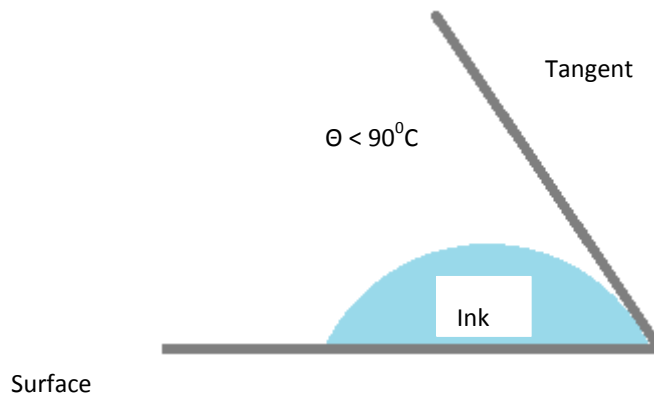
Surface

Figure 6 : Drop profile for good wetting

The primary factors affecting the contact angle are:

- Surface tension-As the surface tension of the ink increases the wettability worsens and the consequently there is an increase in the contact angle
- Surface energy of the powder bed surface-Increasing surface energy results in improved wetting of the powder bed
- Powder bed roughness-Increased roughness results in a smaller contact angle for hydrophilic surface and a larger contact angle in the case of a hydrophobic surface
- Temperature of ink-Higher temperature of the ink lowers surface tension by reducing the intermolecular forces thus decreasing contact angle

The Young's equation makes the following assumption that the substrate surface is homogenous and flat. This is rarely true for powder beds and hence poses a number of challenges.

A survey of scientific literature points to the following methods as a means to measure the contact angle [24].

- Sessile drop method
- Capillary rise or modified Washburn method
- Direct measurements of interfacial energies using heat measurements using microcalorimetry or inverse gas chromatography (very complex and expensive techniques and hence uncommon)

Both the sessile drop and capillary rise techniques are used to evaluate the contact angle and wettability of the powder for different inks. Small contact angles (less than 90^0) indicate good wettability while large contact angles (greater than 90^0) indicate poor wettability. In an ideal case the contact angle of the fluid on the surface would be zero which is indicative of perfect wettability. It is essential for the ink molecules situated at the three phase line to disconnect from the adjoining ink molecules, displace adsorbed gases at the powder surface and form fresh bonds with the powder molecules.

The main problem with using the sessile drop method to evaluate the wettability of porous solids is the penetration of the wetting fluid into the pores of the powder bed during the test for a fluid with a contact angle of less than 90° (critical angle for spontaneous wetting in a porous solid).In the case of the Wilhemy plate method the penetration of the liquid into the pores results in faulty readings of the contact force between the wetting fluid having a contact angle greater than 90° and the powder. Thus these two techniques can be used only in specific cases. The capillary rise or modified Washburn method is a better alternative in this case [22] [25].

1.3.5 GREEN STRENGTH

It is the property of maintaining size and shape during handling [26]. This property is particularly important for parts with complex designs [27].The green strength which is the mechanical strength of the un-sintered printed parts is quite an important factor to facilitate easier handling, minimize production losses and facilitate development of automated part cleaning systems to remove loose powder. The main source of compact green strength is interlocked powder particles [28] due to the geometry and surface irregularities which are considerably reduced in the case of gas atomized

powders due to their geometry. Other factors that increase green strength are decreased particle size, increased printing temperature [29] as well as ink and binder content. The binder used in the ink studied here is Polyvinylpyrrolidone (PVP) $(C_6H_9NO)_x$ which is a white amorphous water-soluble polymer soluble in a large number of hydrophilic and hydrophobic resins [30].An investigation of the effect of different ink and binder content on green strength is necessary and both these variables are varied to evaluate their effect on green strength.

2. EXPERIMENTAL METHODOLOGY

The evaluation of the wetting characteristics of the metal powder involves measurement of properties of different powders including physical and rheological properties, binder properties such as surface tension and rheology as well as the effect of binder loading on green strength and their interactions.

2.1 MATERIALS USED
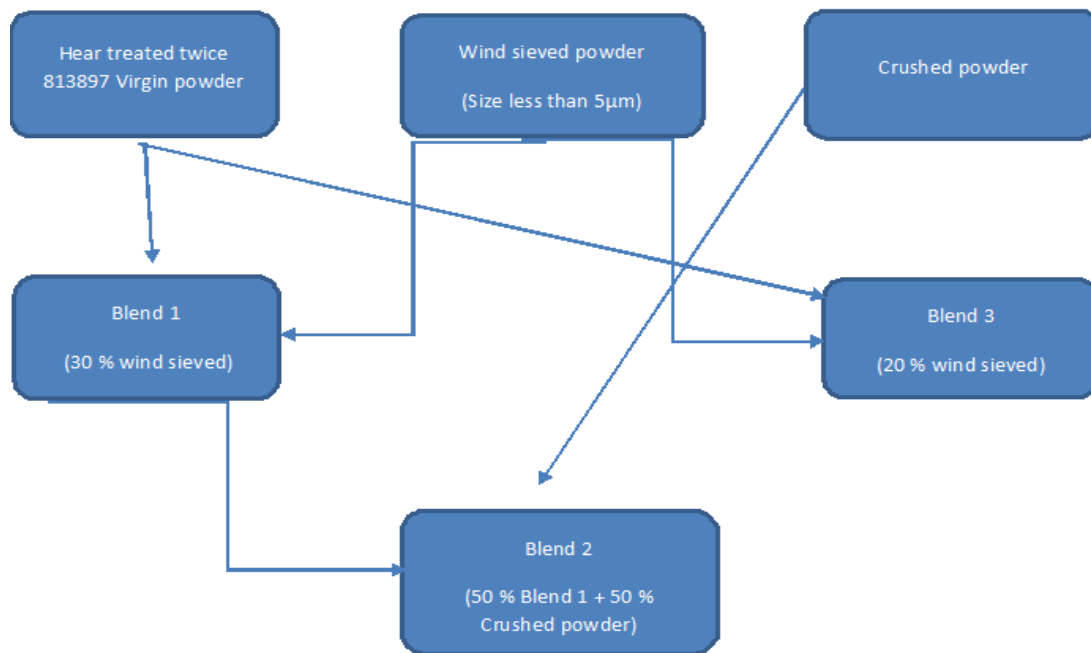
Figure 7: Compositional structure of powder blends

Two different batches of 316L stainless steel powders named 813897 and 816135 will be examined to study differences in wetting behaviour between new or virgin powder and powder heated to 200^0C or recycled powder for each of the powders. A single ink Collins Blue is used as the ink or binder studied during wettability studies. In addition to the four different powders mentioned above three different blends of powders shown in Figure 7 and crushed powder obtained from green printed parts are also prepared to determine which of the powders tested have a rheology that most closely resembles the rheology of the powder found to work best in the machine- 813897 Recycled based on the observations of the machine operator on the shop floor. The crushed powder is quite important as an ingredient in the above

powder blends as its usage would reduce material wastage by utilizing rejected 3D printed parts.

2.2 X-RAY TURBIDIMETRY
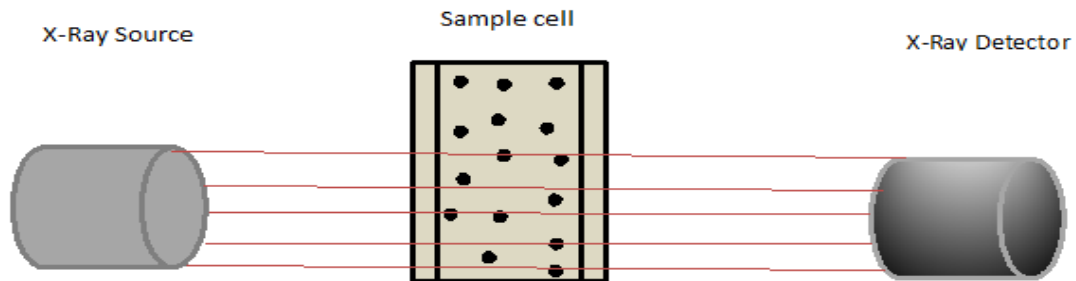
Figure 8: Operation of X-Ray Turbidimeter

The standard is ASTM B 430.This analysis utilizes a sedigraph shown in Figure 8 in which X rays are use together with gravitational forces acting on metal powder particles in a fluid to determine the particle size distribution. The working is based upon Stokes Law which relates the frictional force acting on the powder particle moving through the sedimentation fluid to the velocity, viscosity of the carrying fluid and particle radius.

$$V= (\rho_p-\rho_l)dg^2/18\eta \dots\dots\dots\dots\dots\dots\dots\dots\dots\dots\dots\dots\dots\dots\dots\dots\dots\dots\dots\dots[31](2)$$

Where V=Velocity of the powder particle, cm/s

ρ_p=density of the particle, g/cc

ρ_l=density of the fluid, g/cc

η=viscosity of the fluid, poise

g=acceleration due to gravity,cm^2/s

d=diameter of the particle, cm

The diameter of the particle assumed to be spherical is obtained from the following equation

$$D= [18\eta v/d_r g]^{1/2}\dots\dots\dots\dots\dots\dots\dots\dots\dots\dots\dots\dots\dots\dots\dots\dots\dots[31](3)$$

Where D=Diameter of thee powder particle

       v= settling velocity, cm/s

       d_r =difference in density between liquid and the powder

       g=acceleration due to gravity, cm/s^2

The powder particles whose density is known are kept in a small container which is then subjected to a beam of X-rays. Using the Navier-Stokes equation and noting the rate at which the particles settle and equivalent diameter is obtained. The change in relative intensity of the beam at a particular time and location is used to determine the percentage of particles at or near a certain diameter.

2.3 SURFACE AREA BY BET METHOD
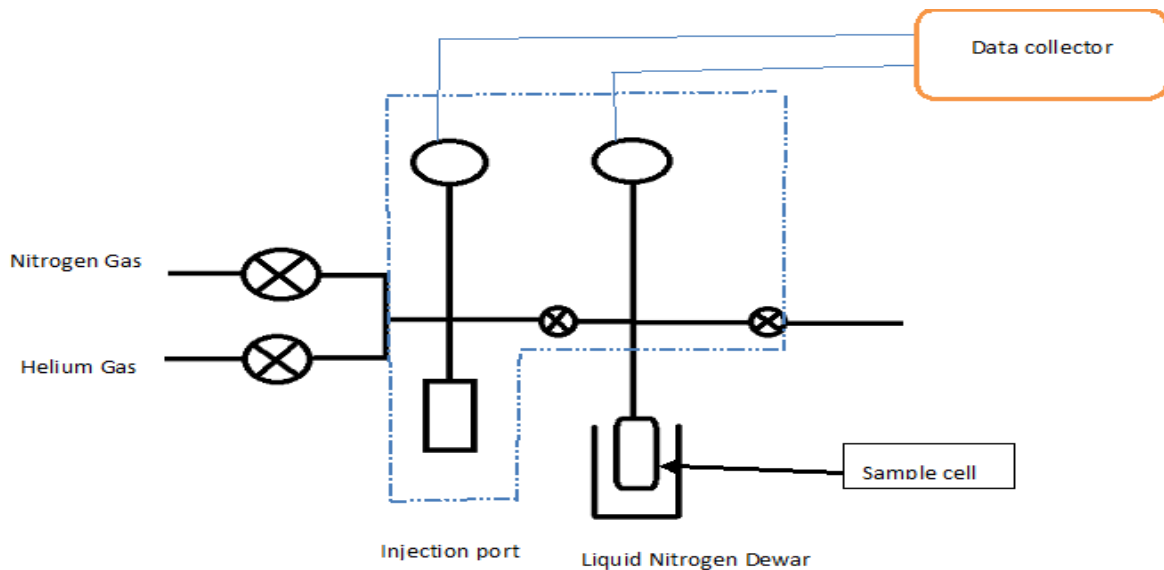
Figure 9: Schematic of BET equipment [32]

The standard for determining the surface area shown in Figure 9 is ASTM B922-10.The surface area of a powder is of great importance in characterizing the wetting behaviour of a powder. This is primarily because the interaction with the ink takes place across the interface which varies with the surface area of the powder. The surface area of the powder increases with an increase in irregularity of geometry and

increase in surface roughness of the powder particles. A measurement of the specific surface area which takes into account the weight of the powder called specific surface area is of even greater importance.

In this method the amount of gas required to deposit a molecular layer on the powder surface is calculated using the Brunauer, Emmett and Teller theory. Nitrogen gas is often utilized. The surface of the powder must however be cleaned at an elevated temperature in vacuum to desorb any previously adsorbed gases. From the calculation of the area of one molecule the area of the sample and the specific surface can be calculated. The amount of gas adsorbed is calculated from the measurements of the volume of gas adsorbed as a function of pressure.

2.4 POWDER RHEOMETRY
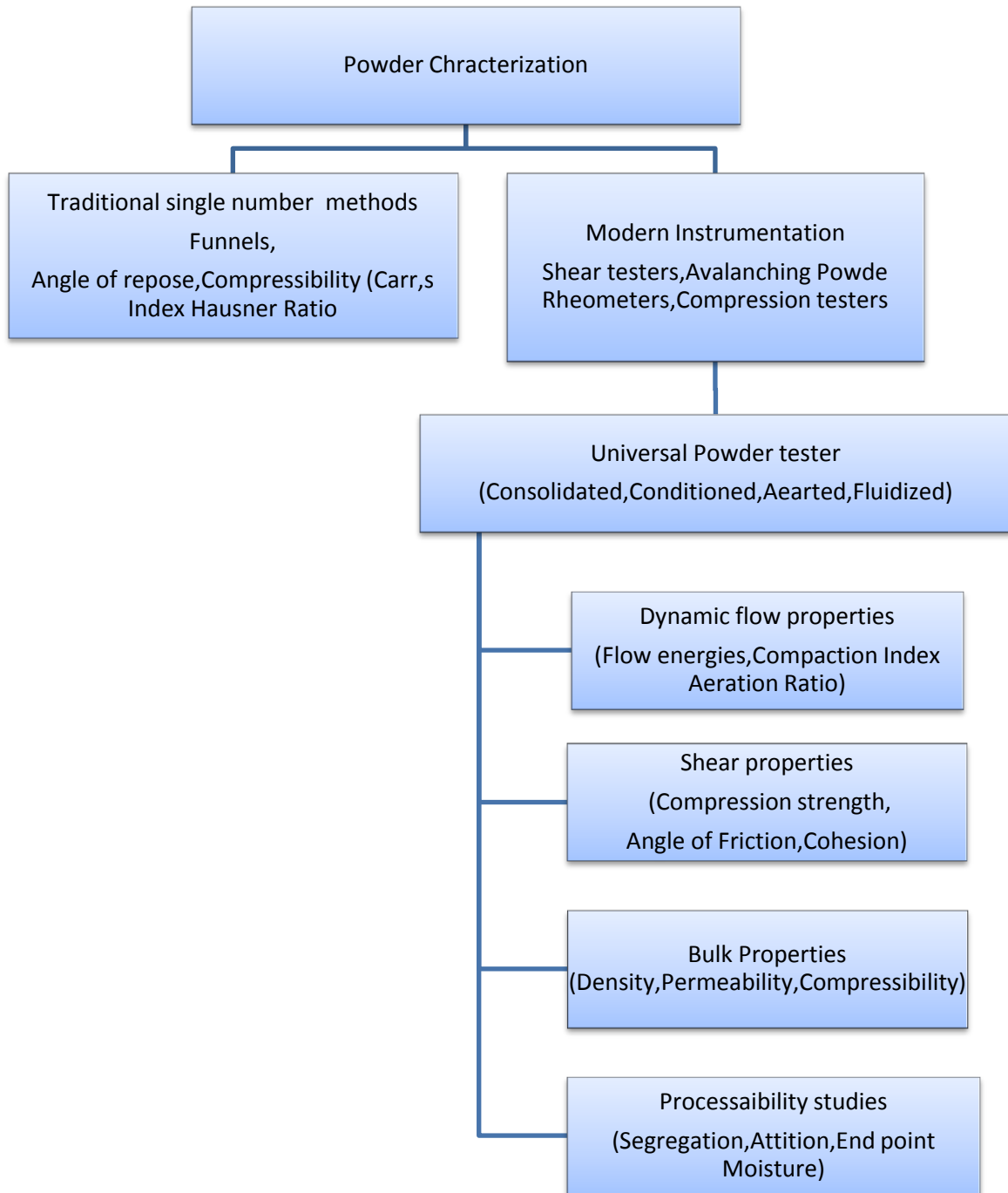
Figure 10: Powder characterization techniques [33]

Traditional tests such as the cone angle or funnel test assign a single value to a powder and do not take into account the effect of aeration or consolidation, etc. Using a FT3 powder rheometer powder behaviour shown in Figure 10 is studied through the measurement of the different properties using a limited sample volume

for modifications if necessary. To avoid the distortion of results by the absorption of moisture by the powders they are dried at 70°C overnight and subsequently placed in a desiccator. A small sample of powder is preconditioned before each test using a blade travelling helically through a vessel to produce a low stress homogenously packed powder bed.

2.4.1 BASIC FLOWABILITY ENERGY (BFE)

It is the energy required to get conditioned powder to flow during the anti-clockwise downwards motion of a blade. It is calculated from the work done in the movement of the blade during the high stress compressive flow from the top of the vessel to the bottom. The value is generally taken as test 7 of the Stability test. It is affected by factors listed in Figure 11.
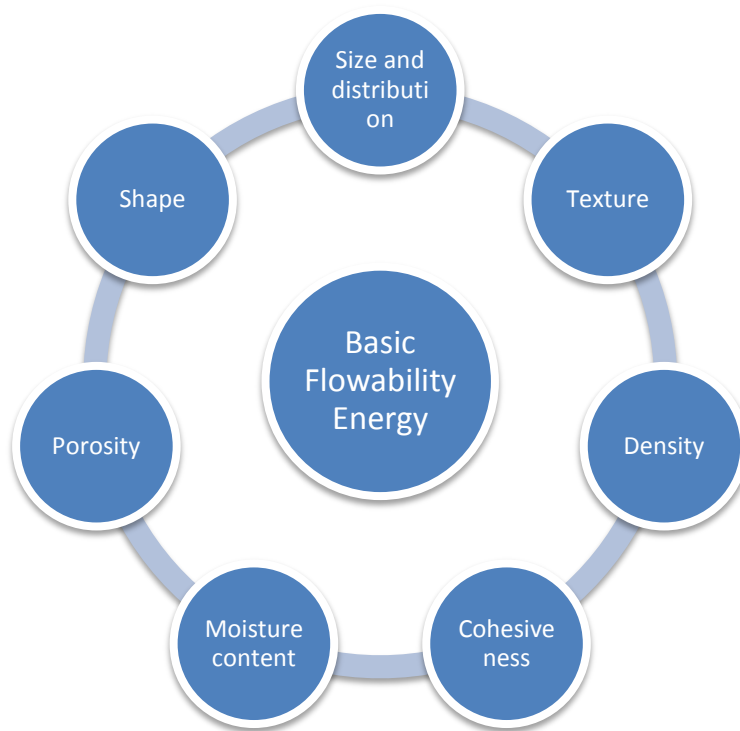
Figure 11; Factors affecting Basic Flowability Energy [39]

Basic Flowability Energy is quite essential to ensure easy powder flow in the machine. In most cases powder with a low BFE will be preferable to a powder with a high BFE for powders that have a different surface texture. Among the above factors particle size is quite critical as finer powders are more cohesive resulting in a high BFE while larger particles being less cohesive give a smaller BFE. For cohesive powders the particles at the blade face can be accommodated by air between

agglomerated particles and hence the stress is transmitted locally while the absence of air in the more efficiently packed non-cohesive powders leading to a flow zone much larger and deeper than in the case of cohesive powders. This is responsible of the situation in powders of different particle sizes where good flow is accompanied by high BFE. The effect of a few variables on the Bulk Flow Energy is shown below in Figure 12.
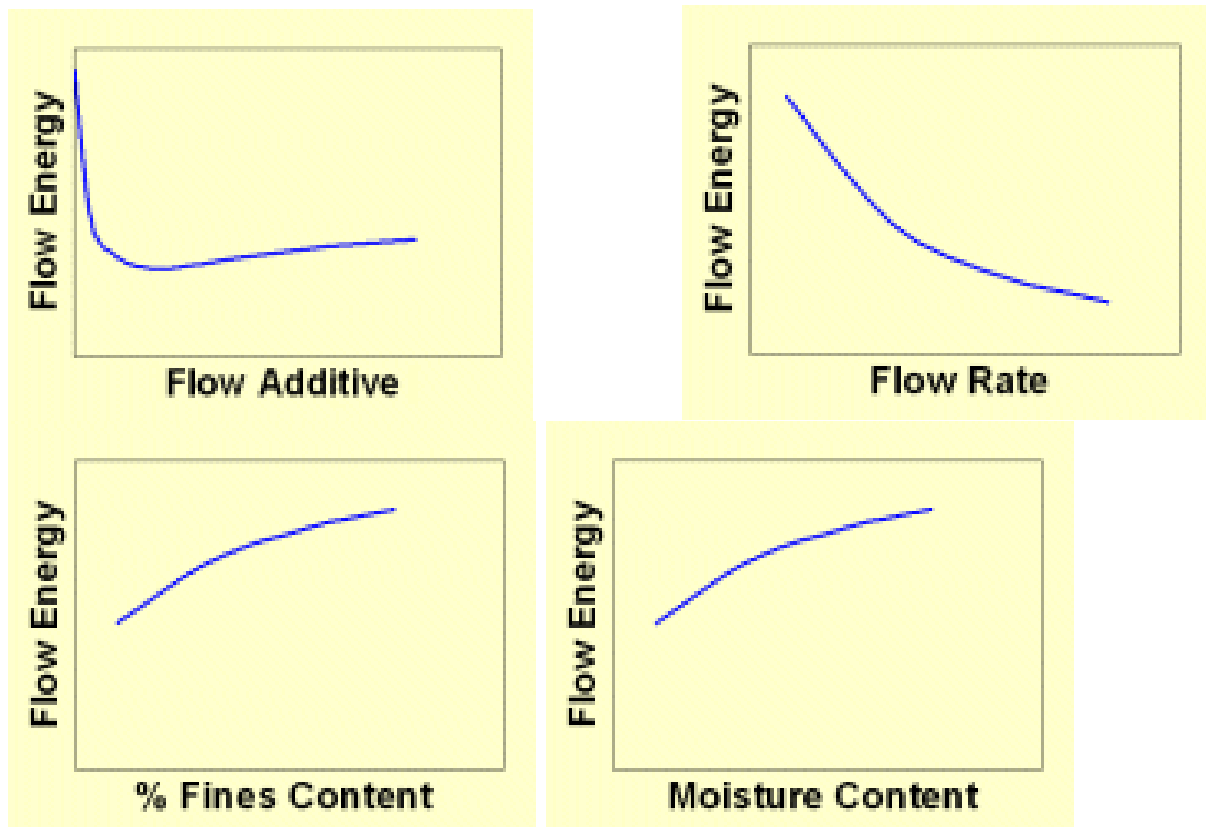
Figure 12: Effect of variables on Bulk Flowability Energy [33]

2.4.2 SPECIFIC ENERGY (SE)
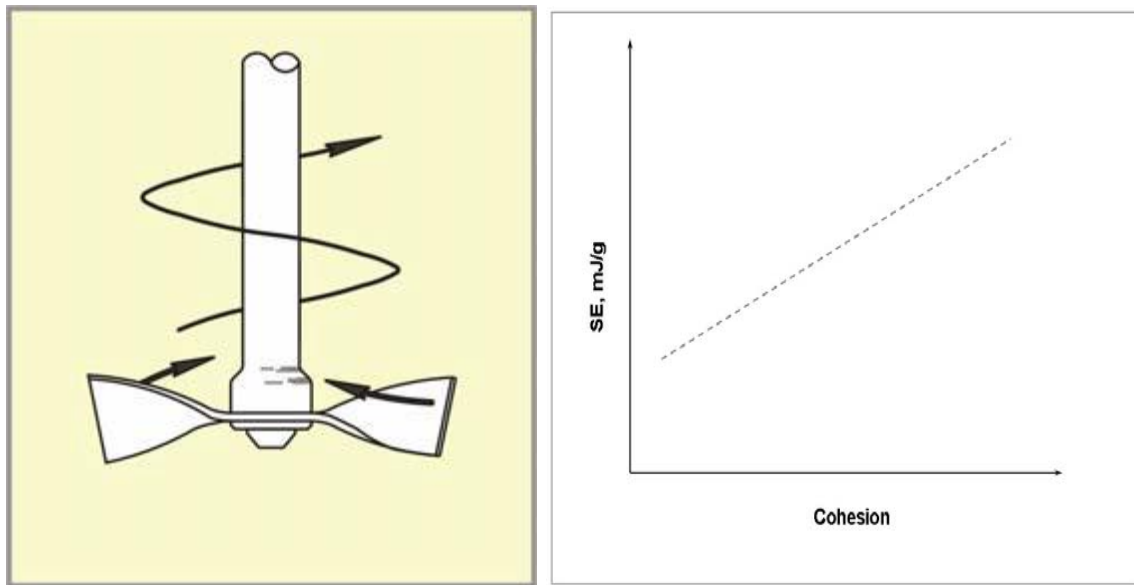
Figure 13: Powder flow and its relationship to cohesion [33]

A measure of powder flow in an unconfined low stress environment it is the energy required to establish an upward clockwise low stress flow pattern in an unconfined powder (no constraint on top as shown in Figure 13).It is indicative of cohesion and shear forces between the powder particles and is obtained from the work done from the movement of the blade normalized against mass. Generally the specific energy is directly proportional to cohesiveness.

2.4.3 STABILITY TEST

To check the validity of the test results it is important to check if there is any change in powder behaviour as a result of rheological testing due to attrition, deformation, caking or agglomeration of the powder. This is usually the first test to be performed as it gives a good indication of the stability of the powder and hence relevance of results during testing. It can be quantified by the Stability Index (SI) obtained from seven conditioning and test cycles.

Stability Index (SI) =Energy consumed during final test/Energy consumed during first test [33]……… (4)

A Stability Index close to 1 indicates a stable and robust powder. However, in case of values significantly lower or higher than one closer examination of the powder is warranted. These deviations from the ideal value could possibly be due to de-

aeration, agglomeration, segregation, moisture uptake and electrostatic charge for values lower than one and attrition, de-agglomeration, over blending of additives or coating of the blade and vessel by additives. In case the powder shows poor stability the number of test cycles can be increased till stability is reached.

2.4.4 VARIABLE FLOW RATE

This test quantifies the behaviour of a powder subject to varying flow rates. This is particularly pertinent in the case of cohesive powders due to higher air content. Initially the flow energy is measured at a flow rate of 100mm/s which is then reduced and the changes in rheology measured. Again cohesive powders are much more sensitive to this due to the higher air content as shown in Figures 8 and 9. This is combined with the stability test because it is only suitable in the case of a stable powder. It is given by the flow rate index (FRI)

Flow rate index (FRI) = Energy of final test ÷ Energy of initial test [33]…………………………………………….. (5)

A guide to the interpretation of the data obtained is given below

Table 1: DATA interpretation guide for flow rate index [39]

Flow Rate Index (FRI)	Typical data
FRI > 3	High flow rate sensitivity-very cohesive powder
1.5 < FRI < 3	Average flow rate sensitivity typical for most powders
FRI ≈ 1	Flow rate insensitive-Large particle size or surface treated powder
FRI < 1	Presence of flow additives
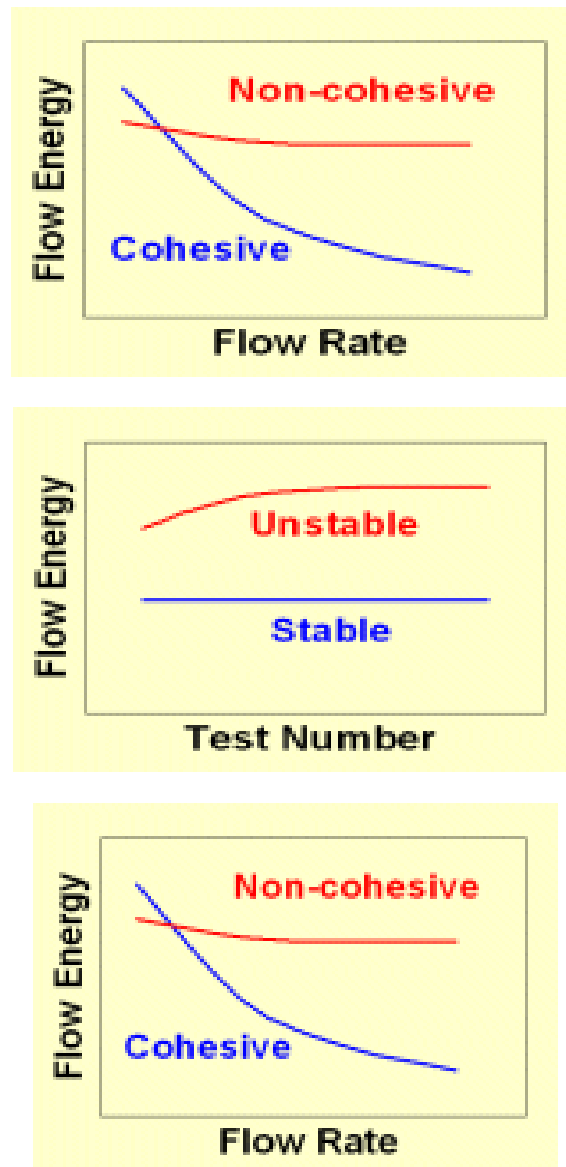
Figure 14: Flow Rate Index for different powder behaviour [33]

2.4.5 TAPPED CONSOLIDATION TEST

In this test the impact of vibration and consequent consolidation on the flow energy of a powder which is likely in real life during transportation and processing. The test is carried out at 50 manual taps but in the case of excessive compaction this may be reduced. The change in flow energy and bulk density can be monitored as part of this process and problem areas identified for process modification if necessary.

2.4.6 PERMEABILITY

It is the measure of permeability of the powder to air and is affected by the particle size and distribution, cohesiveness, shape, surface texture and bulk density. Generally cohesive powders having average size of less than 30 microns are the least permeable as well as powders with a wide size distribution. In this test the air pressure drop for varying normal stress is monitored for constant air velocity. The greater the pressure drop, the lower the permeability. It is quite important in quantifying the effects of storage and flow on powder behaviour. This test uses a vented piston which enables air from the powder to escape uniformly during compression of the powder sample. After powder conditioning the sample the vented piston compresses the sample wile subjecting it to an increasing normal stress for a definite amount of time for equilibration. At the same time air is passed through the bottom of the vessel at a constant rate and the pressure drop across the powder bed is measured. A guide to the interpretation of the data obtained is given below.

Table 2: DATA INTREPRETATION GUIDE FOR PERMEABILITY DATA [33]

Permeability	Typical data
High	Minimal pressure drop Non-cohesive, large particles or granular powder
Medium	Increasing pressure drop with increasing compression Limited particle cohesion/Wide particle size distribution
Low	High air pressure to establish air flow

The permeability is shown for both cohesive and non-cohesive powders in the Figure 15.
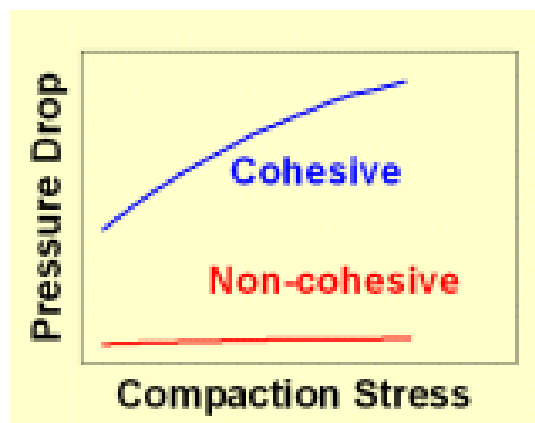
Figure 15 : Permeability for cohesive and non-cohesive powders [33]

2.4.7 COMPRESSIBILITY

It measures the change in density as a function of increasing applied normal stress applied using a vented piston to compress the powder and is affected by the particle size distribution, cohesiveness, stiffness, shape and texture. The compressibility of the powder is determined by measuring the change in volume of a conditioned sample of powder from the traverse of the piston for various applied normal stresses. This is shown for low, medium and high compressibility powders in Figure 16. The bulk density or compressibility index can be determined and evaluated for different normal stresses.

Compressibility Index=Density after compression/Conditioned bulk density [33]………………………….(6)

Table 3: DATA INTERPRETATION GUIDE FOR COMPRESSIBILITY TEST [39]

Compressibility	Typical data
Low	Minimal excess air and efficient particle packing
Medium	Moderate cohesiveness and typical of most powders
High	Small particle size, high cohesiveness and large amount of air
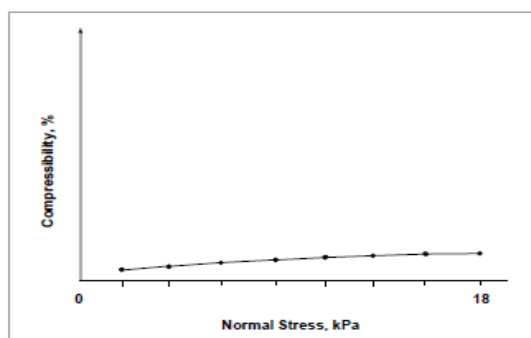
Low compressibility
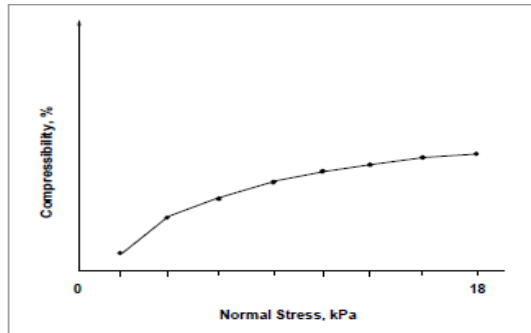
Moderate compressibility
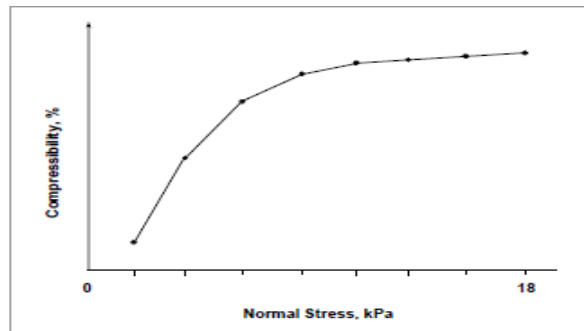
High compressibility

Figure 16: Compressibility for different powders [33]

2.4.8 AERATION

The powder flows under the influence of gravitational forces and due to the influence of cohesive forces between the particles. The differences between cohesive and non-cohesive powders are shown in Figure 17. When a powder flows the gravitational forces exceed the cohesive forces between the particles. Air may be introduced into the powder to improve flow and is highly dependent on the cohesive forces in the powder. In this test air is introduced air is introduced into a vessel filled with powder and measures the change in powder properties. The Aeration ratio quantifies the sensitivity of the powder to aeration.

Aeration ratio, AR: Energy (Air velocity 0)/Energy (Air velocity n)[33]…………………………………………….(9)

Aeration ratio	Typical data
AR ≈ 1	Insensitive to aeration. Very cohesive powders/high levels of binder
2 < AR <20	Average sensitivity to aeration. Typical for most powders
AR >> 20	High sensitivity to aeration. Powder coatings, powders with low cohesive strength
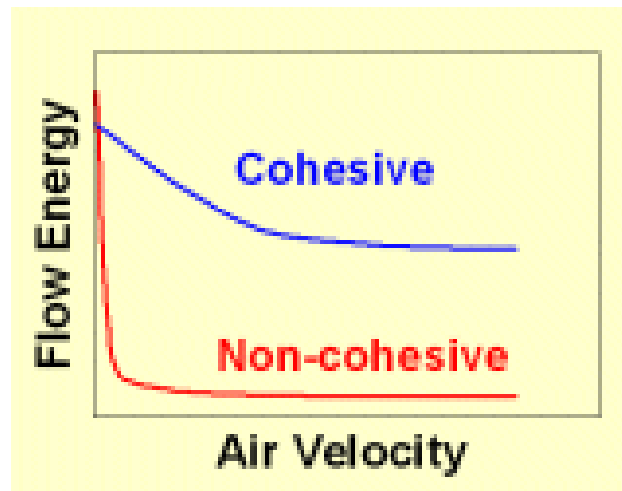
Figure 17: Aeration ratio for cohesive and non-cohesive powders [33]

2.4.9 SHEAR CELL

This test measures how a consolidated powder will flow on overcoming its yield point using a shear cell and thus gives an indication of the probability of flow problems due to either bridging, blockages or stoppages. Initially a normal stress is applied till a certain value is reached after which shear stress is induced through rotation of the blades while maintaining the normal stress at a constant value. The shear stress is increased till the bed fails and this stress is the yield point stress. The shear stress and the normal stress are recorded at the yield point are noted for different lower normal stresses to obtain yield loci. A number of useful parameters can be obtained from the yield loci using Mohr's Stress Circles shown in Figure 18 such as Cohesion and unconfined yield strength. A cohesive powder will have higher values of Cohesion and UYS and a lower flow function. A high value of the flow function on the other hand indicates good flow for stresses similar to those used in the test. The main parameters of the test are given below.

Cohesion: Shear Stress where the Best Fit Line intercepts the y-axis [33]

Unconfined Yield Strength, (UYS): The greater of intercepts of the smaller Mohr's Circle at x-axis [33]

Major Principal Stress: the greater of intercepts of the larger Mohr's Circle at x-axis [33]

Flow function=Major Principal Stress/Unconfined Yield Strength [33]
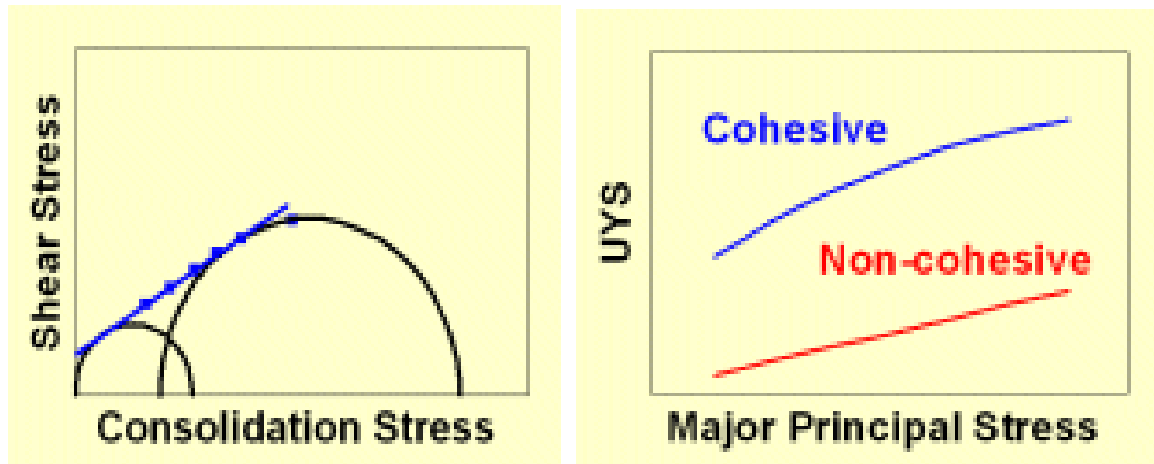
Figure 18 : Unconfined Yield Strength from yield loci using Mohr's Circle Analysis [33]

2.4.10 WALL FRICTION

This test measures the resistance to flow of a consolidated powder in contact with a certain material. Flow occurs on overcoming the friction between the powder and a certain material and is tested for different materials such as machined aluminium, machined steel, machined graphite as well as polished aluminium, polished steel and polished graphite. It is also influenced by the particle size, shape and surface characteristics. In this test a wall friction head of the material to be tested induces vertical and rotational stresses in the powder in a cylindrical vessel. First a constant normal stress is applied to the powder and then the powder is subjected to a shear stress by rotating the wall friction head. The torque increases until the resistance of the powder is overcome and the maximum torque is observed. The head is then continuously rotated at a predetermined velocity for a predetermined amount of time. The torque during this movement is noted from which the steady state shear stress is determined. The wall friction angle can then be determined from the shear stress and the normal stress as shown in Figure 19 below.
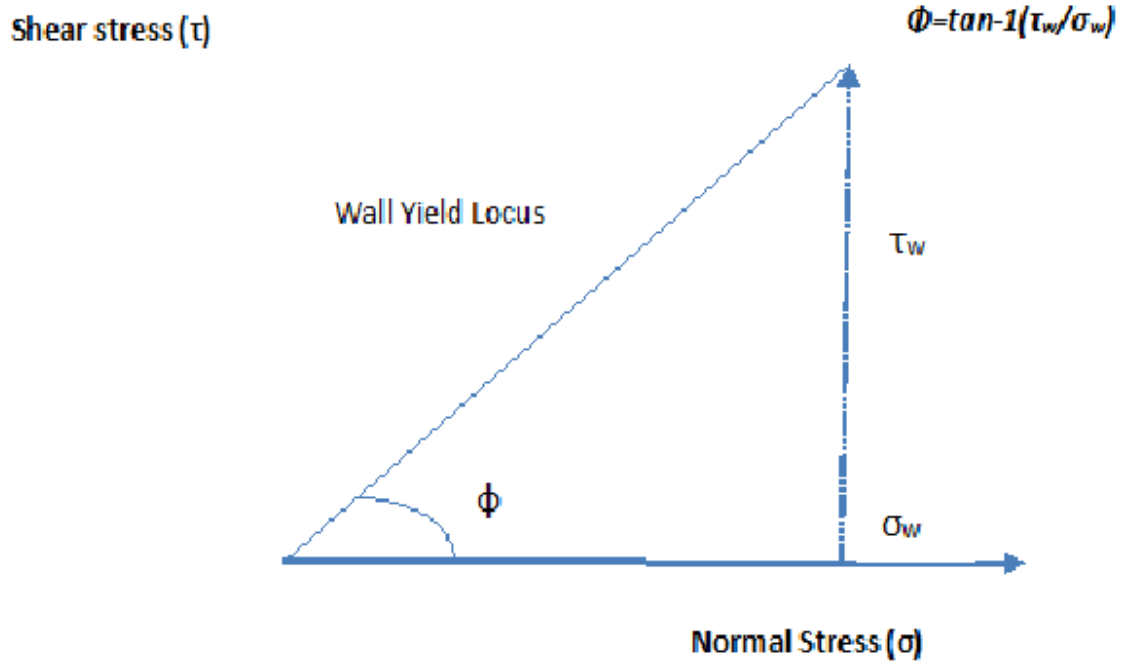
Figure 19: Derivation of wall friction angle from test data [33]

The equation shown in the figure: $\Phi = tan^{-1}(\tau_w / \sigma_w)$

Labels in figure: Shear stress (τ), Wall Yield Locus, ϕ, τ_w, σ_w, Normal Stress (σ)

2.5 GONIOMETRY/OPTICAL TENSIOMETRY
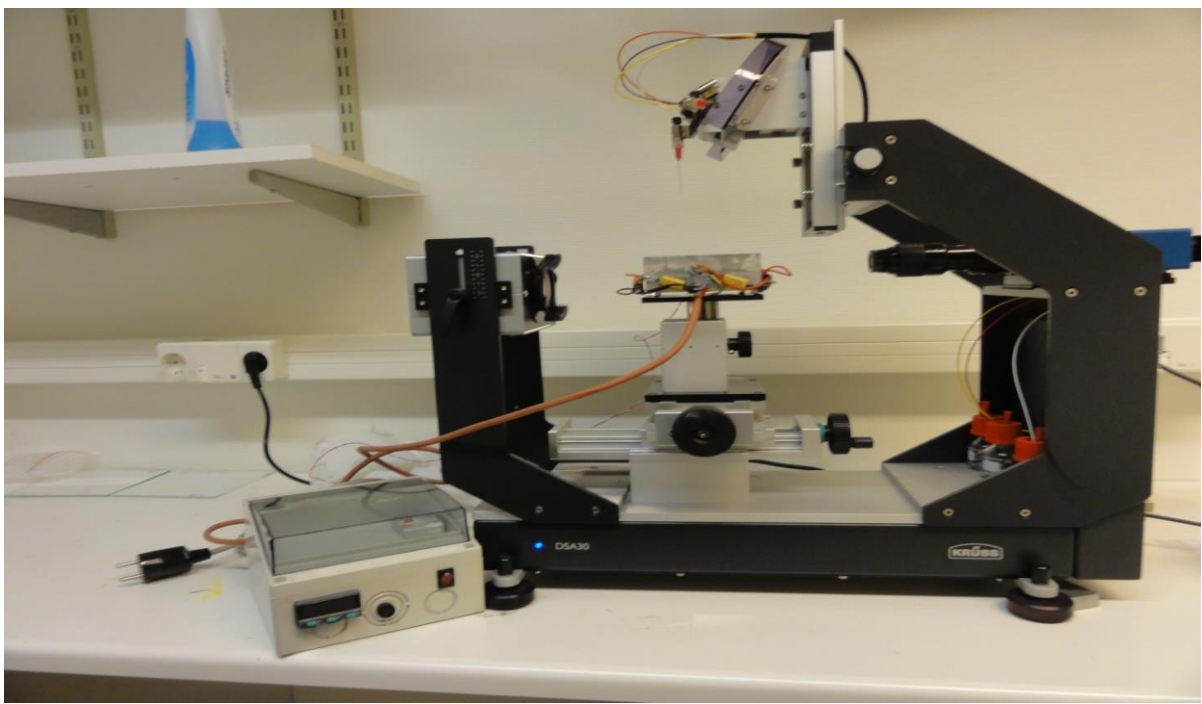
Figure 20: Contact angle goniometer with attached microcontroller and heating plate
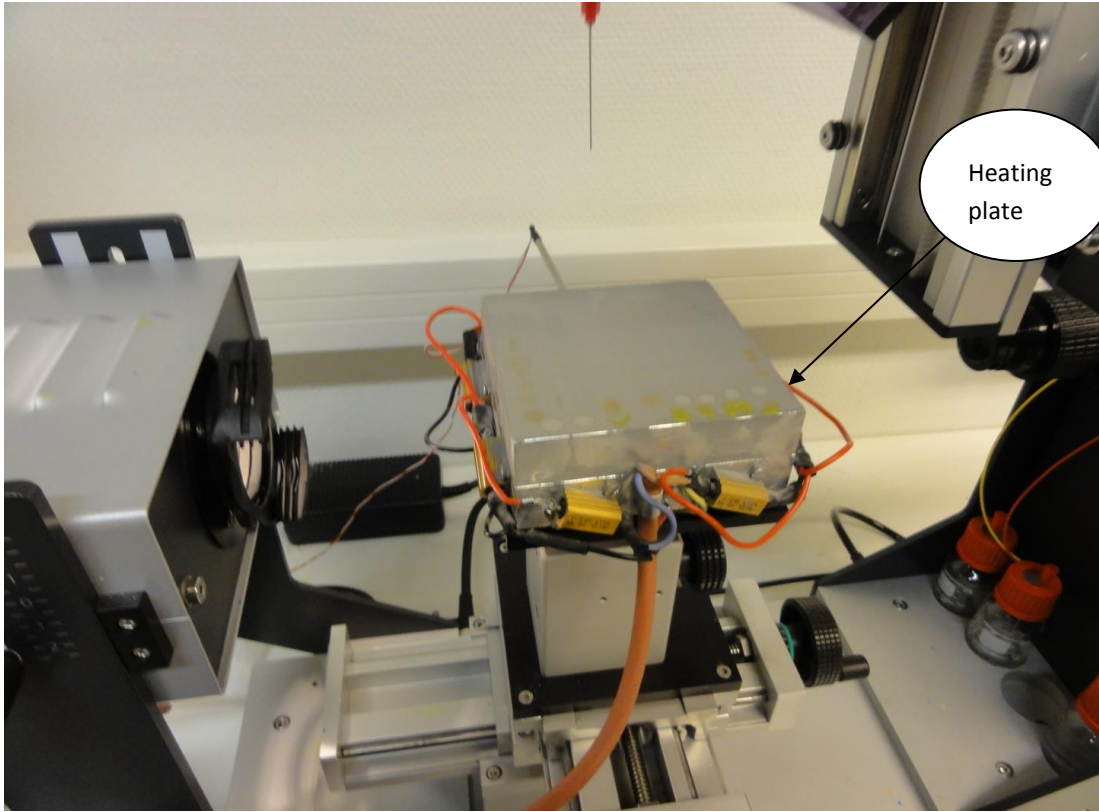
This method employs, using the equipment shown in Figures 20 and 21, drop shape analysis to record the interaction between the ink and powder bed. The sessile drop technique which is most popular in industry [24] determines the wettability by using software to measure the contact angle through the Young's equation based on the surface energies of the powder, ink and the interface between them. An electrically heated aluminium plate having a thickness of about 2 centimetres connected to a microcontroller is used an addition to study the effect of powder bed temperature on wettability. This is quite pertinent as the 3D printing machine is run at an elevated temperature of 80 degrees and the powders used are stored at an elevated temperature of 60 degrees. Different inks with different proportions of binders and surfactants are evaluated to assess the dependence of various factors on wettability. Inks are dropped onto the powder bed manually using a syringe and the process is observed using a microscope at a suitably high magnification. The powder bed baseline is set manually and the contact angle can be computed automatically using the software. The contact angle decreases continuously with time due to a slow penetration of the ink into the powder bed with a consequent decrease in volume.

The drying of the ink drop during measurement and the lack of moisture or environmental control is of concern as it limits the effectiveness of this technique. Surface roughness of the powder bed can cause penetration of the ink drop into the powder bed affecting accuracy of the contact angle measurements. Since a lot of the pre-requisite information such as baseline and tangent placement and the start of measurement are determined manually there is considerable room for error.

2.6 FORCE TENSIOMETRY/DU NOÜY RING METHOD

Used to measure surface tension it consists of a platinum ring which is positioned close to the ink interface and sunk into it. The ring is then gradually withdrawn from the liquid while continuously measuring the force exerted on the ring using a torsion meter till the liquid film formed tears off completely. The surface tension indicated is determined from the diameter of the ring and the force required for tearing through the film. The depth of immersion and the final height to which it rises is irrelevant. Since the accuracy is quite sensitive to surface contamination of the ring, it is heated to red hot condition before each measurement to burn off any contamination. This technique is more robust than goniometry for finding the surface tension. It employs a graduated scale (mJ/m^2).The measured value takes into account the radius of the ring, radius of the wire and the densities of the interface materials. The data so obtained is used in the Washburn test to determine the contact angle.

2.7 MERCURY POROSIMETRY

A porous powder bed composed of small discrete particles imparts many distinctive properties as compared to solid non-porous body such as different permeability and adsorptive capacity [34].This technique can be used to determine the porosity, pore size distribution and pore volume of a powder bed which have a direct effect on the permeability and adsorptive capacity of the powder bed. The technique uses samples where the volume of mercury extruded or intruded is monitored as a function of varying pressure. Mercury is used as it is a non-wetting fluid and inert for most materials. The Washburn equation is used to relate the applied pressure to the pore diameter using the contact angle and surface tension.

r=1530/P…………… …………………………………………………………….. [35](10)

Where r=pore radius (μm)

P=applied pressure (psi)

Both intrusion and extrusion curves for the intrusion of mercury into the pores during the increase in pressure and the extrusion of mercury from the pores during pressure reduction are generated. These curves rarely coincide due to hysteresis caused by trapped mercury which renders the sample subsequently unusable. Mercury porosimtery can identify a wider range of pores in comparison to gas porosimetry. This method had a disadvantage in that assumes that the pores are cylindrical. It also may measure the entrance to a pore rather than the actual size of the pore. Closed pores cannot be analysed.

2.8 WASHBURN CAPILLARY RISE METHOD

A useful technique to obtain a quantitative measurement of powder wettability is the Washburn capillary rise method. This test is based on the principle of the differential between the interfacial energies of the solid-gas and the solid –liquid interface and utilizes the porosity of the powder bed to quantify the rise of a liquid in a powder bed due to the phenomenon of capillary rise. The basic principle of this experiment is similar to the rise of a liquid in a capillary tube due to capillary pressure P_k which in turn depends on the interfacial tension of the liquid γ, capillary radius r and the contact angle θ between the liquid and the capillary [36].

$P_k=2γcosθ/r$... [36] (12)

Assuming laminar flow in the capillary tube and neglecting hydrostatic pressure and the effect of gravity we get the following expression

$dV/dt=(r2ΔPkπ)/(8μh)$ or...[36](13)

$hdh=(rγcosθdt)/4μ$..[36](14)

For the above equation at t=0, h=0 we obtain

$h^2=$ ($\bar{r}$ $\gamma cos\theta.t)/2\mu$.. [36](15)

In terms of liquid mass the above equation can be expressed as

$m^2= (c\rho^2\gamma cos\theta.t)/\mu$... [36](16)

The equation (15) and (16) are most commonly used to determine the contact angle. The constant $\bar{r}$ which is the average capillary radius of the powder bed and c in equation (16) can be obtained experimentally through the use of a completely wetting fluid such as n-hexane or n-heptane for which the contact angle is zero.

This experiment makes the following assumptions:

- The powder packing is reproducible
- The packed column of powder simulates a set of capillaries
- The effect of gravity and liquid can be neglected

The relationship between the contact angle and the mass increase is given by the following relationship

$Cos\theta= (m^2/t).\eta/ (\rho^2\sigma_{Liq}.C_{Solid})$…………………………………………………… [36](17)

Where m=total mass

   T=time

   ρ=density

   σ=surface tension of the liquid

   c=capillary constant which is determined by testing with a perfectly wetting liquid have a   contact angle 0 degrees (n-heptane).

The principle of this experiment is the capillary rise method which we can attempt to simulate. This simulation is used to obtain the capillary rise curve to understand the principle behind its functioning. No further determination of the capillary constant through the use of a non-wetting fluid is performed as it is beyond the scope of this project. The main challenge in this test is to maintain consistent powder bed packing

to obtain relevant and reproducible results. This is done by pouring all the powder in one go and tapping externally after filling the tube with an external tapping machine. Another area of concern is the change in powder packing during the rise of the liquid in the tube which affects the validity of the results [37].The diameter of the tube shown in Figure 23 used is about 1.4cms.The height of the tube is limited to about 9 centimetres so as remain within the limits of the maximum distance of 12 centimetres between the tube support and the base of the weighing scale. The tube is washed with distilled water and acetone and then dried at 150 degrees in a furnace. The base of the tube is fitted with an 11 µm filter as a support for the particles packed into the tube and to allow sufficient ink penetration into the capillary. The powder is packed into a cylindrical tube whose bottom is covered with an 11 µm filter and brought into contact with the ink which rises through the tube through capillary action. The mass data with time is monitored by suspending the tube over an electronic balance shown in Figure 23 and 24.

The graph shown in Figure 22 is then plotted based on the data and the rate of liquid rise is used to determine the contact angle.

$$\cos \theta = \frac{m^2}{t} \frac{\eta}{\rho^2 \, \sigma_L \, c}$$

η = Viskosität der Flüssigkeit (mPa s)
ρ = Dichte der Flüssigkeit (g/cm³)
σ = Oberflächenspannung der Flüssigkeit (mN/m)
θ = Kontaktwinkel (°)
c = Materialkonstante
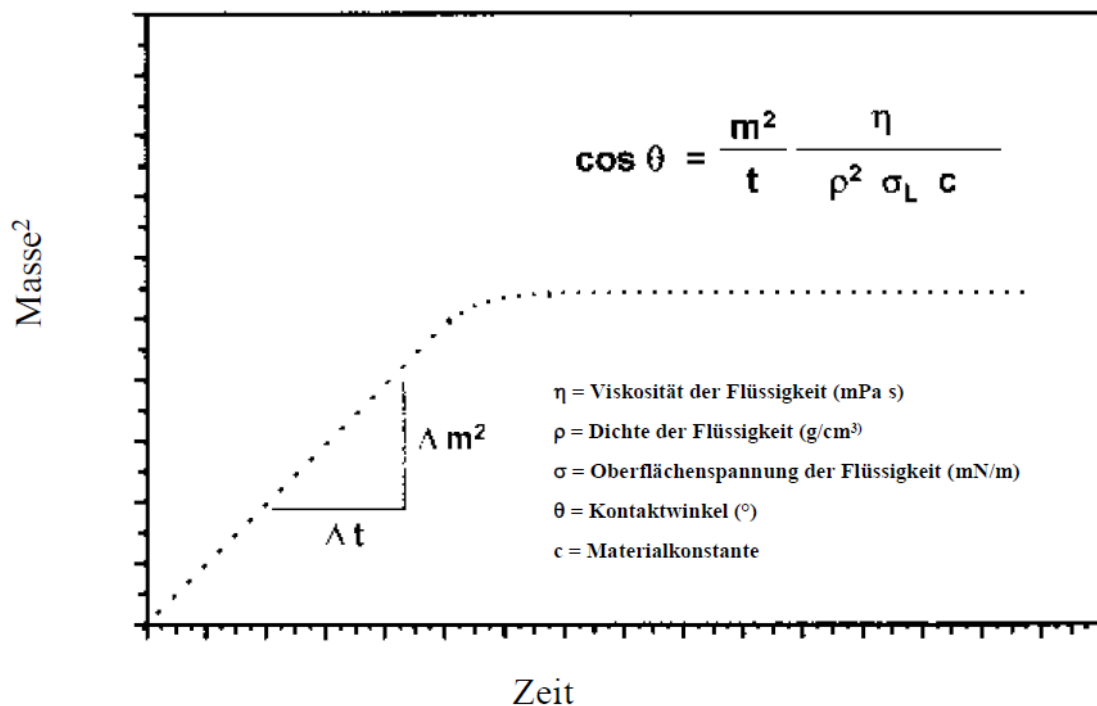
Figure 22: Washburn curve
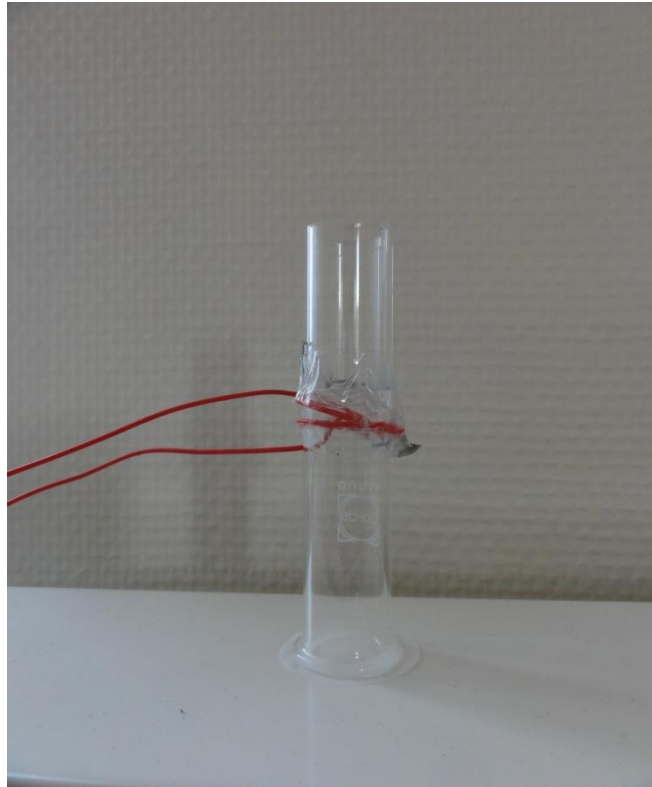
Figure 23:Tube for capillary rise experiment
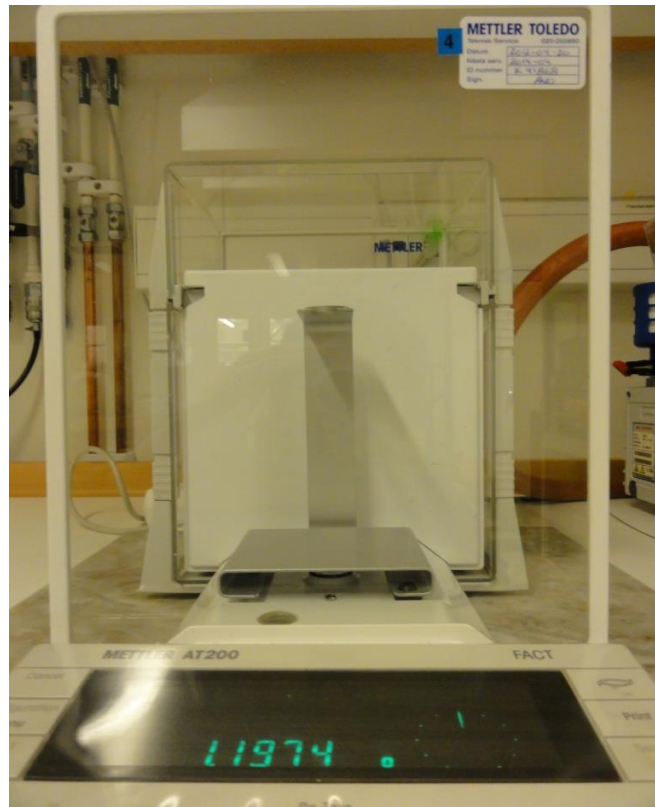
Figure 24: Archimedes weighing scale
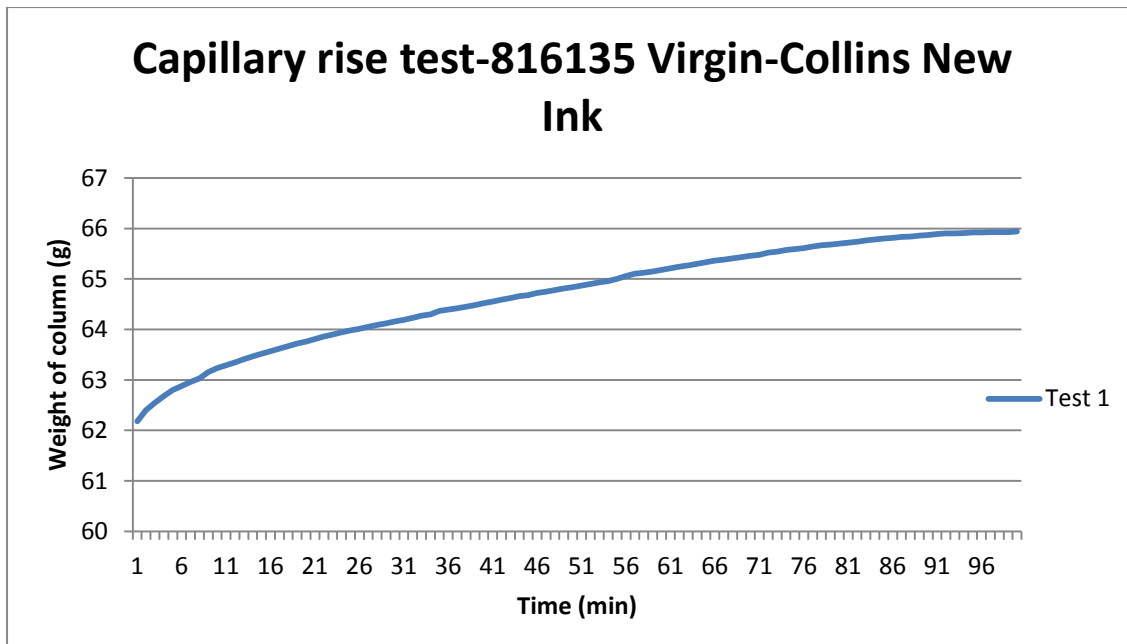
Figure 25: Capillary rise test-816135 Virgin Collins New Ink
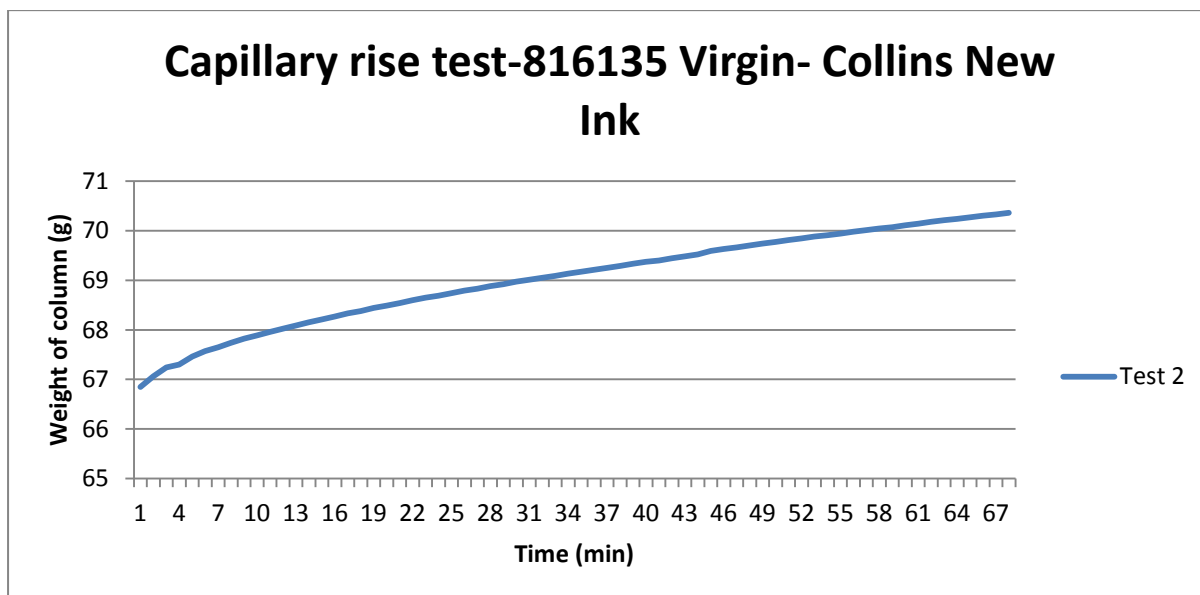
Figure 26: Capillary rise test 2-816135 Virgin Collins New Ink

In addition to the above manual technique an automated tensiometer shown below can used to overcome the difficulties of atmosphere and humidity control and produce more accurate reproducible results. In this technique liquids with known density, viscosity and surface tension should be used. Once the values for these are measured only the material constant needs to be obtained to determine the contact angle.

Table 5: Properties of test fluids

Liquid	Surface tension σ [mN/m]	Density ρ [g/cm³]	Viscosity η [mPa.s]
n-heptane	20.4	0.68	0.41
Collins Ink-New	26	1.03	3.1
Collins Ink-Old	25	1.03	2.9

Initially the capillary constants of the samples was determined using a non-polar test fluid having a contact angle zero and low surface tension (20.14 mN/m) at room temperature such as n-heptane or n-hexane. In the case of the powders to be examined n-heptane was used. The measurements were performed twice and the mean value was noted. Once the capillary constant is determined the contact angle can be determined during the experiment from the plot of m^2/t.

2.9 SCANNING ELECTRON MICROSCOPY

Figure 27: Scanning Electron Microscope

A high energy beam of focussed electrons is deployed to scan the surface to be examined using the apparatus shown in Figure 27. The reaction between the b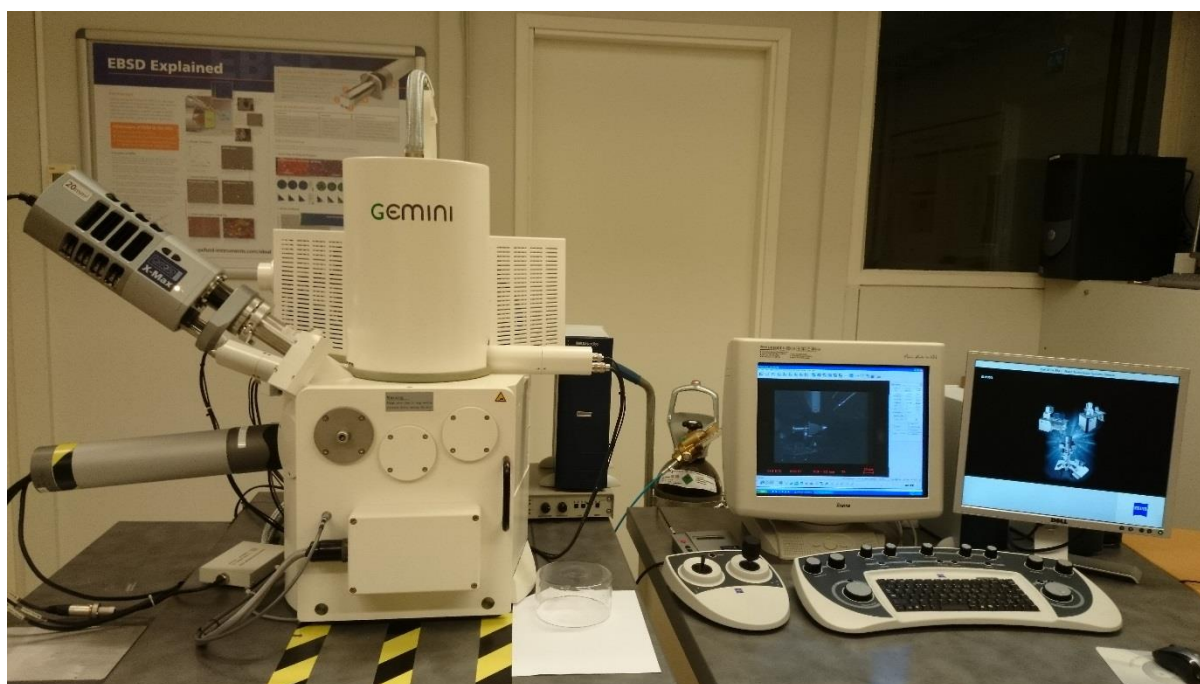eam and the electrons in the sample provides information about the surface morphology and chemistry of the powder. Image magnifications ranging from 100X to 60000X

with good depth of field. In SEM's sample preparation is crucial as it is necessary to ensure it is conductive before placing it in the vacuum chamber. This is done using colloidal graphite paint or double sided adhesive tape to avoid system contamination and consequent image degradation from loose powder. Elemental maps can be generated using the EDS unit attached to evaluate the spatial distribution of various elements. In addition the backscattered electrons can be used to identify different phases by differences in atomic number. Sample preparation is quite crucial in Scanning Electron Microscopy to avoid contamination of the sample chamber and to obtain images with good resolution. Generally the samples must be made conductive to prevent charging and be vacuum compatible. In the case of powder samples having a size larger than 100nm carbon paint, carbon tape or copper tape may be used.

2.10 GREEN STRENGTH

First samples are printed for testing in the 3D printing machine with different amounts of inks classified on a scale with a higher number indicating a larger amount of ink. Two inks having different amounts of binder Polyvinylpyrolidone (PVP) are tested to evaluate the effect of increasing binder content as well. The test used for evaluating green strength is the ASTM B312-09.In this test the force required to fracture an unsintered test specimen subject to an increasing three point transverse load is measured for samples printed with inks having two different binder contents (5% and 10%) and different amounts of ink to determine the relationship between the different variables and green strength.

3. RESULTS

3.1 X-RAY TURBIDIMETRY
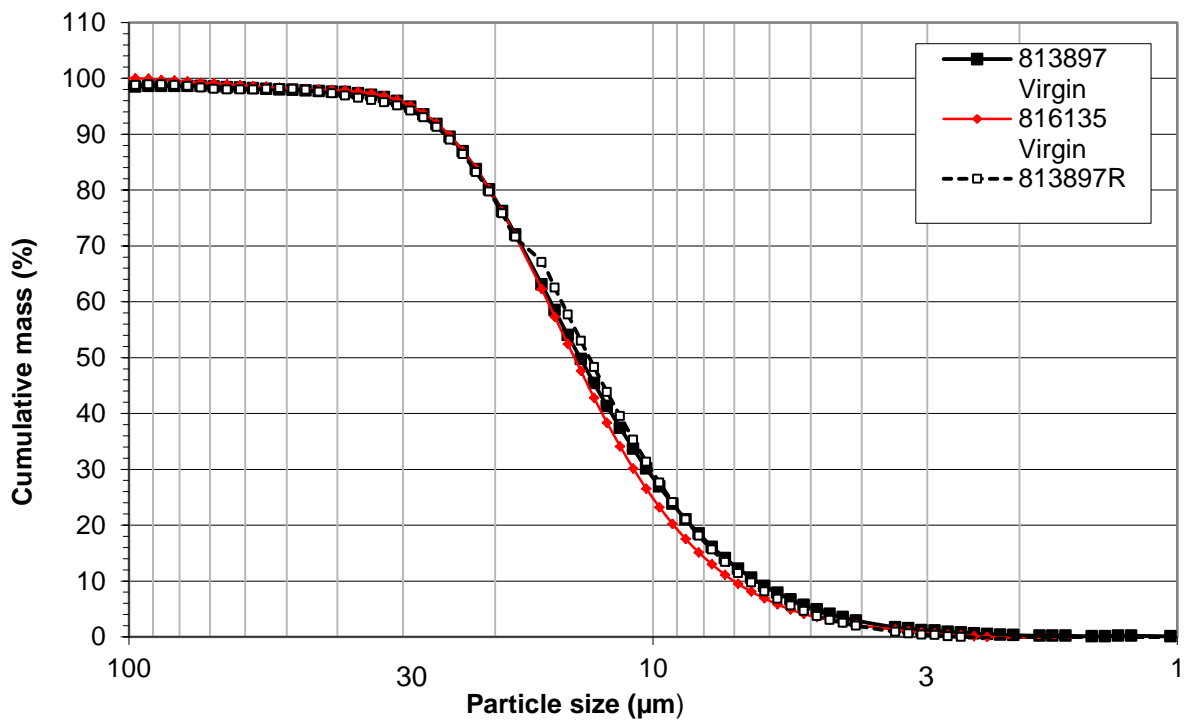
Figure 28: Particle size distribution

From Figure 28 of the particle size distribution we obtain from the X-Ray sedimentation technique the particle sizes as follows

Table 6: Particle size distribution of test powders

Percentile	813897 Virgin	813897 Recycled	816135 Virgin
d_{10}	6.49	6.49	6.87
d_{50}	13.72	13.72	14.53
d_{90}	24.40	25.85	24.40

The particle size distribution of the measured powders is similar within the likely margin of error.

3.2 SURFACE AREA/BET METHOD

Table 7: BET measurements for test powders

Powder	Density (g/cc)	Sample tube Empty (g)	Sample tube Tube+ Powder (g)	After degassing Tube+ Powder(g)	Sample weight Powder (g)	Sample Volume (cm^3)	Reference 2,53 Glass balls (g)	BET m^2/g	Particle size (µm)
813897 Virgin	8	14.6	49.1	49.1	34.5	4.3	10.9	0.088	13
813897 Recycled	8	14.5	53.5	53.5	39.0	4.9	12.3	0.09	13
816135 Virgin	8	14.2	51.0	51.0	36.8	4.6	11.6	0.099	14

As can be seen from the above test data the surface area of the 813897 Recycled powder is much greater than the virgin powder.

3.3 POWDER RHEOMETRY

3.3.1 BASIC FLOWABILITY ENERGY (BFE) TEST

Table 8: Basic flowability Energy measurements for test powders

Powder	Basic Flowability Energy (mJ)	Consolidated Bulk Density (g/ml)
813897 Virgin	470	4.6
813897 Recycled	490	4.6
816135 Virgin	448	4.7
816135 Recycled	636	4.5
Blend 1	474	4.5
Blend 2	522	4.4
Blend 3	440	4.7
Crushed powder	660	4.1

From the above data it can be seen that Bulk Flowability Energy (BFE) of both of the virgin powders-813897 and 816135 is lower than that for the recycled powders for a similar particle size distribution. The low bulk density of recycled 816135 powders indicates poor flow. The Bulk Flowability Energy (BFE) of Blend 1 is closest to that of the recycled 813897 Recycled powder. The consolidated bulk density of Blend 1 is

closest to that of 813897 Recycled powder. Since the particle size distribution of the virgin and recycled powders is similar we cannot make inferences from the proportion of fines.

3.3.2 SPECIFIC ENERGY TEST

Table 9: Specific energy measurements for test powders

Powder	Specific Energy (mJ/g)
813897 Virgin	2.6
813897 Recycled	2.6
816135 Virgin	2.2
816135 Recycled	2.9
Blend 1	2.6
Blend 2	2.8
Blend 3	1.9
Crushed powder	3.7

Also the specific energy values being higher for the 816135 Recycled powders indicate greater cohesiveness in comparison to the virgin powders. The specific energy of Blend 1 is closest to that of the 813897 recycled powder.
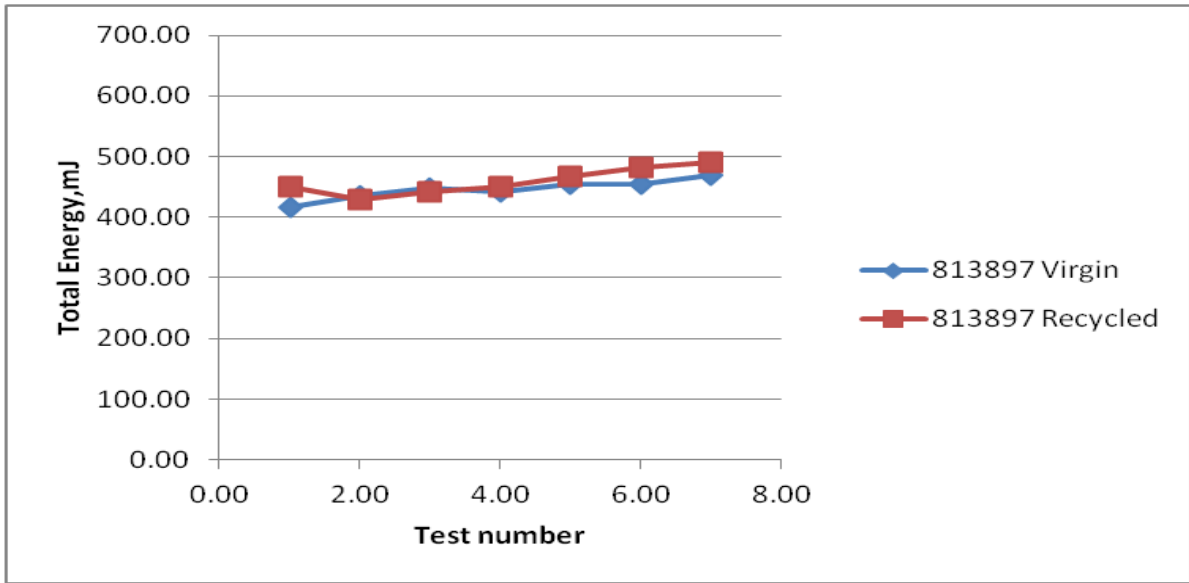
3.3.3 STABILITY INDEX (SI) TEST

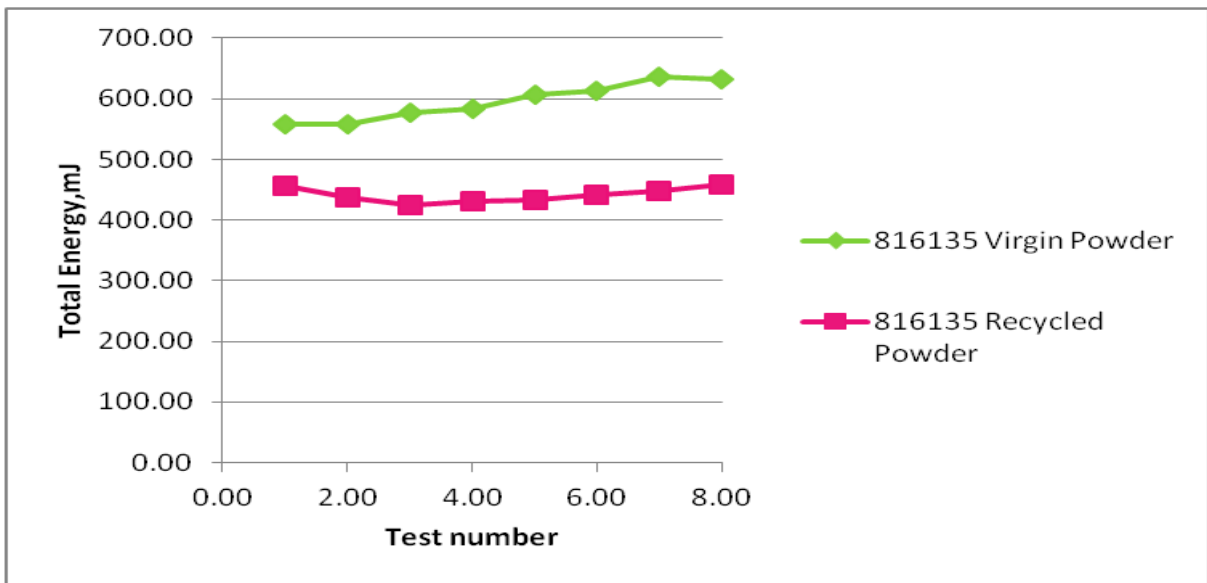**Figure 29: Stability test for 813897 powder**

Figure 30: Stability test for 816135 powder
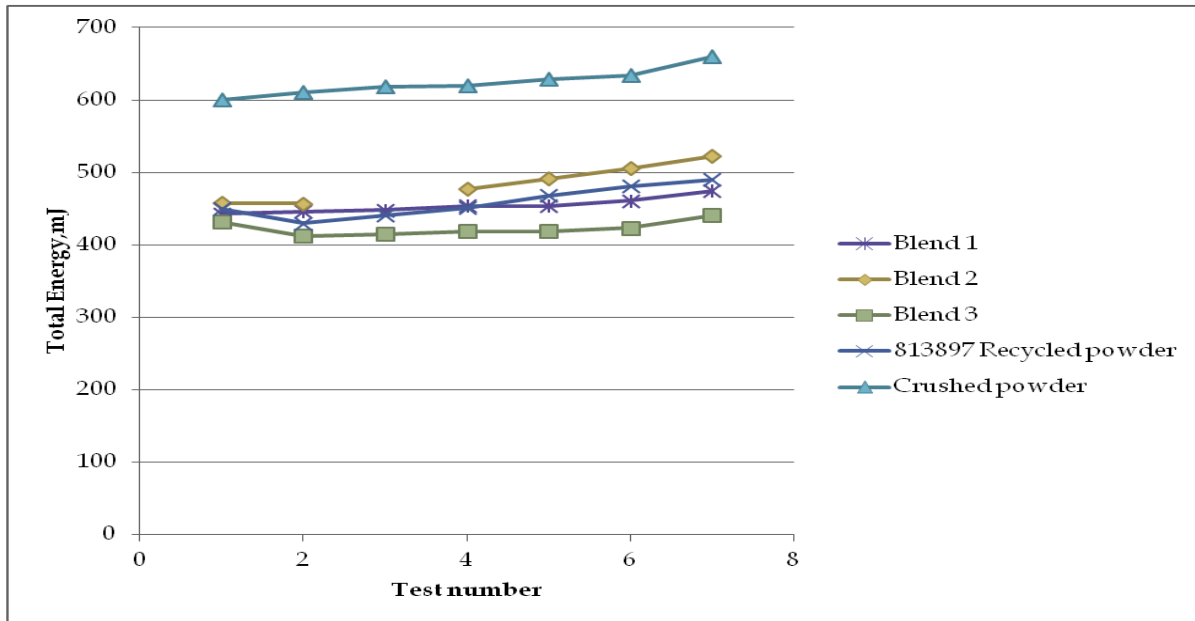
As can be seen in Figures 29, 30 and 31 the measured powders are quite stable and do not undergo any significant rheological changes during measurement due to caking and powder agglomeration. To examine this more closely it is important to examine another parameter the Stability Index. The values are typical for a stable powder.

Table 10: Stability Index measurements for test powders

Powder	Stability Index
813897 Virgin	1.1
813897 Recycled	1.1
816135 Virgin	1.0
816135 Recycled	1.1
Blend 1	1.1
Blend 2	1.1
Blend 3	1.0
Crushed powder	1.1

Table 11: Stability test measurements for 813897 powder

Test Number	Total Energy, mJ	
	813897 Virgin Powder	813897 Recycled powder
1.00	418	450

2.00	436	430
3.00	448	441
4.00	442	451
5.00	454	468
6.00	454	481
7.00	470	490

Table 12: Stability test measurements for 816135 powder

Test Number	Total Energy, mJ	
	816135 Virgin Powder	**816135 Recycled powder**
1.00	558	456
2.00	558	438
3.00	578	426
4.00	583	431
5.00	607	433
6.00	613	442
7.00	636	448

3.3.4 VARIABLE FLOW RATE TEST

Table 13: Flow Rate Index measurement for test powders

Powder	Flow rate index
813897 Virgin	1.6
813897 Recycled	1.6
816135 Virgin	1.5
816135 Recycled	1.4
Blend 1	1.5
Blend 2	1.6
Blend 3	1.5
Crushed powder	2.6

Since the Flow Rate Index is quite close to the range of 1.5 to 3 their flow rate sensitivity is normal. This can also be seen in the plots below of the energy for different blade tip speeds.
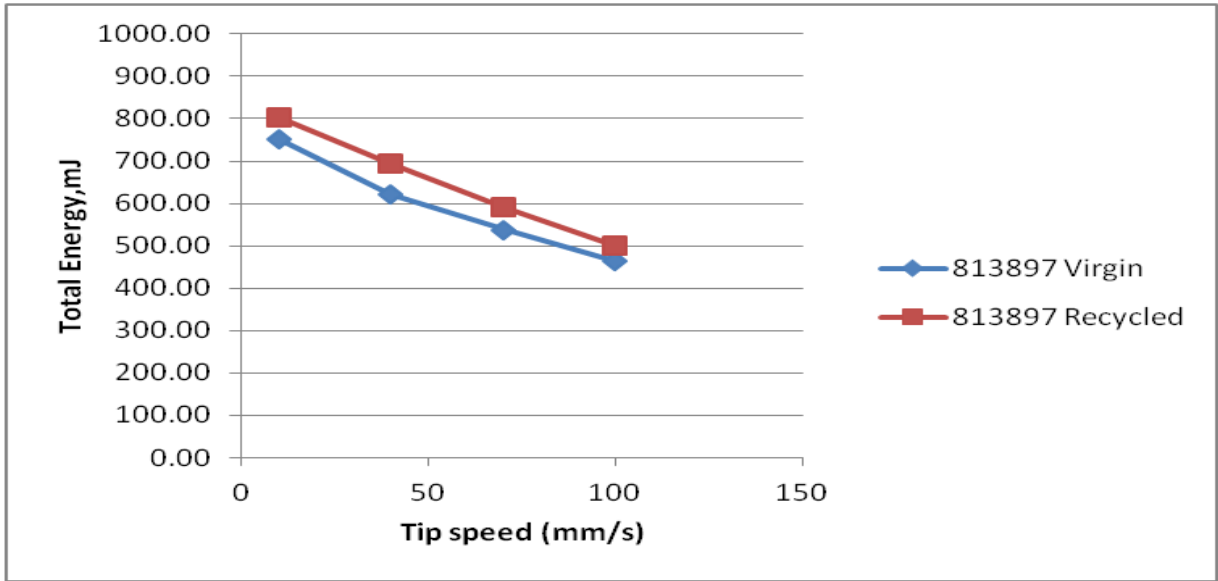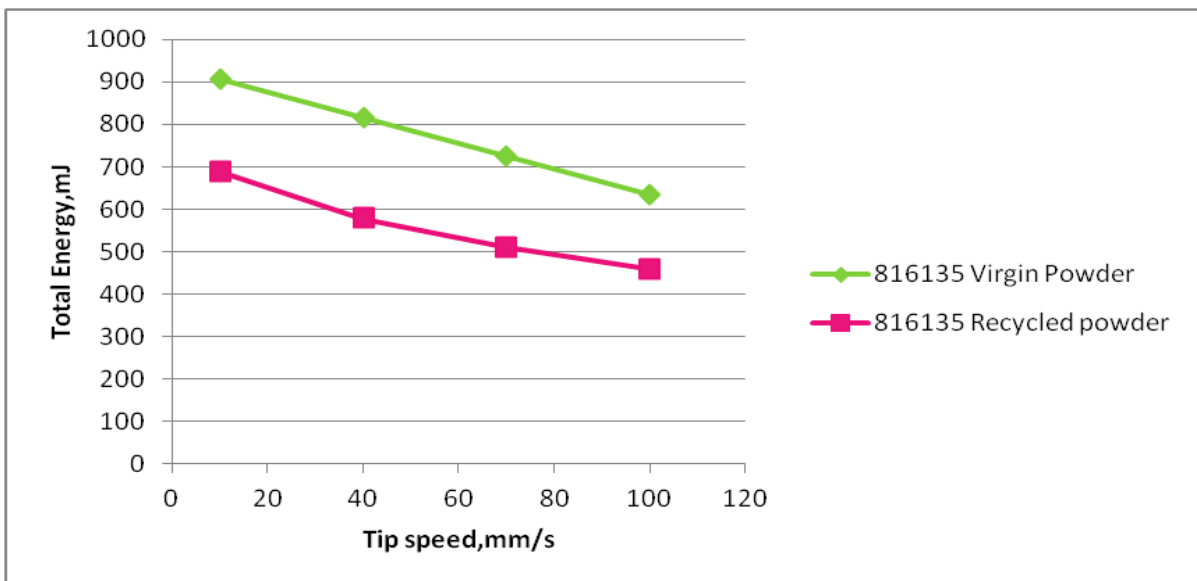
Figure 32: Variable flow rate test for 813897 powder

Table 14: Variable flow rate measurements for 813897 powders

Tip speed, mm/s	Total Energy,mJ	
	813897 Virgin Powder	813897 Recycled Powder
10	753	804
40	623	694
70	539	592
100	463	501

Figure 33: Variable flow rate test for 816135 powder

Tip speed, mm/s	Total Energy,mJ	
	816135 Virgin Powder	816135 Recycled Powder
10	906	690
40	816	578
70	725	511
100	633	459
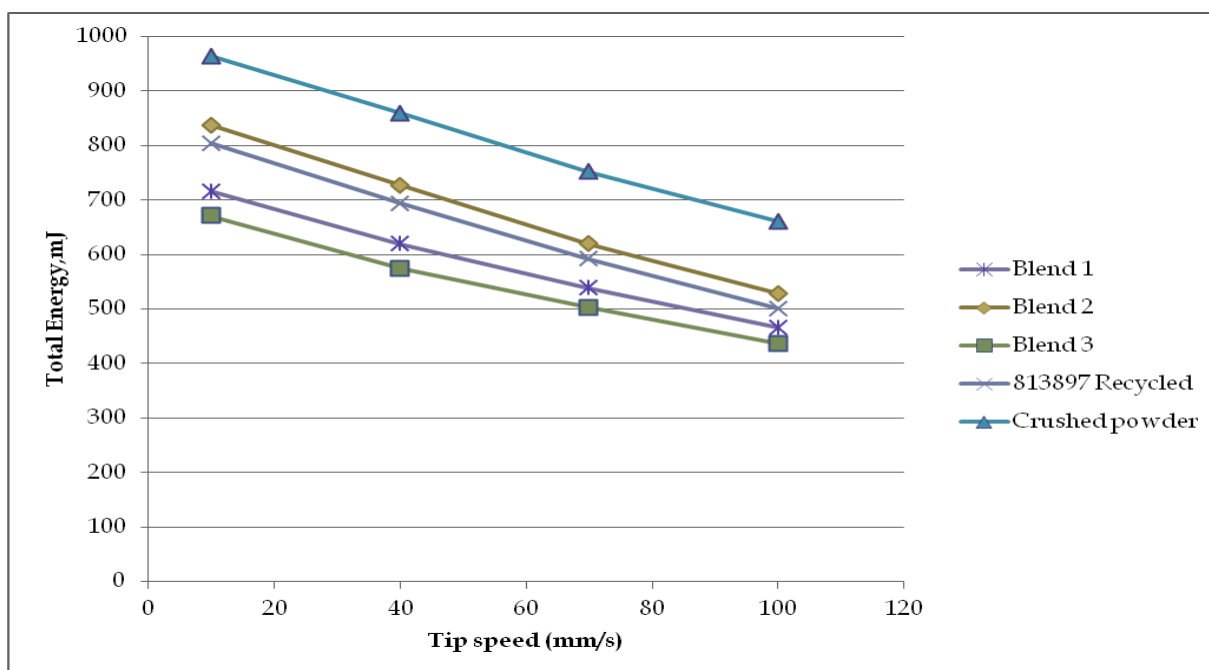
Figure 34: Variable flow rate test-powder blends

3.3.5 TAPPED CONSOLIDATION

As can be seen in the data below the 816135 Virgin and 813897 Recycled are more prone to consolidation on being subjected to vibration. For the powder blends the crushed and Blend 2 seem to be closer than the others to the 813897 recycled powders

Table 16: Total Energy values for test powders

Powder	Total Energy, mJ
813897 Virgin	1039
813897 Recycled	1377
816135 Virgin	1107

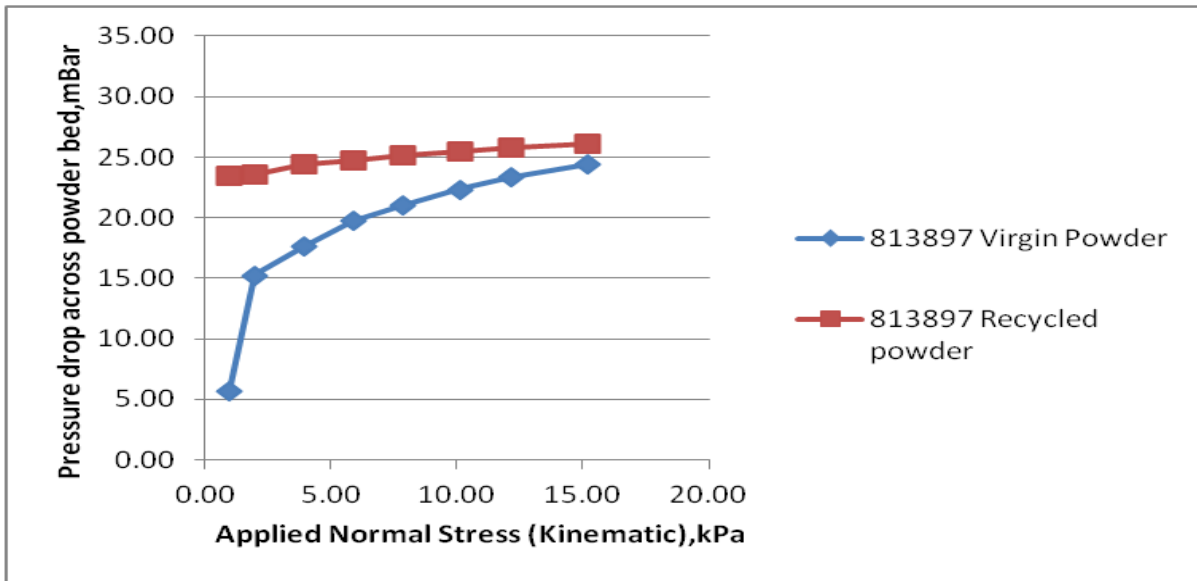| 816135 Recycled	987
Blend 1	1074
Blend 2	1190
Blend 3	1185
Crushed powder	1527

3.3.6 PERMEABILITY TEST
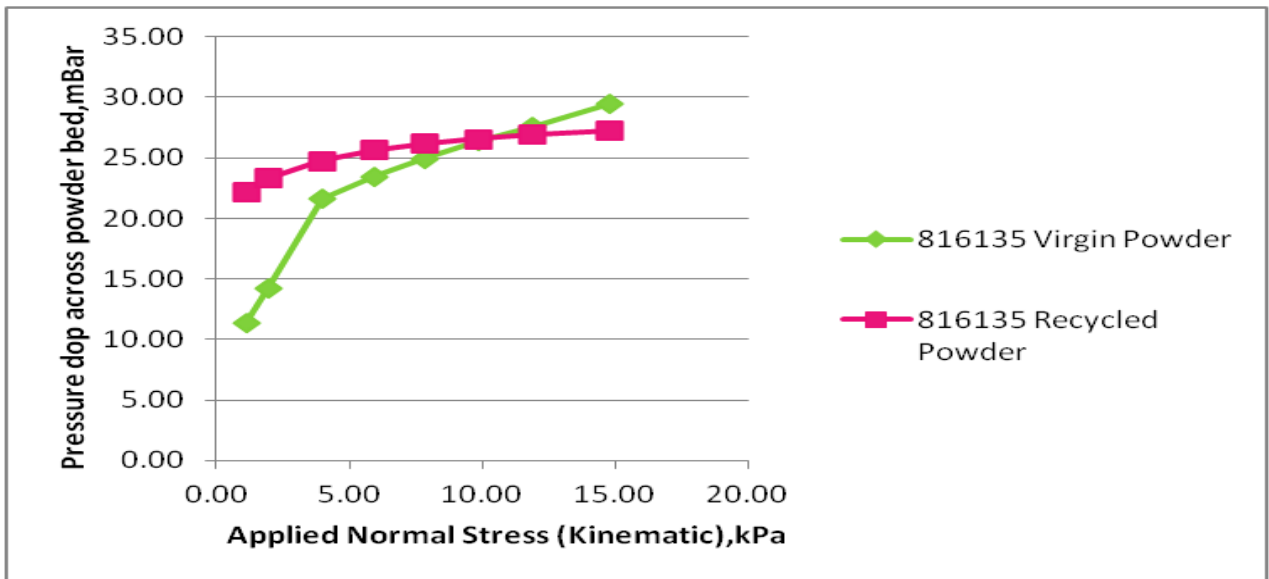

Figure 35: Permeability test 813897 powder

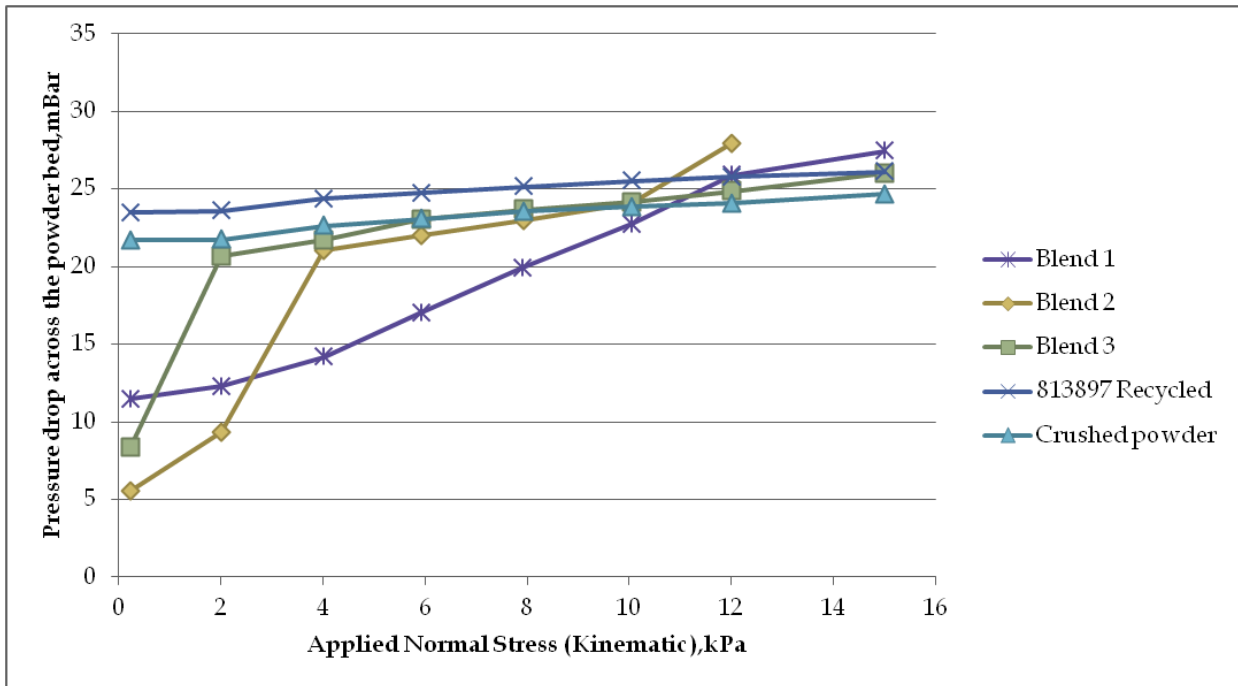Figure 36: Permeability test 816135 powder

51

Figure 37: Permeability test powder blends

Table 17: Permeability measurements for test powders

Powder	Pressure drop at 15kPa (mBar)	Consolidated Bulk Density (g/ml)
813897 Virgin	24.37	4.80
813897 Recycled	26.11	4.54
816135 Virgin	29.49	4.72
816135 Recycled	27.27	4.55
Blend 1	27.45	4.66
Blend 2	27.94	4.65
Blend 3	26.02	5.10
Crushed powder	24.66	4.63

Table 8: Permeability measurements for test powders

As can be seen in Figure 35 and Figure 36 the recycled powders 813897 Recycled and 816135 Recycled have a lower degree of permeability at low normal applied stress and a smaller permeability change at increasing levels of compressive stress than the 813897 Virgin powder and the 816135 Virgin powder. The 813897 Virgin powder has a lower pressure drop and a higher bulk density. The 816135 Virgin powder has a higher pressure drop and a higher bulk density. For the powder blends Blend 3 seems to have a permeability that most closely resembles that of the 813897 Recycled powder.
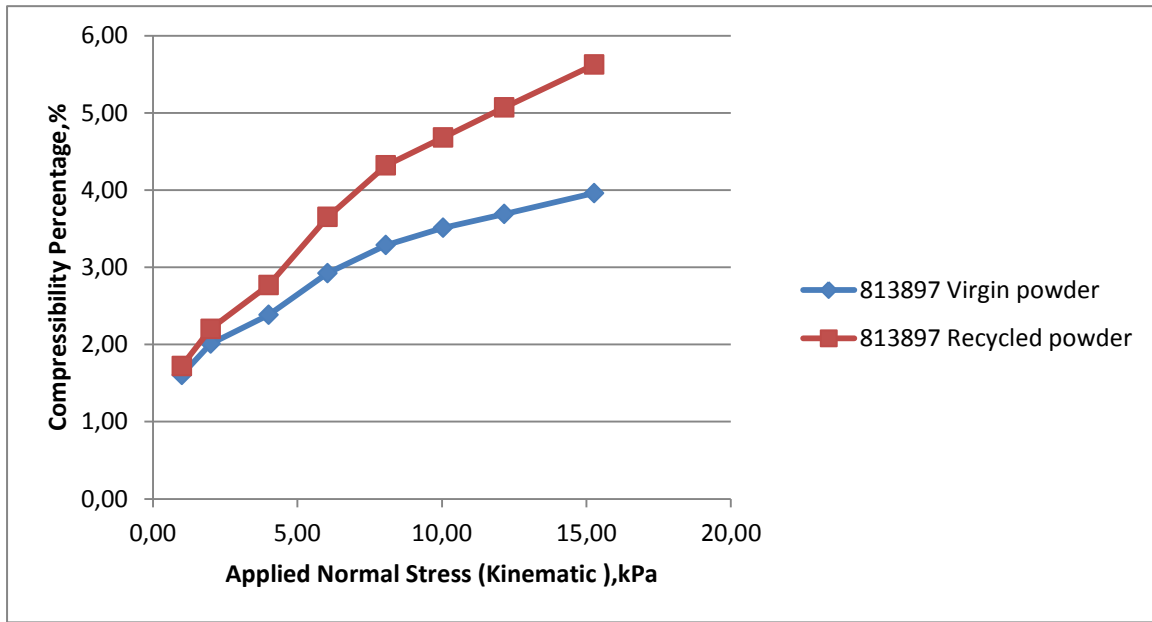
3.3.7 COMPRESSIBILITY TEST

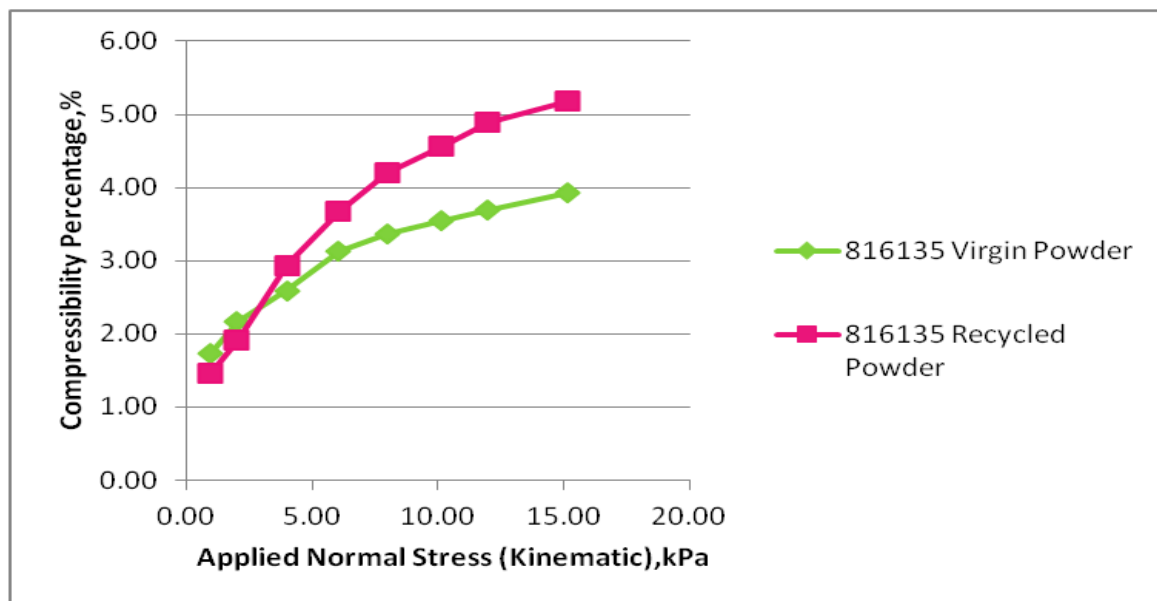**Figure 38: Compressibility test 813897 powder**

Figure 39: Compressibility test 816135 powder
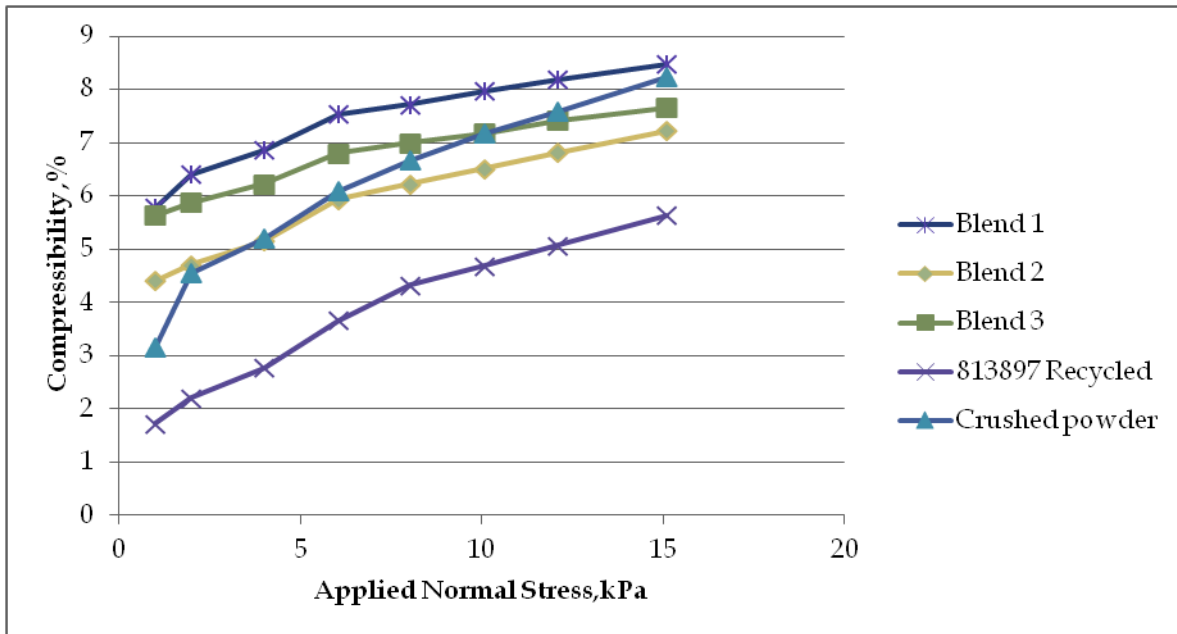
Figure 40: Compressibility test powder blends

Table 18: Compressibility test results for test powders

Powder	Conditioned Bulk Density (g/ml)
813897 Virgin	4.64
813897 Recycled	4.57
816135 Virgin	2.18
816135 Recycled	2.90
Blend 1	4.66
Blend 2	4.65
Blend 3	5.10
Crushed powder	4.63

The Conditioned Bulk Density values for the 813897 are higher than the 816135 powders. From the Figure 38 and Figure 39 of compressibility it can be seen that the recycled powders have a greater compressibility than the virgin powders. For the powder blends as seen in Figure 40, the Blend 3 has the most similar compressibility characteristics to 813897 Recycled powder. The conditioned bulk density on the other hand is quite close for Blend 1, Blend 2 and the crushed powder but Blend 3 has the highest conditioned bulk density.

3.3.8 AERATION TEST
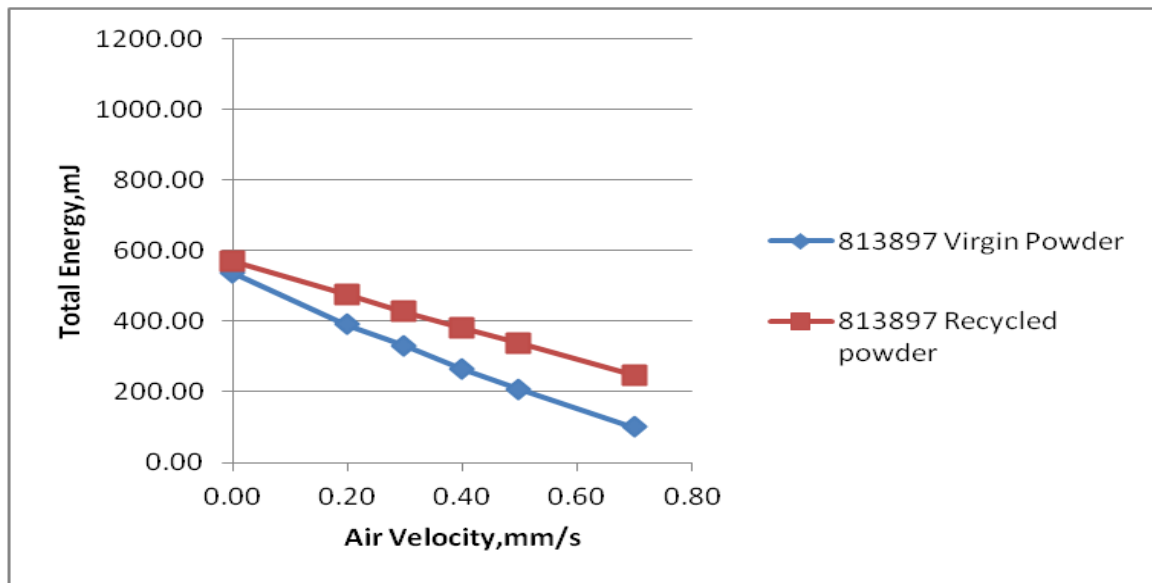
Figure 41: Aeration test 813897 powder
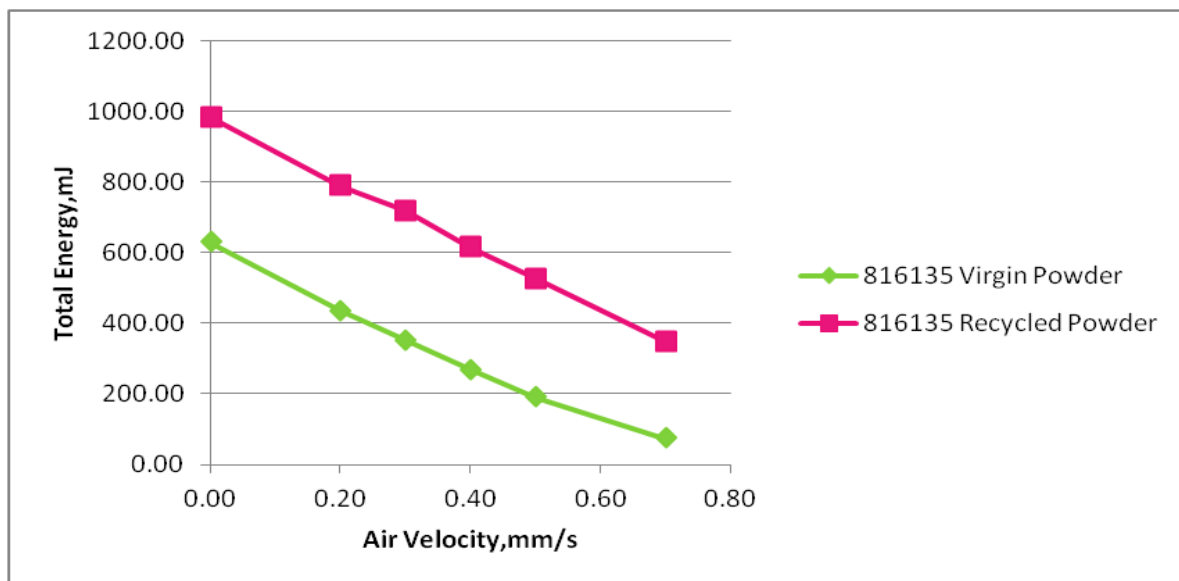
Figure 42: Aeration test 816135 powder
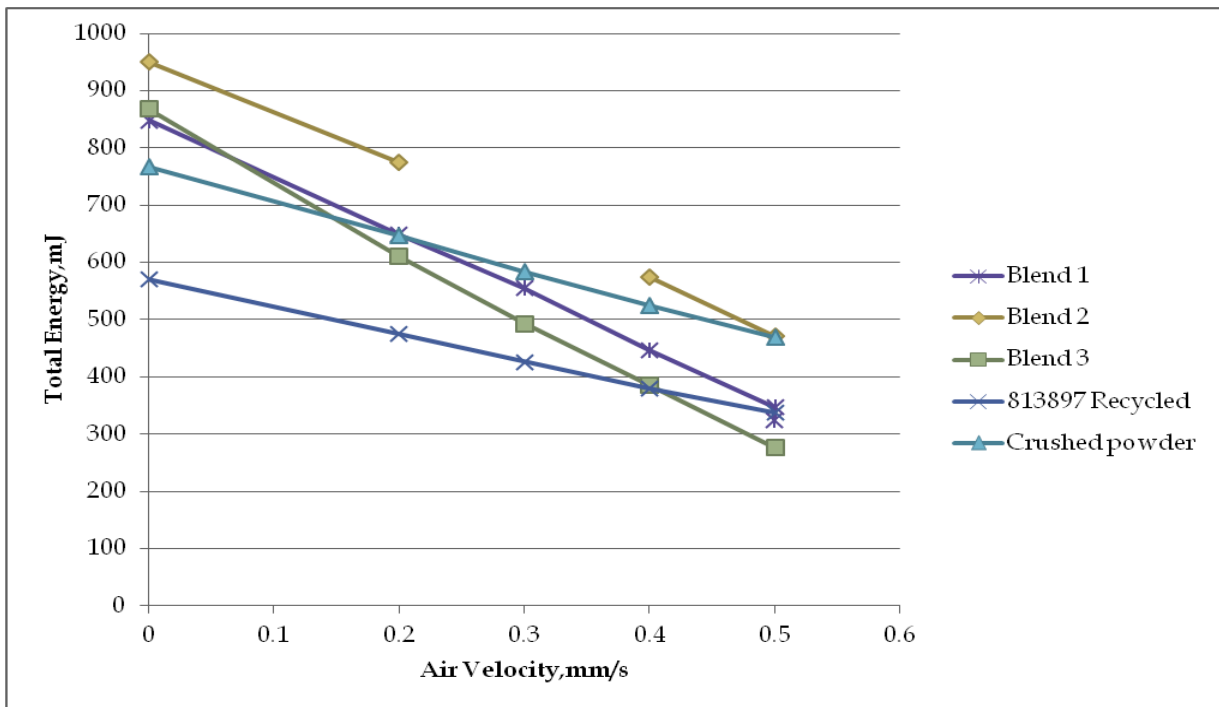
Figure 43: Aeration test-test powders

Table 19: Aeration ratios for test powders

Powder	Aeration ratio
813897 Virgin	5.37
813897 Recycled	2.33
816135 Virgin	8.54
816135 Recycled	2.83
Blend 1	2.61
Blend 2	2.05
Blend 3	3.15
Crushed powder	1.66

As can be seen in Figure 41 and Figure 42 the virgin powders were more easily aerated than the recycled powders. From Figure 43 we can see that among the powder blends, Blend 3 shows the best aeration response but Blend 1 and Blend 2 show a response closest to the 813897 Recycled.

3.3.9 SHEAR CELL TEST
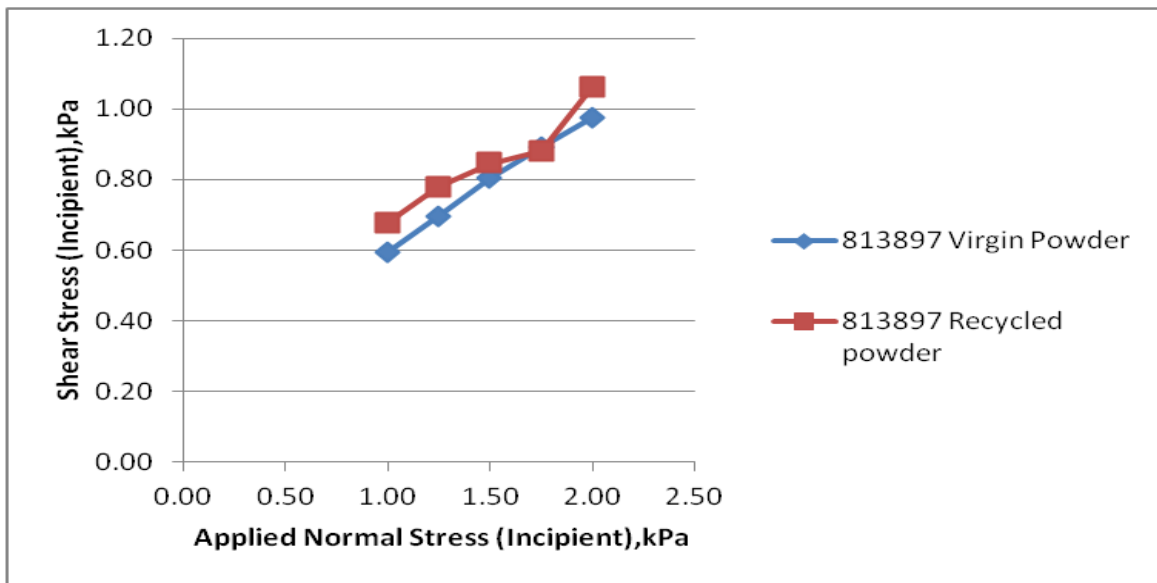
Figure 44: Shear cell test 816135 powder
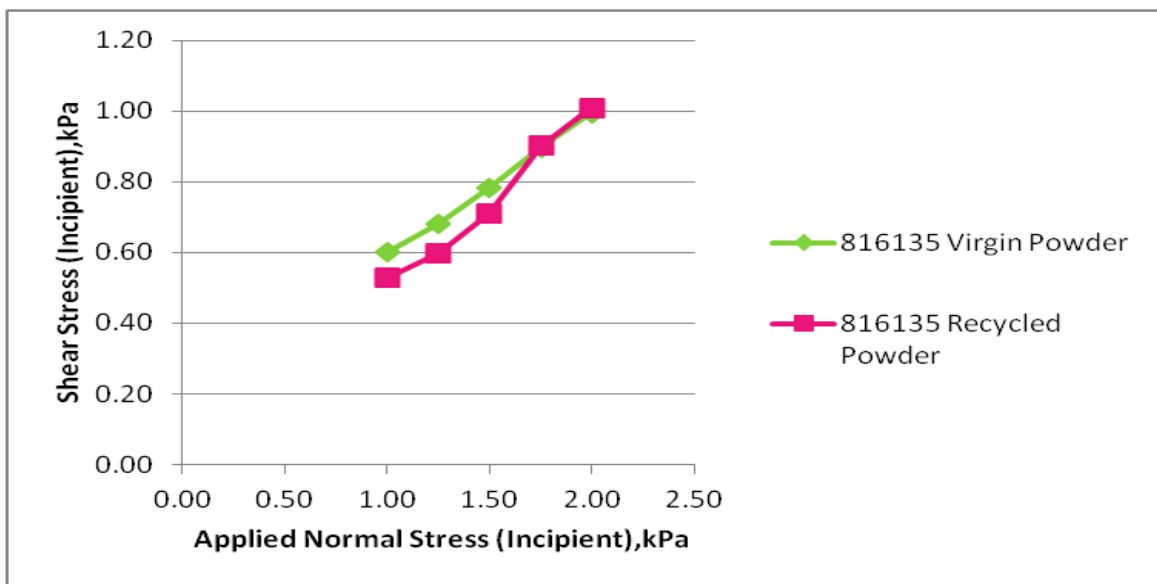
Figure 45: Shear cell test 816135 powder
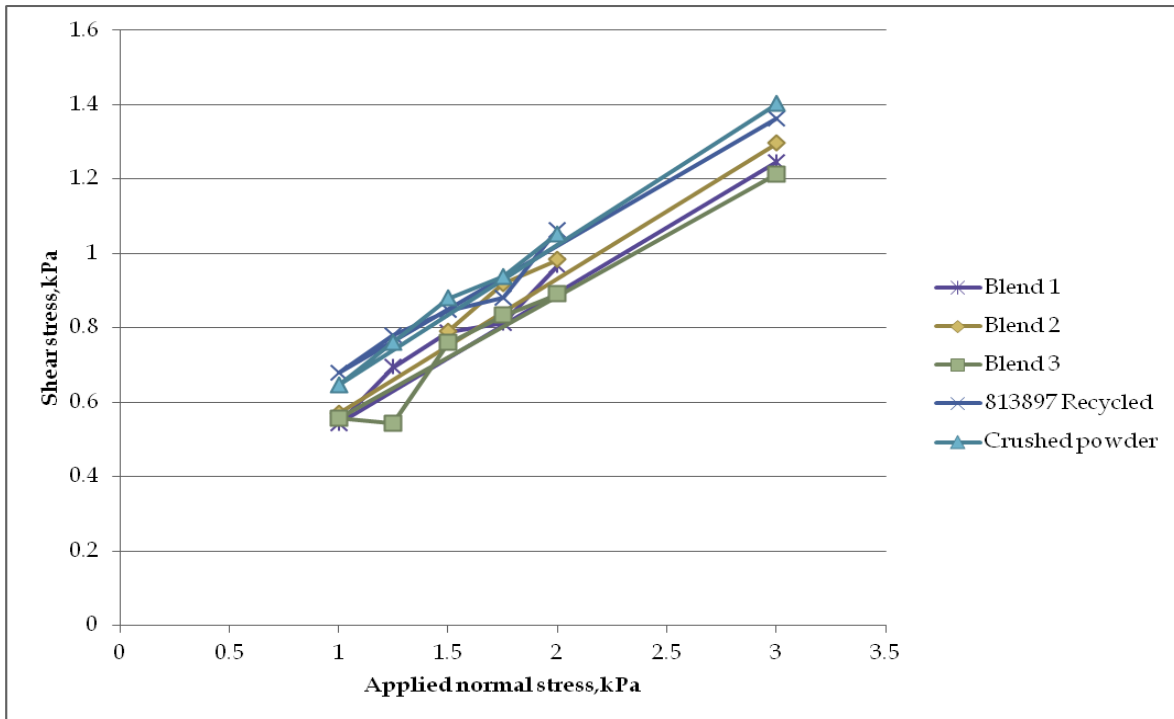
Figure 46: Shear cell test powder blends

Table 20: Shear test results for test powders

Powder	Cohesion	Unconfined Yield Strength,kPa	Flow function
813897 Virgin	0.22	0.63	6.62
813897 Recycled	0.31	0.88	5.18
816135 Virgin	0.19	0.56	7.57
816135 Recycled	0.02	0.08	15.30
Blend 1	0.23	0.65	6.71
Blend 2	0.11	0.35	12.01
Blend 3	0.21	0.60	7.46
Crushed powder	0.27	0.27	5.90

The cohesion between the particles of the 813897 powder is much greater than the 816135 powders. The crushed powder shows a degree of cohesion similar to 813897 powders. The yield stress which reflects the friction or cohesion between the powder particles is also much higher for the 813897 powders and highest for the recycled 813897 powder. The yield stress in the Blend 1 powder most closely resembles that of the 813897 Recycled powder. The flow function indicating powder fluidity shows better flow for the 816135 powders with the best flow for the recycled

816135 powder. The flow function for the crushed powder is closest to that of the 813897 recycled powders indicating a similar degree of powder fluidity.

3.3.10 WALL FRICTION
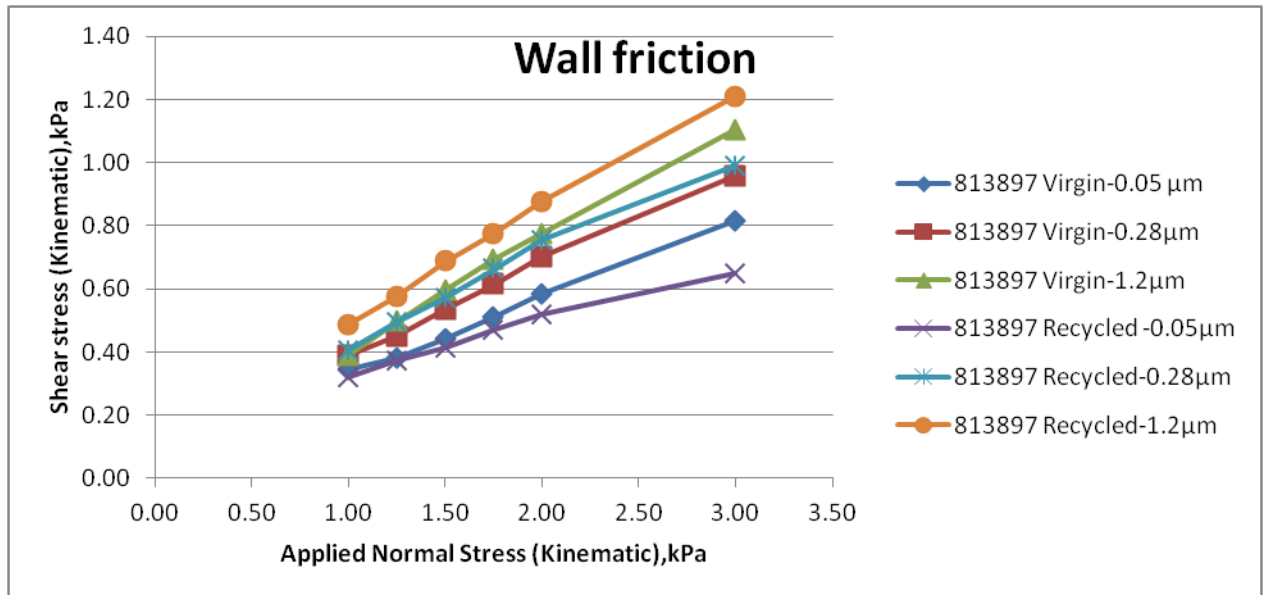
Figure 47: Wall friction test 813897 powder
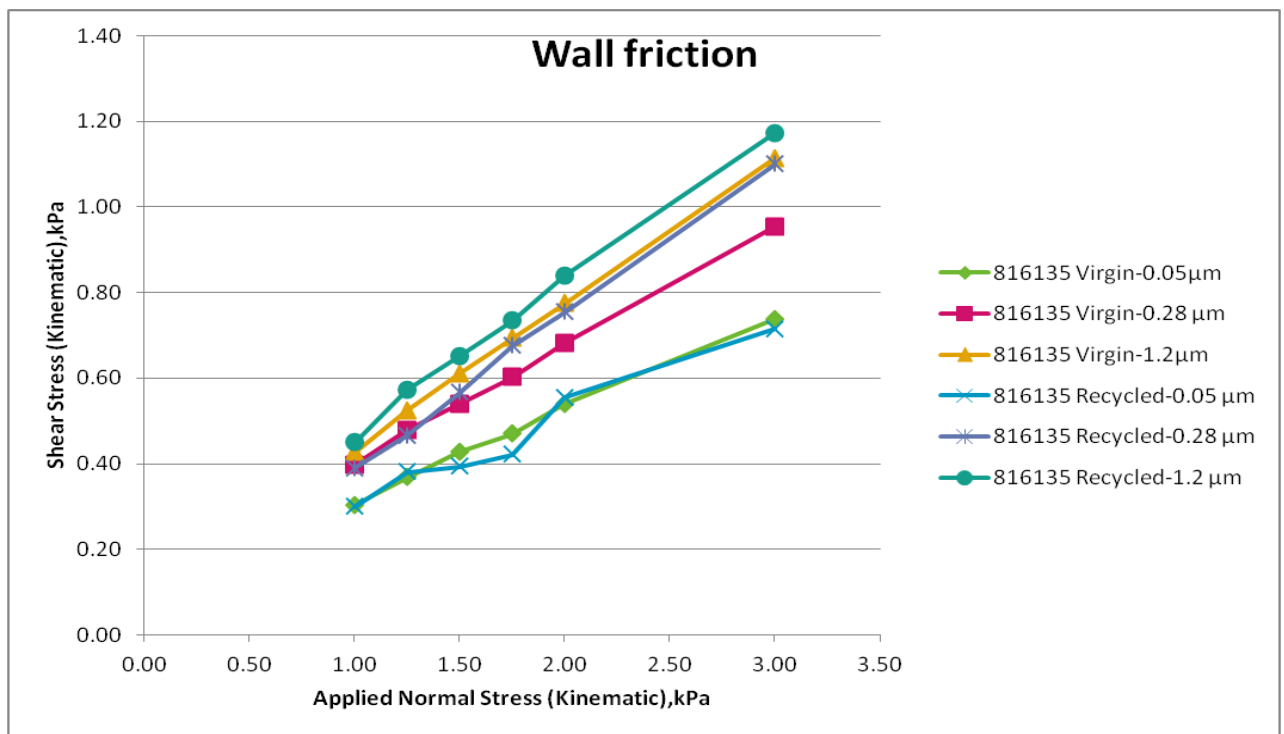
Figure 48: Wall friction test 816135 powder

Table 21: Wall friction test results for test powders

Powder	Surface roughness (μm)	Wall friction angle (°)
813897 Virgin	0.05	16.02
	0.28	18.82
	1.2	20.94
813897 Recycled	0.05	14.08
	0.28	19.84
	1.2	23.30
816135 Virgin	0.05	14.82
	0.28	18.74
	1.2	21.23
816135 Recycled	0.05	14.39
	0.28	20.49
	1.2	22.46
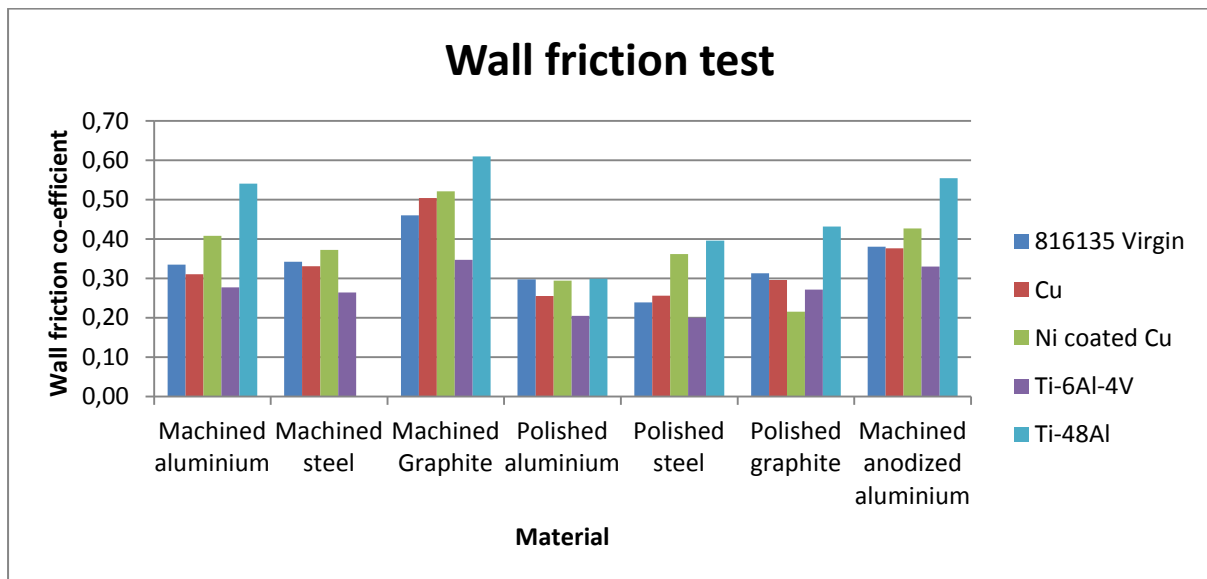
Figure 49: Friction co-efficient for different materials

As can be seen in the Figure 49 above the friction co-efficient does not change much between different powders and materials except of Ti-48Al powder.
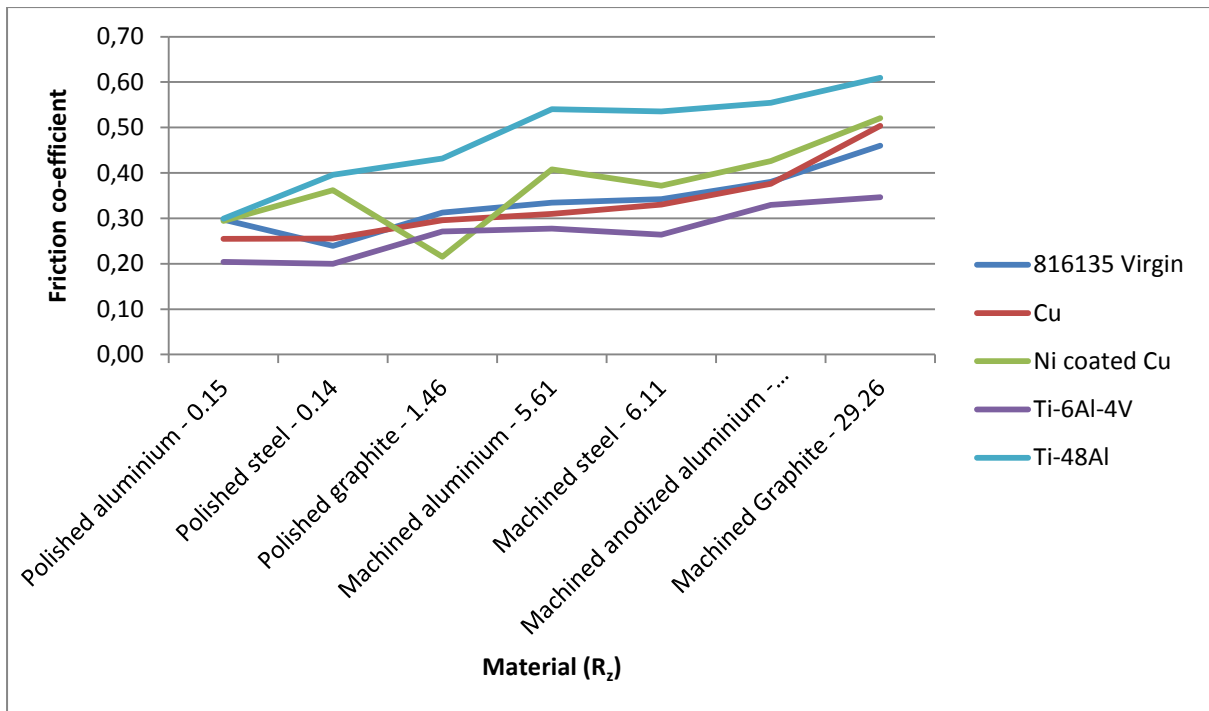
Figure 50: Friction co-efficient vs. Rz for different materials

Figure 51: Friction co-efficient vs Ra for different materials

Also the friction co-efficient is plotted against the surface roughness parameters R_a and R_z in Figure 50 and Figure 51 to evaluate the relationship between them.

3.4 CONTACT ANGLE GONIOMETRY

Table 22: Contact angle measurements in degrees for 816135 powder

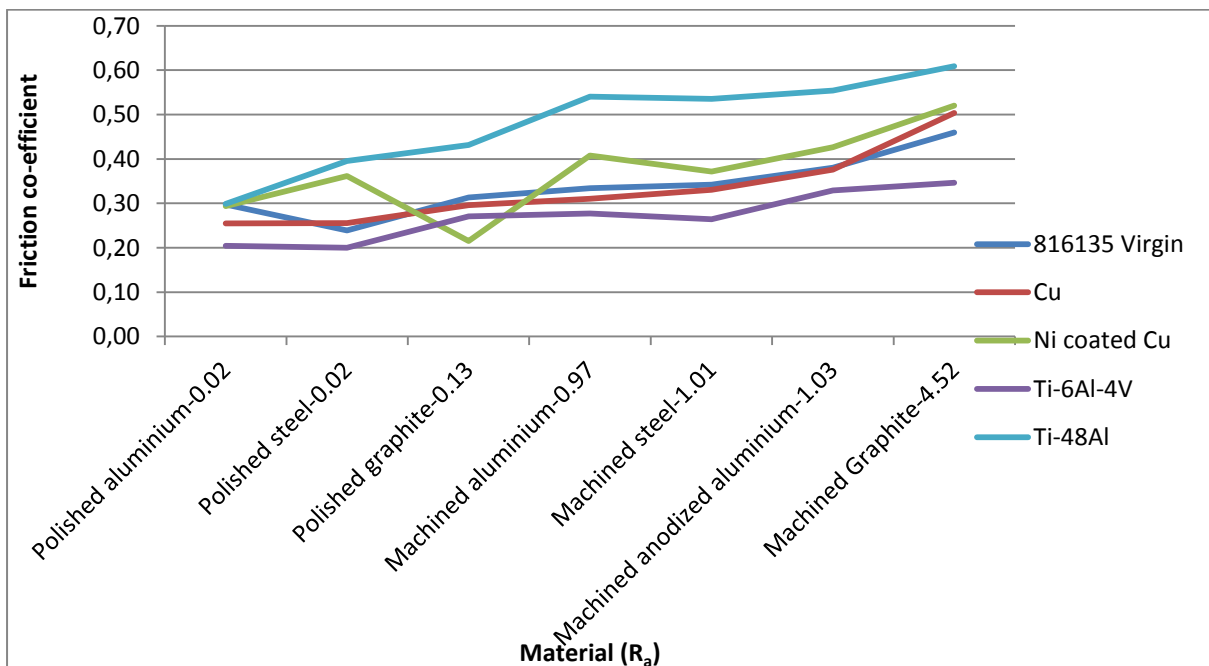| Ink	Virgin Powder-816135		Recycled powder-816135	
	Mean	Standard deviation	Mean	Standard deviation
New 15777-5	106	3	118	0
AQUARES Y	86	3	134	0
AQUARES HYVIS	86	2	120	1
INKIT 120926-3	77	2	121	2
130122-1	87	3	112	0
130121-1	117	1	117	1
HP	42	3	119	0

The wetting of the virgin 816135 powder is better than that for the recycled 816135 powder except for the 130121-1 ink. The experiment is also performed using a heated plate as shown in Table 23 indicating worse wetting at higher temperatures for most inks especially the Collins Blue ink.

Table 23: Contact angle measurements in degrees for different inks and 816135 powder

Temperature (°C)	Collins New-15777-5	AQUARES Y	AQUARES HYQUIS	INKIT 120926-3	130122-1	130121-1	HP
25	106	86	86	77	87	117	42
30	115	113	94	118	103	107	114
50	115	111	101	116	114	103	80
90	117	115	123	121	109	102	114

3.5 FORCE TENSIOMETRY/DU NOÜY RING METHOD

Table 24: Surface tension measurements using goniometry and Du Nuouy Ring technique

Ink	Goniometer (mJ/m^2)	Du Nuoy Ring technique (mJ/m^2)
New 15777-5	24	25
130122-1	28	27
130121-1	45	28
120926-3	36	25
HP	34	22

3.6 MERCURY POROSIMETRY

Differential Intrusion vs Diameter
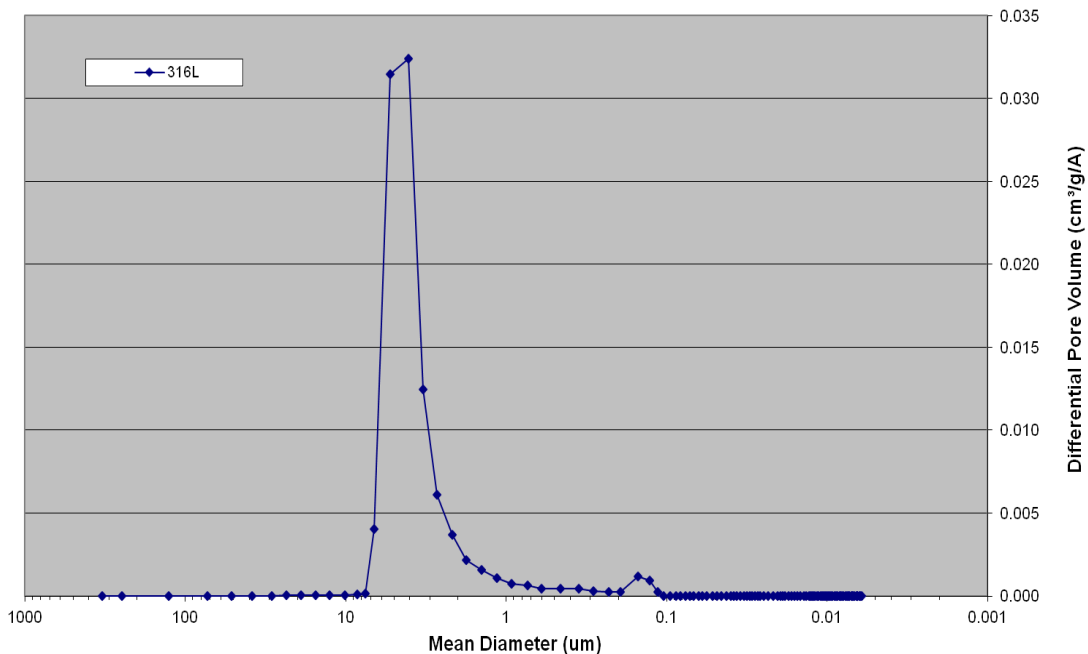
Figure 52: Mercury porosimtery intrusion curve

Cumulative Intrusion vs Diameter
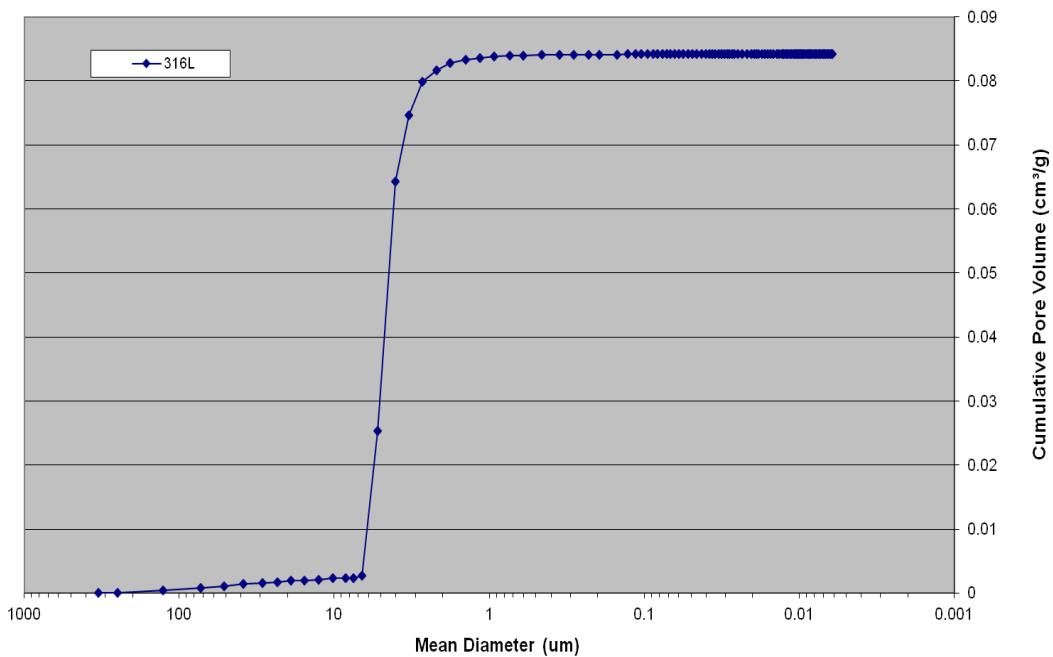
Figure 53: Cumulative mercury intrusion curve

As can been seen in Figure 51 and Figure 52 the average pore diameter in the pore bed is 3.7 μm. The percentage porosity is determined to be 40 %.The majority of the pore size lie in the range of 3-5 μm.

3.7 WASHBURN CAPILLARY RISE METHOD
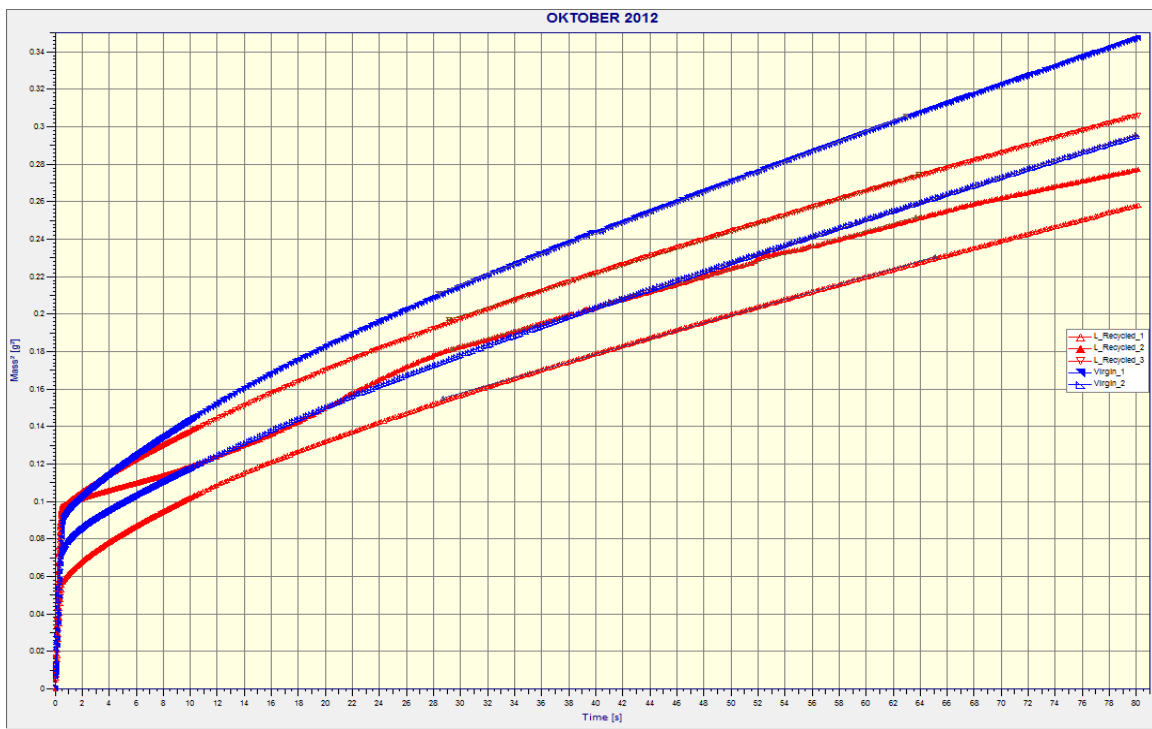
Figure 54: Capillary rise curve for 813897 Virgin and Recycled powder for Collins Old Ink

Figure 55: Capillary rise curve-813897 Virgin and Recycled powder for Collins Old ink
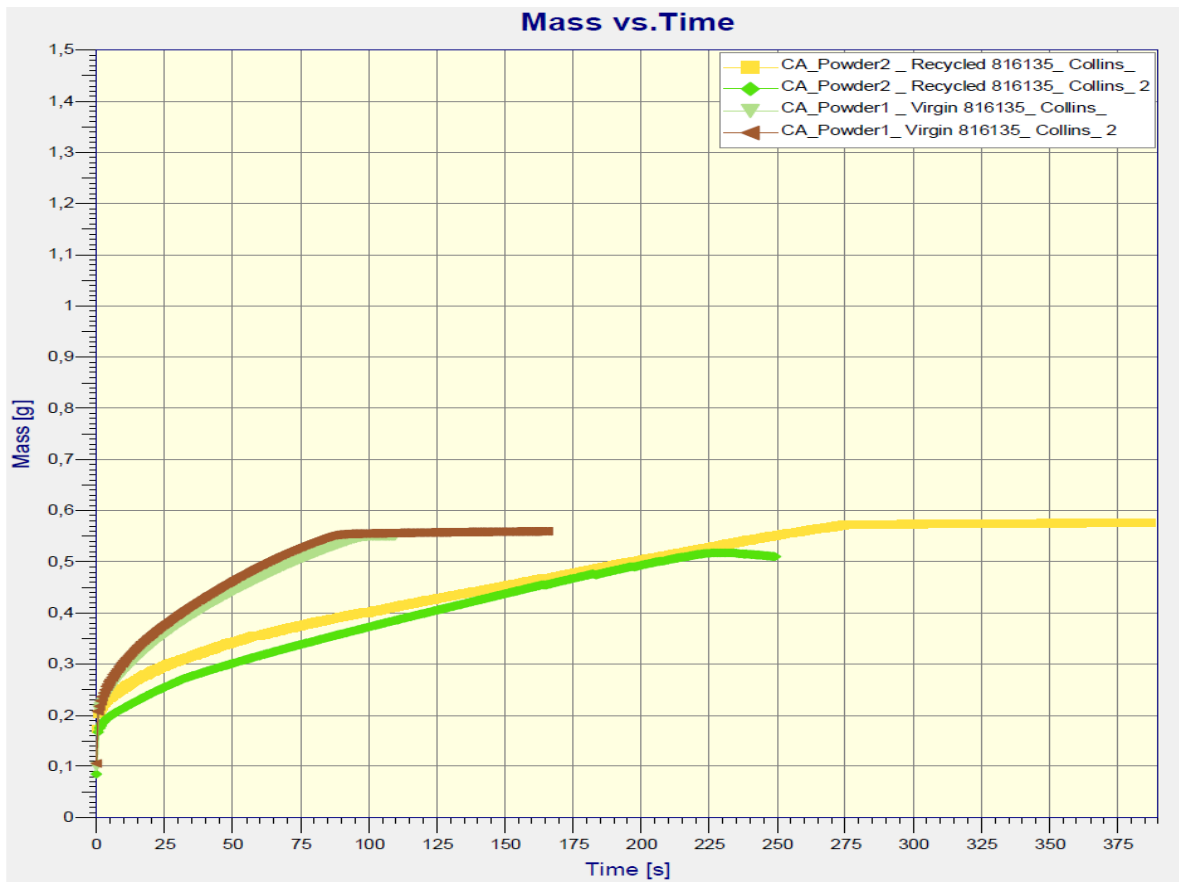
Table 25: Washburn technique measurements for test powders

Figure 56: Capillary rise curve for 816135 powder and Collins New Ink

Powder	Capillary constant c [cm^5]	Contact angle [^{o}]
813897 Virgin	3.5E-6	44.34
813897 Recycled	2.8E-6	34.43
816135 Virgin	5.59E-6	57.79
816135 Recycled	4.63E-6	75.11

In the case of the 813897 powders the virgin powder exhibits a larger capillary constant and a larger contact angle. In the case of the 816135 powder the virgin powder exhibits a larger capillary constant but smaller contact angle than the recycled powder.

3.8 SCANNING ELECTRON MICROSCOPY
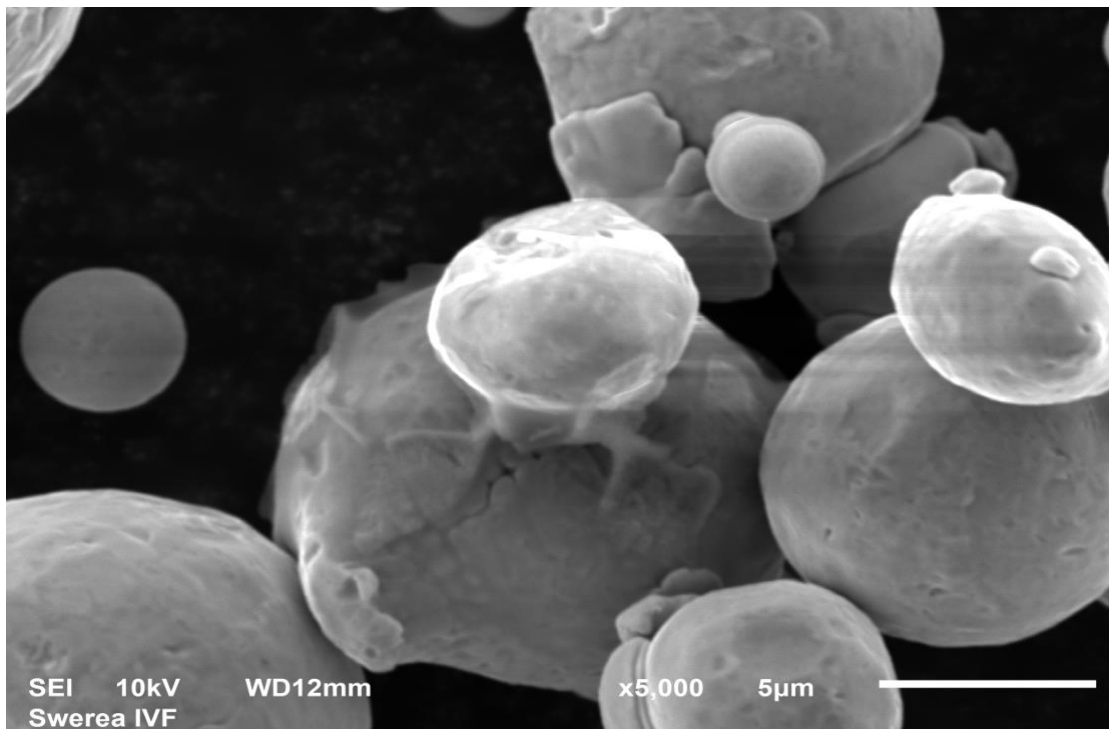
Figure 57: 816135 Recycled powder 5000X Secondary Electron Image showing surface topography
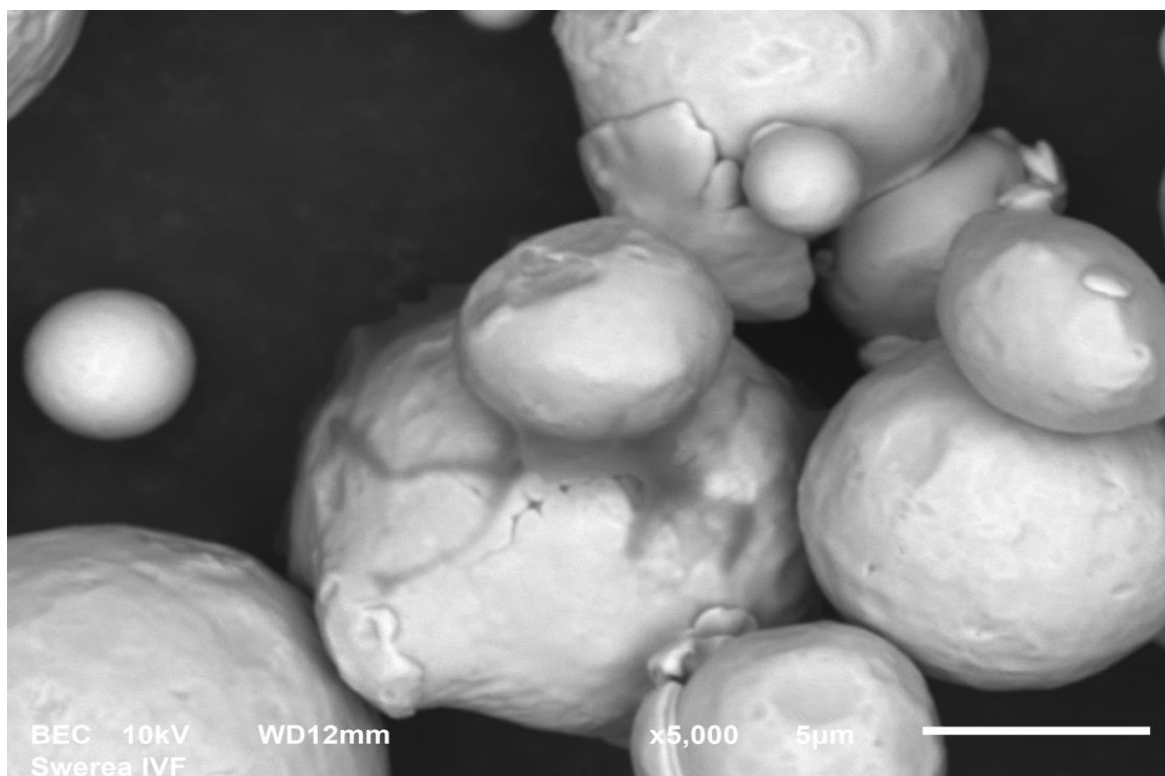
Figure 58: 816135 Recycled 5000X Backscattered Electron Image with carbon at contact point (dark region)
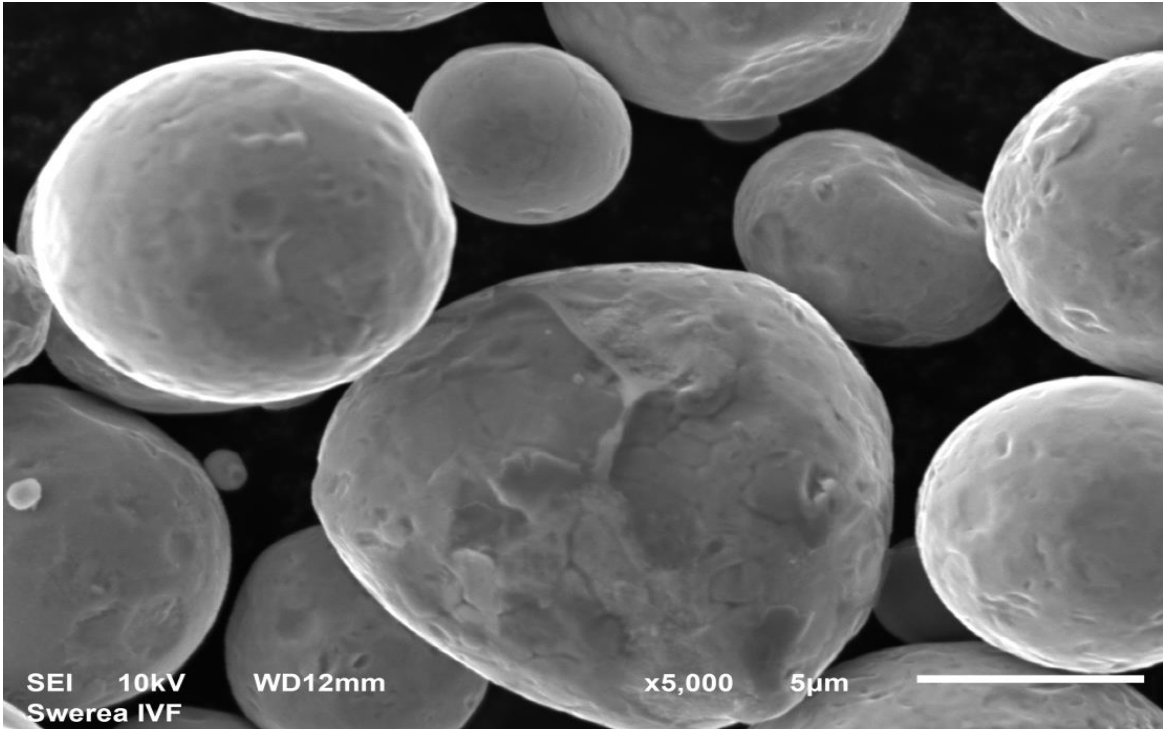
Figure 59: 816135 Recycled powder 5000X Scanning Electron Image showing surface topography
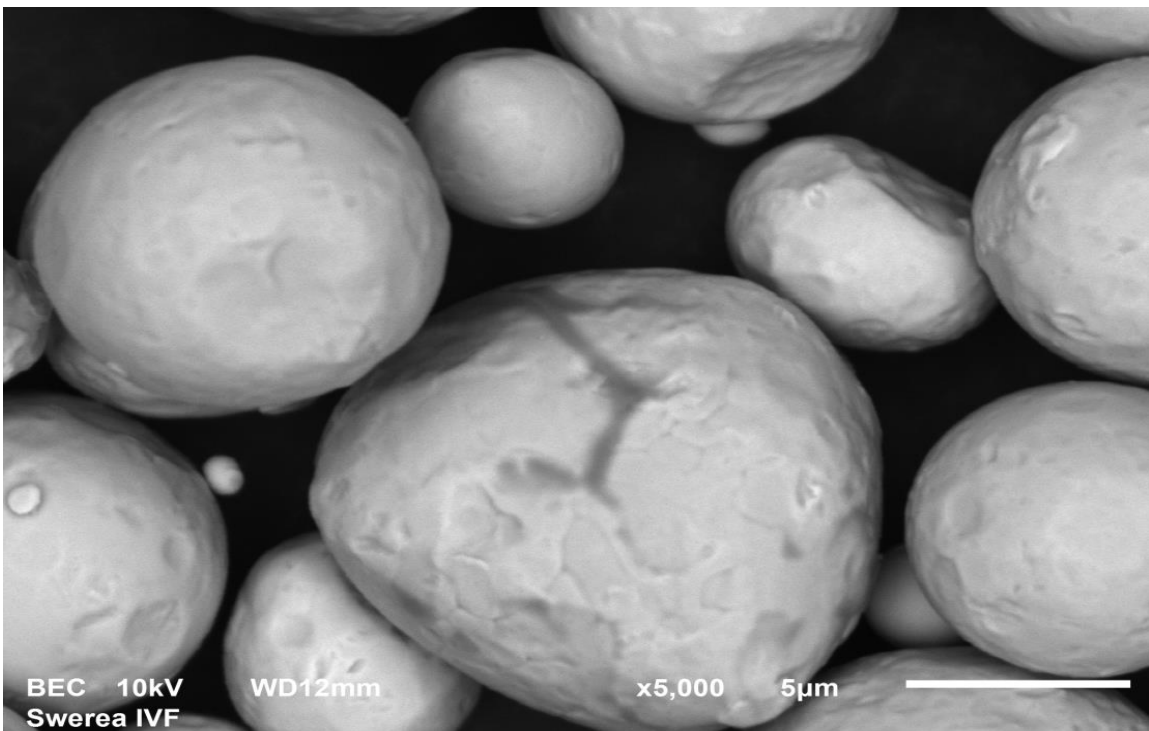
Figure 60: 816135 Recycled powder 5000X Backscattered Electron Image showing carbon at surface (dark region)
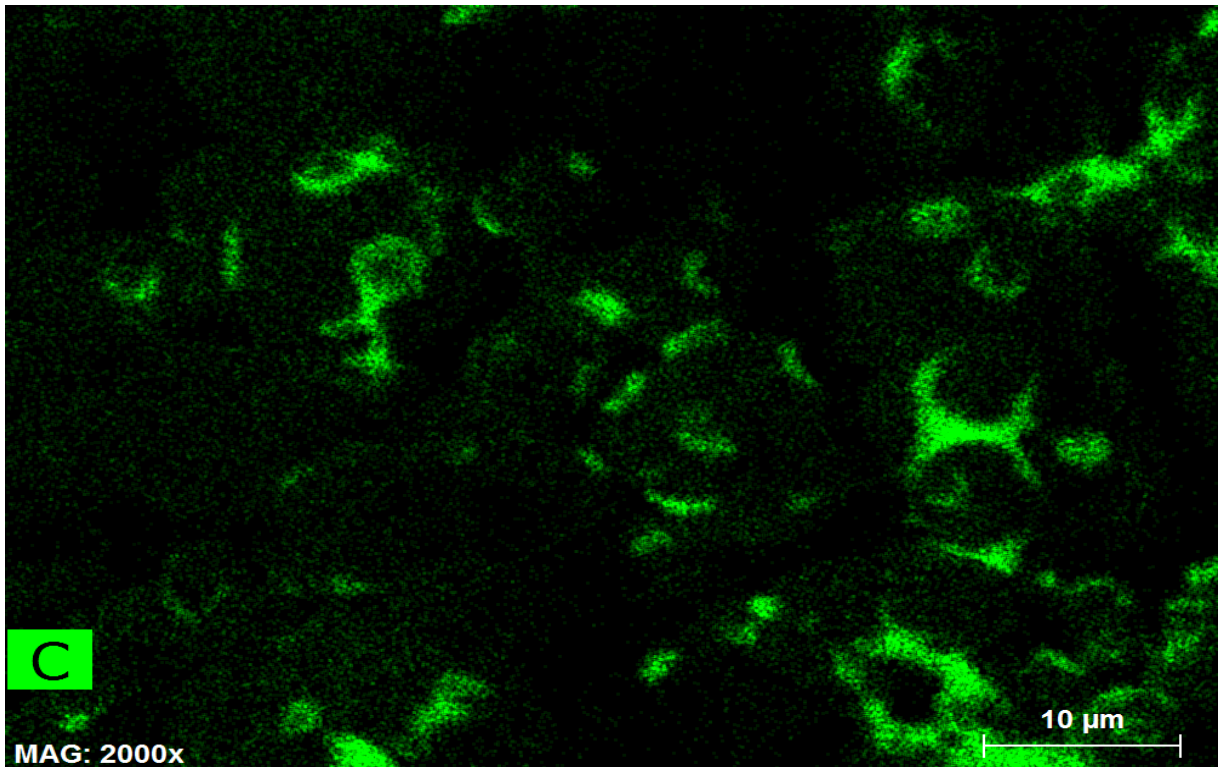
Figure 61: Elemental map- Carbon 816135 Recycled powder -Inked showing carbon concentrated at contact points
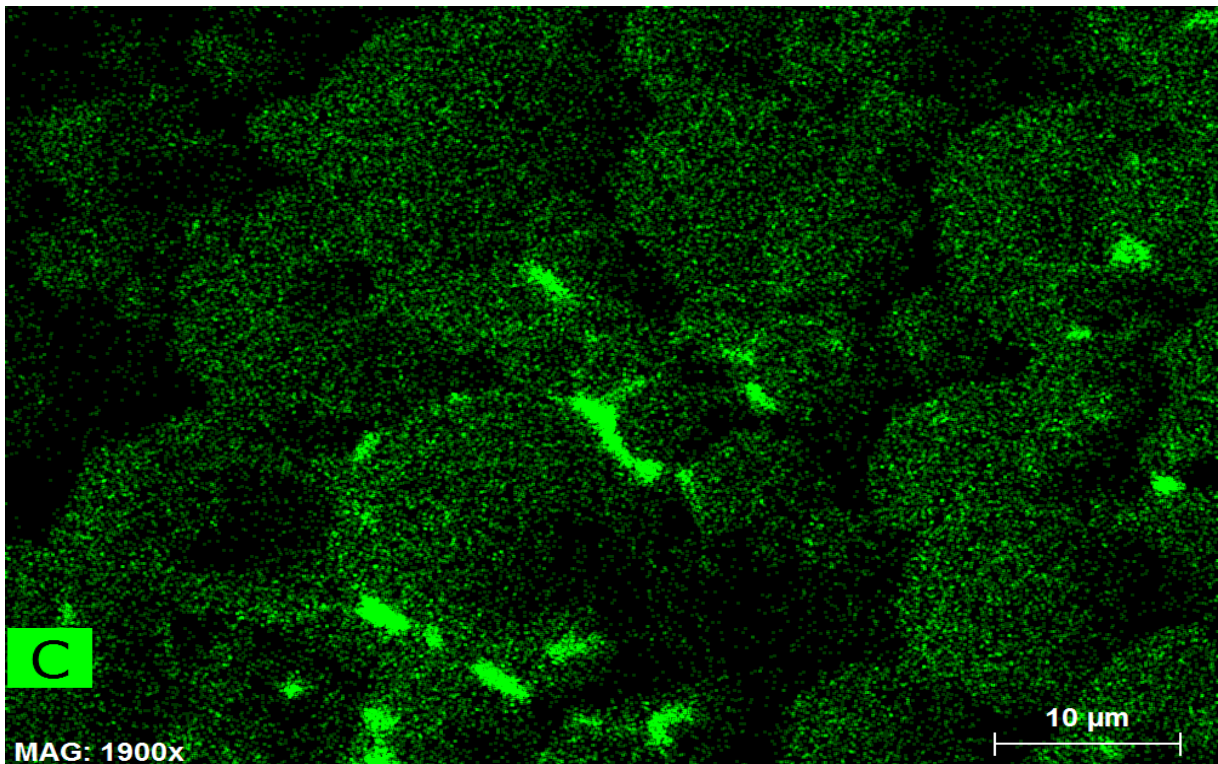
Figure 62: Elemental map-Carbon 816135 Recycled powder Inked showing carbon concentrated at contact points
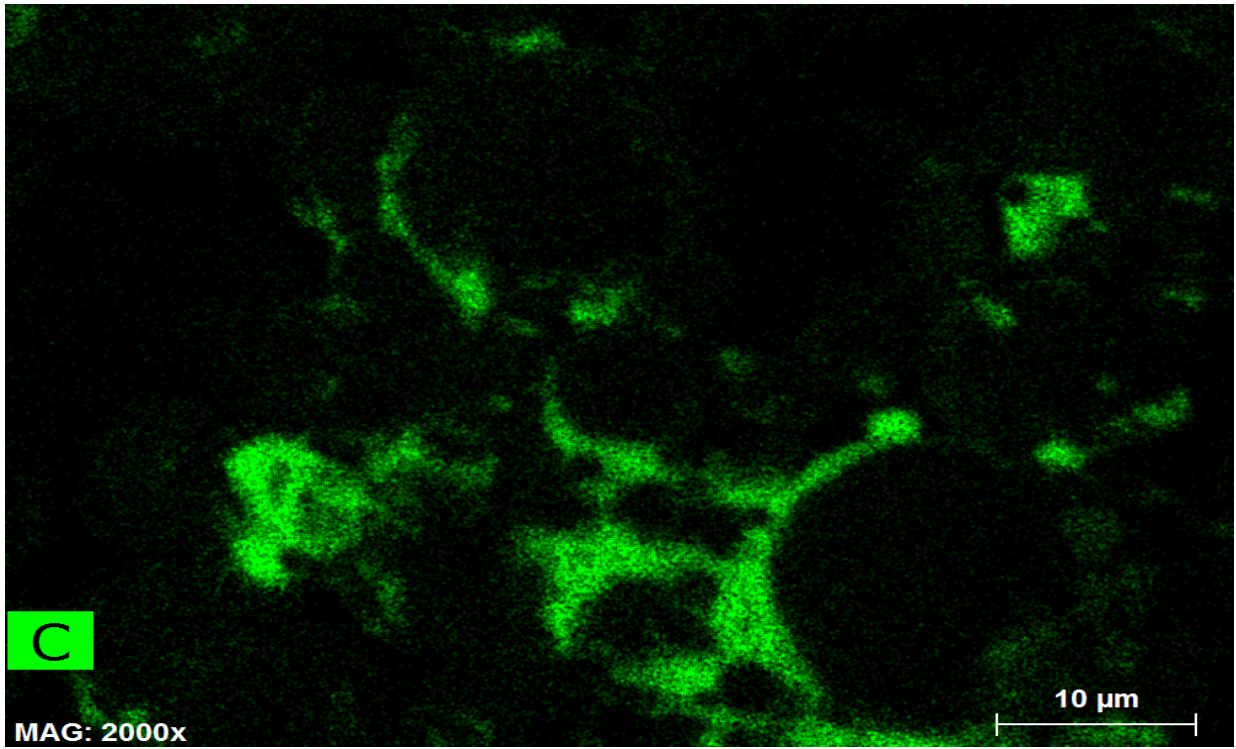
Figure 63: Elemental map carbon 816135 Virgin Inked showing carbon at contact points
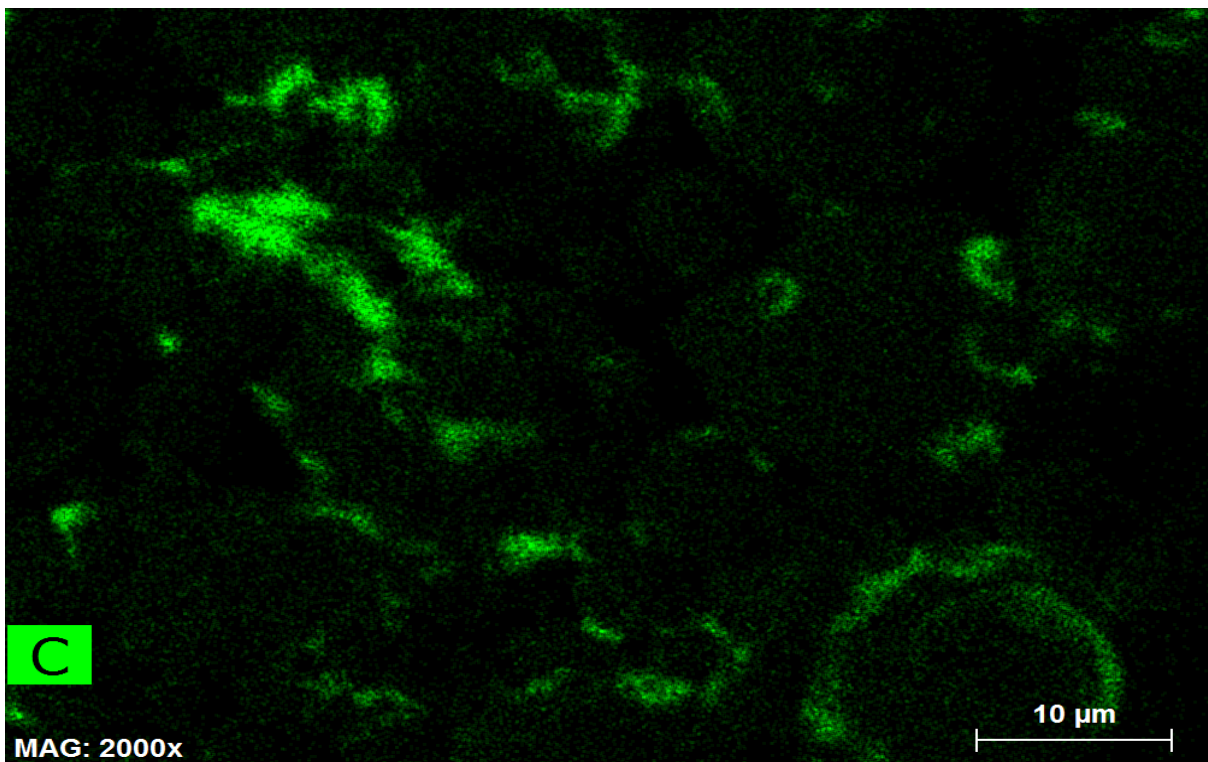
Figure 64: Elemental map-carbon 816135 Virgin powder inked showing carbon at contact points

An SEM examination of a printed part can also provide a good idea of binder deposition and spreading during printing.
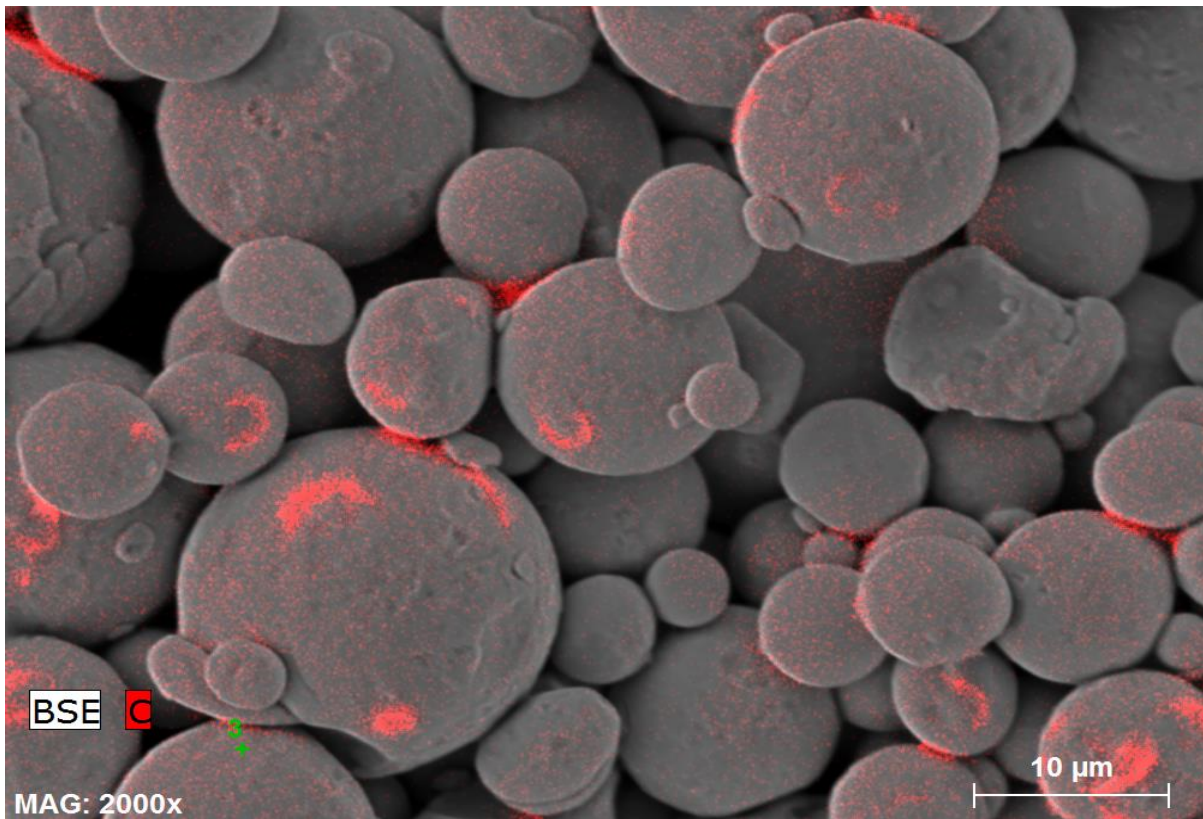
Figure 65: Carbon distribution in printed part 813897 powder (shown in red)
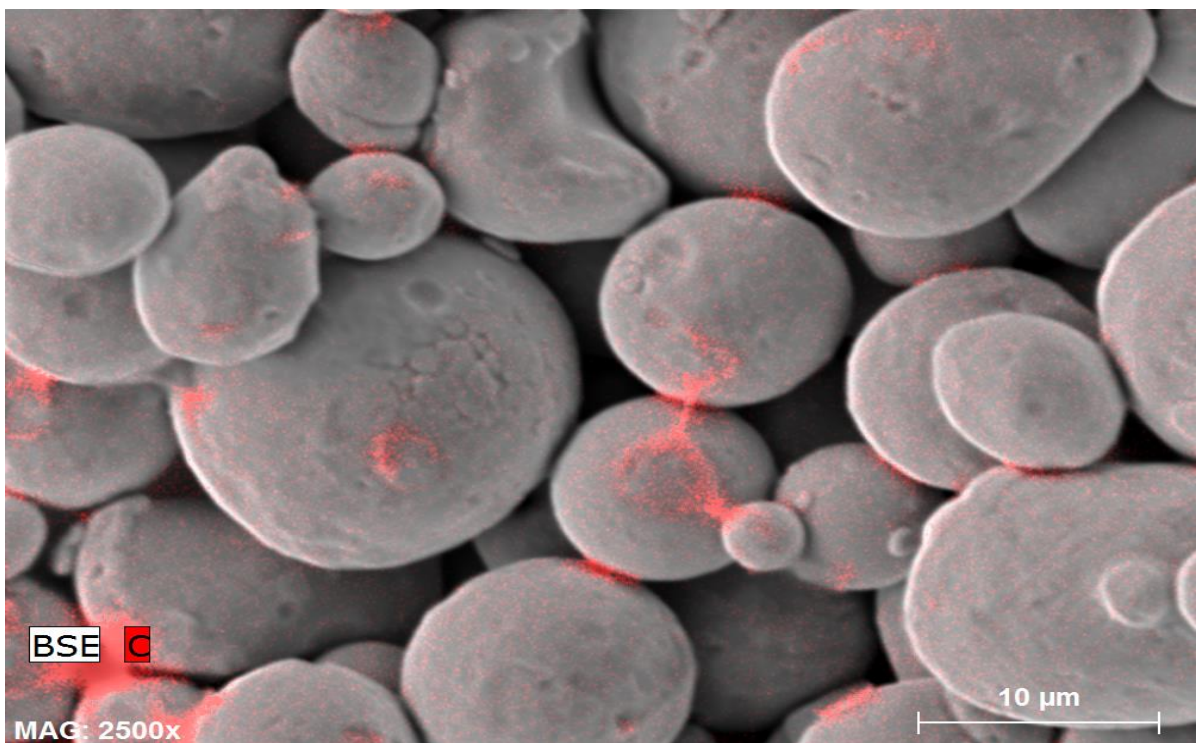
Figure 66: Carbon distribution in printed part 813897 powder (shown in red)

3.9 GREEN STRENGTH
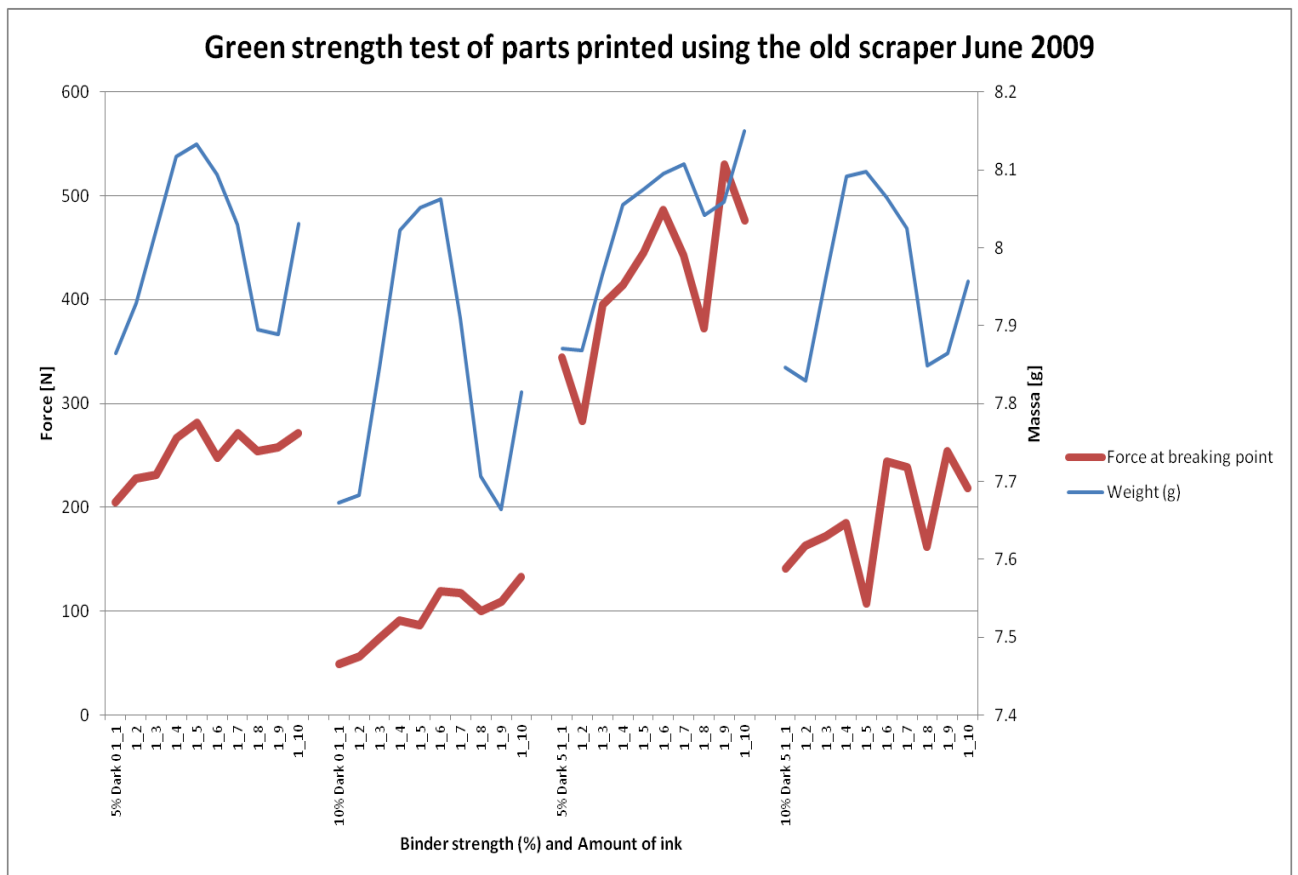
Figure 67: Green strength test using 813897 powder Old Collins Ink

The graph above shows the effect of an increase in the ink strength and binder content on the green strength of the part. The printing process itself affects the behaviour of the ink and the green strength significantly. The test was performed with 5% and 10 % PVP for two different ink strengths. The strength is measured at various points along the part to account for variations along the length. The weight of the parts is also examined.

4. DISCUSSIONS

4.1 X RAY TURBIDIMETRY

The particle size distribution of the measured powders is the same and any difference can be attributed to the margin of error during measurement.

4.2 SURFACE AREA/BET METHOD

The larger surface area of the 813897 Recycled powder is co-related with a smaller average particle size. Since the particle size distribution of the powders is similar it can be taken as an indicator of surface roughness or the number of satellites.

4.3 POWDER RHEOMETRY

For a similar particle size distribution the powder rheology showed significant differences. The rheology of the powder which most closely resembles the powder 813897 Recycled is Blend 1 based on the data obtained from rheological testing and listed in Table 26 below.

Table 26:Results of rheological testing of test powders

Powder	BFE (mJ)	SE(mJ/g)	SI	FRI	Pressure drop 15kPa (mBar)	CBD$_{tap}$	Aeration Ratio
813897 Virgin	470	2.6	1.1	1.6	24.37	4.64	5.37
813897 Recycled	490	2.6	1.1	1.6	26.11	4.57	2.33
816135 Virgin	448	2.2	1	1.5	29.49	2.18	8.54
816135 Recycled	636	2.9	1.1	1.4	27.27	2.90	2.83
Blend 1	474	2.6	1.1	1.5	27.45	4.66	2.61
Blend 2	522	2.8	1.1	1.6	27.94	4.65	2.05
Blend 3	440	1.9	1	1.5	26.02	5.10	3.15
Crushed powder	660	3.7	1.1	2.6	24.66	4.63	1.66

4.3.1 BASIC FLOWABILITY ENERGY (BFE) TEST

The BFE of the virgin powder especially the 815135 powder is significantly lower than that of the recycled powders. This also needs to be co-related to the consolidated bulk density data to obtain a better idea of flow properties [33]. Since this is the same for the 813897 powders we can take the lower BFE of the 813897 Virgin powders as an indicator of better flow. The low bulk density of 816135 Recycled powder in combination with the higher BFE indicates poor flow in comparison to the 816135 Virgin powders. The BFE and bulk density of the Blend 1 powder is closest to that of the 813897 Recycled powders.

4.3.2 SPECIFIC ENERGY TEST

A specific energy value of between 5 and 10 indicates moderate cohesion in the powder. This is the case for all of the measured powders. The specific energy values being higher for the recycled powders indicate greater cohesiveness and better packing in comparison to the virgin powders [33]. The specific energy of Blend 1 is closest to 813897 recycled powders thus indicating a similar degree of cohesiveness.

4.3.3 STABILITY INDEX (SI) TEST

The BFE of the virgin powder especially the 815135 powder is significantly lower than that of the recycled powders. The stability index of the measured powders is similar and hence the powder does not change much during measurement due to de-aeration, agglomeration, segregation or moisture uptake.

4.3.4 VARIABLE FLOW RATE TEST

This is a measure of the sensitivity of the powder rheology to the flow rate. Since the Flow Rate Index is quite close to the range of 1.5 to 3 their flow rate sensitivity is normal [33].

4.3.5 TAPPED CONSOLIDATION TEST

The 816135 Virgin and 813897 Recycled are more prone to consolidation on being subjected to vibration. For the powder blends the crushed and Blend 3 seem to be closer than the others to the 813897 recycled powders.

4.3.6 PERMEABILITY TEST

The recycled powders 813897 Recycled and 816135 Recycled have a lower degree of permeability at low normal applied stress and a smaller permeability change at increasing levels of compressive stress than the 813897 Virgin powder and the 816135 Virgin powder. The 813897 Virgin powder has a lower pressure drop and a higher bulk density probably due to the surface texture. The 816135 Virgin powder has a higher pressure drop and a higher bulk density. For the powder blends Blend 3 seems to have a permeability that most closely resembles that of the 813897 Recycled powder.

4.3.7 COMPRESSIBILITY TEST

The higher values for the Conditioned Bulk Density values for the 813897 powders show it is more cohesive than the 816135 powders. From the graphs of compressibility it can be seen that the recycled powders have a greater compressibility than the virgin powders thus indicating greater cohesiveness. These more compressible powders are more likely to compact when compressed and thus more prone to flow related problems. For the powder blends the Blend 3 has the most similar compressibility characteristics to 813897 Recycled powder. The conditioned bulk density on the other hand is quite close for Blend 1, Blend 2 and the crushed powder indicating a similar degree of cohesiveness but Blend 3 has the highest conditioned bulk density and hence is a good match.

4.3.8 AERATION TEST

The data and the aeration ratios of between 2 and 20 indicate average sensitivity to aeration which is typical for most powders. However the virgin powders were more easily aerated than the recycled powder which is correlated with a lower

cohesiveness which has been confirmed by the compression test above. Among the powder blends Blend 1 and Blend 2 show ratios that most closely match that of the 813897 Recycled powder.

4.3.9 SHEAR CELL TEST

The cohesion between the particles of the 813897 powder is much greater than the 816135 powders. The crushed powder shows a degree of cohesion similar to 813897 powder. The yield stress which reflects the friction or cohesion between the powder particles is also much higher for the 813897 powders and highest for the recycled 813897 powder. The yield stress in the Blend 1 powder most closely resembles that of the 813897 Recycled powder. The flow function indicating powder fluidity shows better flow for the 816135 powders with the best flow for the recycled 816135 powder. The flow function for the crushed powder is closest to that of the 813897 recycled powder indicating a similar degree of powder fluidity.

4.3.10 WALL FRICTION TEST

The friction co-efficient does not change much between different powders and materials except of Ti-48Al powder. Thus minimal gains in powder flow can be expected from surface coating of the scraper blades which is in itself a rather expensive process.

4.4 CONTACT ANGLE GONIOMTERY

The wetting of the 816135 Virgin powder is better than that for the 816135 Recycled powder. The experiment performed using a heated plate shows worse wetting with Collins Blue ink at higher temperatures.

4.5 FORCE TENSIOMETRY/DU NOÜY RING METHOD

This data is necessary for the Washburn test and is of use when measuring the contact angle.

4.6 MERCURY POROSIMETRY

The average pore diameter in the pore bed is 3.7 μm. The percentage porosity is determined to be 40 %.The majority of the pore size lie in the range of 3-5 μm. The percent porosity is only an approximate measure due to limitations in replicating powder bed packing due to sample holder and sample loading technique.

4.7 WASHBURN CAPILLARY RISE METHOD

In the case of the 813897 powders the virgin powder exhibits a larger capillary constant and a larger contact angle which indicates poorer wetting compared to the recycled powder. In the case of the 816135 powder the virgin powder exhibits a larger capillary constant but better wetting than the recycled powder. Surface chemistry is the likely cause and could be further examined for quantification and easier comparison using ESCA.

4.8 SCANNING ELECTRON MICROSCOPY

During the printing process selective deposition of the ink by the print head stitches the powder particles. As ink in the debinding oven maintained at 200°C begins to evaporate surface tension pulls the ink to the contact points between the powder particles increasing the saturation of the liquid and preferentially deposition of the suspended particles at the necks [38].The green body mostly consists of 30-70% powder, 10 % ink with the remaining portion occupied by void space [39].It is impossible to compare and quantify the various residues on the surface of the powder using SEM. This is best done through better tools to investigate the surface chemistry such as X-ray photoelectron spectroscopy (ESCA), Auger electron spectroscopy, Secondary ion mass spectroscopy and Ion scattering spectroscopy. The surface chemistry difference is the most likely cause of the difference in wetting characteristics between the 816135 powder and the 813897 powder.

4.9 GREEN STRENGTH

For the parts printed with ink containing 5 % PVP an increase in the mount of ink from Dark 0 to Dark 5 significantly increases the green strength. However this increase is minimal in the case of the ink with 10% PVP. Also for a fixed amount of ink there is actually a decrease in strength with an increase in the amount of PVP. This is not the same as in the case of tablets used in diametral compression tests to measure the green strength. This is possibly as the increase in PVP significantly increases the viscosity which reduces penetration ability of the ink which along with the decreased time for penetration possibly significantly reduces the contact between powder particles thus reducing the green strength.

5. CONCLUSIONS

The following can be inferred from the results of this study

- For a similar particle size distribution the powder rheology showed significant differences
- Greater energy to establish flow in recycled powders
- Greater cohesion and compressibility for recycled powders
- Easier aeration for the virgin powders
- Blend 1 is the best rheological match for use in the machine
- In the case of the powder blends crushed powder seems to have a very different and undesirable property profile
- Coating the scraper blade with different materials to improve flow may not be justifiable for the cost due to minimal change in powder flow
- The Washburn test is a far more reliable and robust method of measuring the contact angle compared to contact angle goniometry
- Wetting studies from the Washburn test indicate better wetting for the 816135 Virgin powder than the recycled powder and better wetting for the 813897 recycled powder than the 813897 Virgin powder
- The wetting results from the 813897 powders are in agreement with shop floor experience and are expected while this is not the case in the 816135 powders. This discrepancy in the case of the 816135 powders is likely due to the difference in surface chemistry
- Temperature of the powder bed has a poor effect on wetting behaviour
- The binder migrates to the contact point between the powder particles. Increasing the amount of PVP in the ink would also likely increase the contact between the powder particles
- An increase in binder content increases the green strength of the part for low binder content but this is not the case at higher binder content

6. FUTURE WORK

To develop a better understanding of the wetting phenomena in different virgin and recycled powders further studies would be helpful. As the differences in the wetting characteristics of the virgin and recycled powders vary quite widely despite similarities in measured properties further examination including an examination of the surface chemistry of the powders would be quite helpful. Also as the machine is run at an elevated temperature of about $80^{o}C$ the powder rheology could be examined using a modified apparatus to overcome the limitations of the current plastic testing devices. The exposure to moisture during goniometric measurements and the drying effect on the ink need to be avoided to avoid the modifying effects of these variables on the readings. Real life tests could be performed on a machine to correlate this data to experimental simulations to improve accuracy of readings and develop a better understanding of the limitations of the current setup.

7. ACKNOWLEDGEMENT

REFERENCES

1. Laurence Galet , Severine Patry, John Dodds, Determination of the wettability of powders by the Washburn capillary rise '[method with bed preparation by a centrifugal packing technique

2. A comparison of contact angle measurement techniques applied to highly porous catalyst supports, Emilia Nowak , Gary Combes, E. Hugh Stitt , Andrzej W. Pacek

3. Determination of contact angles and pore sizes of porous media by column and thin layer wicking, C.J. Van Oss, R.F. Giese, Z. Li, K. Murphy, J. Norris, M.K. Chaudhury, et al.,

4. Laser Fabrication and Machining of Materials, By Narendra B. Dahotre, Sandip P. Harimkar

5. Powder Technology: Fundamentals of Particles, Powder Beds, and Particle Generation, H Masuda, K Higashitani, H Yoshida - 2010 - CRC Press

6. Moon, Jooho, et al. "Ink-Jet Printing of Binders for Ceramic Components."Journal of the American Ceramic Society 85.4 (2002): 755-762.

7. Godlinski,D. and S. Morvan, Steel parts with tailored material ingredients by 3D-pinting using nano-particlulate ink Materials Science Forum,2005.492-493 (Functionally graded materials VIII):p679-684

8. Berend-Jan de Gans,Paul C.Duineveld, Inkjet printing of polymers: State of the art and future developments

9. Greil, P., Polymer derived engineering ceramics, Advanced Engineering Materials, 2000.2(6): p 339-348.

10. Moon, J., et al., Slurry chemistry control to produce easily dispersible ceramic powder compacts. Journal of the American Ceramic Society, 2000. 83 (10):p. 2401-2408.

11. Baskaran, S., Graff,Gordon L.,Method of freeform fabrication by selective gelation of powder suspensions,USPTO,Editor,1997,Battelle Memorial Institute: United States

12. Seerden,K.A.M., et al.,Ink-jet printing of wax-based alumina suspensions. Journal of the American Ceramic Society,2001,84(11):p.2514-2520.

13. Wang, T. and B.Derby, Ink-jet printing and sintering of PZT. Journal of the American Ceramic Society,2005.88(8):p 2053-2058.

14. Tim Freeman, Quantifying experience in powder processing, *Pharmaceutical Technology Europe;* Mar 2009; 21, 3; ProQuest Central

15. Sachs E.M., Powder dispensing apparatus using vibration, USPTO, Editor, 2000, Massachusetts Institute of Technology: United States.

16. Sachs E.M., Cima, Michael J., Caradonna, Michael A., et al., Jetting layers of powder and the formation of fine powder beds thereby, USPTO, Editor,2003, Massachusetts Institute of Technology: United States

17. Cima, M., Sachs, Emanuel, Fan, Tailin., et. al., Three-dimensional printing techniques, USPTO, Editor, 1995, Massachusetts Institute of Technology: United States

18. Cima,L.G., Cima, Michael J., Preparation of medical devices by solid freeform fabrication methods,USPTO,Editor,1996,Massachusetts Institute of Technology: United States

19. Bredt,J.,F., Andersson, Timothy C., Russell, David B., Three dimensional printing materials system,USPTO,Editor,2002,Z Corporation: United States

20. I. Gibson, D.W. Rosen, B. Stucker, Additive manufacturing technologies: rapid prototyping to direct digital manufacturing, Springer, US (2010) p. 24

21. Kruth JP, Leu MC, Nakagawa T (1998) Progress in additive manufacturing and rapid prototyping.
Ann CIRP 47(2):525–540

22. Burns M (1993), Automated fabrication: improving productivity in manufacturing. Prentice
Hall, Englewood Cliffs, NJ

23. Chua CK, Leong KF (1998) Rapid prototyping: principles and applications in manufacturing.
Wiley, New York

24. I. Gibson, D.W. Rosen, B. Stucker, Additive manufacturing technologies: rapid prototyping to direct digital manufacturing, Springer, US (2010) p. 174

25. I. Gibson, D.W. Rosen, B. Stucker, Additive manufacturing technologies: rapid prototyping to direct digital manufacturing, Springer, US (2010) p. 182

26. Sachs, E. M., Hadjiloucas, C., Allen, S., and Yoo, H. J., 2003, "Metal and Ceramic Containing Parts Produced From Powder Using Binders Derived From Salt," U.S. Patent No. 6,508,980

27. Liu, J., and Rynerson, M., 2003, "Method for Article Fabrication Using Carbohydrate Binder," U.S. Patent No. 6,585,930.

28. B.R. Utela, D. Storti, R.L. Anderson, M. Ganter,Development process for custom three-dimensional printing (3DP) material systems,J Manuf Sci Eng – Trans ASME, 132 (1) (2010)

29. Rulison, C. Wettability studies for porous solids including powders and • brous materials. Technical note 302. KRÜSS: Instruments for surface chemistry, Charlotte, Krüss, 1996.

30. Lund, J.A., "Origin of Green Strength in Iron Compacts," Int. J. Powder Metall. Powder Technol., vol 18. (no. 2),pp 117-127,1982.

31. Vyal, E., Laptev, M., Use of certain binders to increase the strength of green compacts, Powder Metallurgy and Metal Ceramics, 44, 614-618,2005

32. Capus, J.M.: Metal Powders – A Global Survey of Production, Applications and Markets1996–2005, Third Edition; Oxford, Elsevier Advanced Technology 2000

33. K.P. Hapgood, J.D. Litster, S.R. Biggs, T. Howes, Drop penetration into loose packed powder beds, submitted to J. Colloid Interface Sci., 253 (2002), pp. 353–366

34. Marmur, A., *J. Colloid Interface Sci.* 124**,** 301 (1988)

35. J.I. Goldstein, D.E. Newbury, P. Echlin, D. Joy, C.E. Lyman, E. Lifshin, L. Sawyer, J.R. Michael, Scanning electron microscopy and x-ray microanalysis, 3rd ed., Kluwer Academic/Plenum /Springer, New York, 2003, pp. 92–93.

36. 'Metals Handbook', Vol. 7, 9th edn, 'Powder metallurgy', 6; 1984, Metals Park, OH, American Society for Metals.

37. S. Arima, D. Banyash, J. Breidenbaugh, S. Masuhara, and M. Takada: 'Advances in powder metallurgy and particulate materials', Vol. 3, 91–101; 1994, Princeton, NJ, MPIF.

38. E. Klar and W. M. Shafer: 'Modern developments in powder metallurgy', Vol. 9, 91–113, 1976, Princeton, NJ, MPIF

39. Freeman, R., Measuring the Flow Properties of Consolidated, Conditioned and Aerated Powders - A Comparative Study Using a Powder Rheometer and a Rotational Shear Cell, Powder Technology, 174, pp. 25-33, 2007.

40. Gianangelo Bracco, Bodil Holst., Surface Science Techniques, Volume 51 (2013)

41.   H.   R.   Allcock,   "*Introduction   to   Materials   Chemistry.*", 1st edition, Wiley, Hoboken 2008

42.   P.C. Angelo, R. Subramanian, Powder metallurgy: science, technology and applications, Prentice-Hall of India, New Delhi, 2008.

43. Kaufui V.Wong, Aldo Hernandez, A Review of Additive Manufacturing, Department of Mechanical and Aerospace Engineering, University of Miami, Coral Gables, FL 33146, USA

44. Terry Wohlers, Tim Caffrey, Additive Manufacturing: Going Mainstream, Manufacturing Engineering, ISSN 0361-0853, 06/2013, Volume 150, Issue 6, p. 6

45. Gibson I, Rosen DW, Stucker B. Additive manufacturing technologies: rapid prototyping to direct digital manufacturing. US: Springer; 2010. p. 41–59

46. Mustaffa Ibrahim, Takayuki Otsubo, Hiroyuki Narahara, Hiroshi Koresawa and Hiroshi Suzuki, Investigation on Fabricating 3D Structures Using Inkjet Printing Technology, Department of Mechanical Information Science and Technology, Kyushu Institute of Technology

47. Magdassi, Shlomo, Chemistry of Inkjet Inks, World Scientific; 2010

48. Grohowski, J. "Understanding the effects of atmosphere type on thermal debinding behavior." Industrial Heating(USA) 67.10 (2000): 61-64.

49. Leach, Robert H., ed. The printing ink manual. Springer, 1993,pp 678-698

50. Cooke, April, and John Slotwinski. Properties of Metal Powders for Additive Manufacturing: A Review of the State of the Art of Metal Powder Property Testing. US Department of Commerce, National Institute of Standards and Technology, 2012.

51. Neikov, Oleg D., et al. Handbook of non-ferrous metal powders: technologies and applications. Access Online via Elsevier, 2009.

52. Klar, Erhard, and Prasan K. Samal. Powder Metallurgy Stainless Steels: Processing, Microstructures, and Properties. ASM international, 2007.

53. Freeman, Tim. "The importance of powder characterization." Pharma Technol Eur 22 (2010): 21-26.

54. Prescott, James K., and Roger A. Barnum. "On powder flowability." Pharmaceutical technology 24.10 (2000): 60-84.

55. Siebold, A.; Nardin, M.; Schultz, J.; Walliser, A.; Oppliger, M. Colloids Surf.A 2000, 161, 81

56. Grundke, K.; Augsburg, A. J. Adhesion Sci. Technol. 2000, 14, 765

57. Gooch, Jan W., ed. Encyclopedic dictionary of polymers. Vol. 1. Springer, 2010,p 577.

58. Kitaoka, Nobuyuki, and Yoshiaki Ono. "Water-based ink composition for ballpoint pen and ballpoint pen comprising the same." U.S. Patent No. 7,441,976. 28 Oct. 2008.

59. Connexions. 2013. *BET Surface Area Analysis of Nanoparticles*. [online] Available at: http://cnx.org/content/m38278/latest/?collection=col10700/latest [Accessed: 15 Oct 2013].

60. Connexions. 2013. BET Surface Area Analysis of Nanoparticles. [online] Available at: http://cnx.org/content/m38278/latest/?collection=col10700/latest [Accessed: 15 Oct 2013].

61. Lowell, Seymour, and Joan E. Shields. Powder surface area and porosity. Vol. 2. Springer, 1991.

62. Nowak, Emilia, et al. "A comparison of contact angle measurement techniques applied to highly porous catalyst supports." Powder Technology (2012).